Lawrence Berkeley National Laboratory
Recent Work

Title
SPECTRA AND KINETICS OF THE HYDROPEROXYL FREE RADICAL IN THE GAS PHASE

Permalink
https://escholarship.org/uc/item/2199x0ct

Author
Paukert, Thomas Theodore.

Publication Date
1969-11-01

eScholarship.org Powered by the California Digital Library
University of California

UCRL-19109

cy. 2

RECEIVED
LAWRENCE
RADIATION LABORATORY

DEC 17 1969

LIBRARY AND
DOCUMENTS SECTION

SPECTRA AND KINETICS OF THE HYDROPEROXYL FREE RADICAL IN THE GAS PHASE

Thomas Theodore Paukert
(Ph.D. Thesis)

November 1969

AEC Contract No. W-7405-eng-48

TWO-WEEK LOAN COPY

This is a Library Circulating Copy which may be borrowed for two weeks. For a personal retention copy, call Tech. Info. Division, Ext. 5545

LAWRENCE RADIATION LABORATORY
UNIVERSITY of CALIFORNIA BERKELEY

UCRL-19109

cy. 2

DISCLAIMER

This document was prepared as an account of work sponsored by the United States Government. While this document is believed to contain correct information, neither the United States Government nor any agency thereof, nor the Regents of the University of California, nor any of their employees, makes any warranty, express or implied, or assumes any legal responsibility for the accuracy, completeness, or usefulness of any information, apparatus, product, or process disclosed, or represents that its use would not infringe privately owned rights. Reference herein to any specific commercial product, process, or service by its trade name, trademark, manufacturer, or otherwise, does not necessarily constitute or imply its endorsement, recommendation, or favoring by the United States Government or any agency thereof, or the Regents of the University of California. The views and opinions of authors expressed herein do not necessarily state or reflect those of the United States Government or any agency thereof or the Regents of the University of California.

TABLES OF CONTENTS

January 7, 1970

UNIVERSITY OF CALIFORNIA

Lawrence Radiation Laboratory
Berkeley, California

AEC Contract No. W-7405-eng-48

ERRATA

TO: Recipients of UCRL-19109

FROM: Technical Information Division

SUBJECT: "Spectra and Kinetics of the Hydroperoxyl Free Radical in the Gas Phase" by Thomas Theodore Paukert, Ph.D thesis, November 1969

Please make the following corrections to your copy of subject report.

Page	and line	
4	15	Reads 1.7 ± 4 Should read 1.7 ± 0.4
46	9	in Figure 12a and at 1368, 1378, and 1425 cm^{-1} Delete
69	15	Reads The phase shift .....are found from Table IV. Should read The phase shift of the radical at each frequency can be found from the theoretical curve in Figure 19, and the phase shift of the reactant corresponding to the radical phase shift is found from Table IV.
73	1	Reads 1/4 Hz in Table V Should Read 1/4 Hz are listed in Table V
93	23	Reads and 3505 cm^{-1} Should read 3505, and 3550 cm^{-1}
98	24	Reads $HO_2 + HO \rightarrow H_2O_2 + O_2$ Should read $HO_2 + HO_2 \rightarrow H_2O_2 + O_2$

SPECTRA AND KINETICS OF THE HYDROPEROXYL FREE RADICAL IN THE GAS PHASE

Thomas Theodore Paukert

Inorganic Materials Research Division, Lawrence Radiation Laboratory, and Department of Chemistry, University of California, Berkeley, California

ABSTRACT

The absorption spectrum of the hydroperoxyl radical (HO_2) has been obtained by the molecular-modulation technique. The radical was formed by the photolysis of hydrogen peroxide at 2537 A and by the photolysis of ozone in the presence of hydrogen peroxide at 2537 A. The vibrational frequencies of HO_2 have been observed to be 1095, 1390, and 3410 cm^{-1}. Details of the vibrational spectrum are consistent with the molecular geometry: H-O bond distance 0.96 A, O-O bond distance 1.3 A, and H-O-O angle approximately 108°. The absorption spectrum of HO_2 in the ultraviolet has a maximum at 2100 A.

Kinetic analysis of the modulated absorption signals shows that the HO_2 radical decays by a process second order in HO_2 concentration. The rate constant for the disproportionation reaction $HO_2 + HO_2 \rightarrow H_2O_2 + O_2$ was found to be $3.6 \pm 0.5 \times 10^{-12}$ cm^3/molecule·sec in agreement with a reported value of 3×10^{-12} cm^3/molecule·sec.

The absorption coefficient of HO_2 at 1420 cm^{-1}, the absorption maximum of the 1395 cm^{-1} band is approximately 5×10^{-20} cm^2/molecule. The absorption coefficient at 2100 A is 4.5×10^{-18} cm^2/molecule.

I. INTRODUCTION

The direct observation of free radical intermediates in chemical reactions is of interest for two reasons. First, the information gained can provide detailed knowledge of the radicals themselves. Second, in the case of some complex chemical reactions, the mechanism of reaction cannot be uniquely determined without direct observation of one or more of the intermediates involved.[1] The most successful techniques for experimental detection of free radicals have been flash photolysis and matrix isolation. The high light intensities used in flash photolysis (up to 10^{22} quanta/cm^2 sec) generate sufficiently high concentrations of radicals to permit direct spectroscopic detection. A large number of radicals have been observed and mechanisms clarified by this technique.[2,3,4,5,6] Because the absorption coefficients of radicals are generally unknown, it is difficult to determine the radical concentrations. Hence, in most cases, the rate constants for radical-radical reactions cannot be determined.[2] The method of matrix isolation has likewise been very successful in the observation and identification of radicals;[7,8] but since its success lies in the isolation of the radicals in a non-reactive environment, no kinetic data can be obtained. A third technique is that of molecular modulation now being developed in this laboratory.[9,10,11] This method complements the other two because it permits the detection of free radicals in chemical systems under moderate light intensities (approximately 10^{16} quanta/cm^2 sec) and rate constants can be easily extracted from the experimental data. The application of this last technique to the hydroperoxyl radical (HO_2) is the subject of this paper.

A. Indirect Evidence of HO_2

The hydroperoxyl radical was first proposed by Marshall[12] and by Taylor[13] as part of the mechanism of the reaction of hydrogen and oxygen. Marshall proposed the following steps:

$$H + O_2 \rightarrow HO_2$$

$$HO_2 + H_2 \rightarrow H_2O_2 + H$$

$$2H_2O_2 \rightarrow H_2O + O_2$$

He subsequently showed that the mercury photo-sensitized oxidation of hydrogen produces hydrogen peroxide and has a large quantum efficiency as predicted by the mechanism.[12]

The formation of the hydroperoxyl radical by the termolecular process

$$H + O_2 + M \rightarrow HO_2 + M$$

in the $H_2 + O_2$ reaction has long been established,[14] but the fate of HO_2 is a matter of controversy. The mechanistic treatment by Lewis and von Elbe,[15] which agrees well with the data of many workers, presumes the removal of HO_2 at the walls and does not include the homogeneous reaction

$$HO_2 + HO_2 \rightarrow H_2O_2 + O_2 \quad .$$

Hence the authors conclude the reaction must proceed very slowly (once in every 10^7 collisions), if at all. On the other hand Baldwin, et al.[16,17] report evidence of this reaction occurring in the oxidation of hydrogen in vessels with a different surface composition. Furthermore, Burgess and Robb[18] conclude from their studies of the mercury photo-sensitized $H_2 + O_2$ reaction that the HO_2--HO_2 disproportionation reaction occurs very rapidly at a rate very close to the rate of collision. A serious difficulty in the study of the hydrogen-oxygen system is a strong surface effect on the overall reaction

rate[19] which may account for the wide discrepancy in the estimates of the rate of the disproportionation reaction.

Another chemical system in which the presence of the HO_2 radical is presumed is the photolysis of ozone with water or hydrogen peroxide in the ultraviolet. In several studies of the photolysis of ozone, the quantum yield of ozone decomposition varied widely depending on the oxygen-to-ozone ratio, the decomposition of ozone being retarded by oxygen.[20,21,22] Each of these studies compared the quantum yield in the presence of water or hydrogen peroxide to the quantum yield in the absence of these hydrogen containing substances. In all three, the quantum yields were substantially larger (by a factor of four to six) when water or hydrogen peroxide was present. Volman[21] found that at 2537 A the quantum yield of ozone decomposition varied from 0.04 to 0.22, depending on foreign gases, with no hydrogen peroxide and from 0.23 to 0.71 with the peroxide. Heidt and Forbes[20] conducted photolytic experiments on ozone at 2100, 2540, and 2800 A with and without water. With water present, the quantum yield lay between 1.6 and 130 depending on total pressure, ozone-to-oxygen ration, and water pressure; without water the quantum yield varied from 0.5 to 6.3 for a similar range of total pressure and ozone-to-oxygen ratio. Finally, Norrish and Wayne[22] observed a quantum yield of 6.5 at 2537 A for pure dry ozone at 1 cm of Hg; at the same ozone pressure with about 1 cm of water the quantum yield was greater than 25.

These results strongly indicate the action of a chain due to the presence of the hydrogen-containing molecule. Volman[23] presents the following chain to account for quantum yield dependence on the oxygen-to-ozone ratio and on the presence of water or hydrogen peroxide.

$$O_3 + h\nu \rightarrow O_3^* \qquad (1)$$

$$O_3^* + M \rightarrow O_3 + M \qquad (2)$$

$$O_3^* \rightarrow O_2 + O \qquad (3)$$

$$O + O_2 + M \rightarrow O_3 + M \qquad (4)$$

$$O + O_3 \rightarrow 2O_2 \qquad (5)$$

$$O + H_2O_2 \rightarrow HO_2 + OH \qquad (6a)$$

$$O + H_2O \rightarrow 2OH \qquad (6b)$$

$$OH + O_3 \; HO_2 + O_2 \qquad (7)$$

$$OH + H_2O_2 \rightarrow HO_2 + H_2O \qquad (8)$$

The presence of the hydroxyl radical OH has been confirmed by Mc Grath and Norrish[14] who observed it spectroscopically following the flash photolysis of wet ozone. They did not, however, detect HO_2.

The photolysis of hydrogen peroxide is also believed to produce HO_2. Volman[25] found the quantum yield for hydrogen peroxide decomposition at 2537 A to be 1.7 ± 4. This result is consistent with the very simple mechanism

$$H_2O_2 + h\nu \rightarrow 2OH \qquad (1')$$

$$OH + H_2O_2 \rightarrow HO_2 + H_2O \qquad (8)$$

$$HO_2 + HO_2 \rightarrow H_2O_2 + O_2 \qquad (10)$$

which predicts a quantum yield of 2.

Numerous workers[17,26,27,28] studying the $H_2 + O_2$ system and others[29,30,31,32] studying the decomposition of hydrogen peroxide have used a reaction between OH and H_2O_2 to interpret their results. The flash photolysis of hydrogen peroxide by Greiner[32] showed, by observation of OH, that the hydroxyl radical is formed in the photolysis and that it decays by a process first order in both OH and H_2O_2 concentrations. Greiner also searched for an absorption by HO_2 in the region 2500 is 10,000 A but found nothing. That

HO_2 is, indeed, the product of reaction (8) was demonstrated by Foner and Hudson[33] as described in the next section.

The photolyses of ozone in the presence of hydrogen peroxide and of hydrogen peroxide by itself are thus expected to be rich in HO_2 radicals.

B. Direct Evidence of HO_2

Direct observation of HO_2 was first accomplished by Foner and Hudson[34] who succeeded in producing hydroperoxyl radicals by the reaction

$$H + O_2 + M \rightarrow HO_2 + M$$

and detecting them by mass spectrometry. This radical has also been observed mass spectrometrically by Robertson[35] who added O_2 to a stream of H atoms, Ingold and Bryce[36] who reacted O_2 with H atoms and with methyl radicals, and Fabian and Bryce[37] who studied the reaction of methane with oxygen molecules. Foner and Hudson[33] have since reported observing the mass spectrum of HO_2 formed in six different ways: the reactions of H atoms with O_2 and H_2O_2, of O atoms with H_2O_2, of OH radicals with H_2O_2, the photolysis of H_2O_2, and a low-power electrical discharge of H_2O_2.

Spectroscopic detection of HO_2 has been achieved by Milligan and Jacox[38] using the matrix isolation technique. They photolyzed an HI-O_2 mixture in an argon matrix at 4°K and obtained infrared absorption peaks in the regions 1040-1101 cm^{-1}, 1380-1390 cm^{-1}, and at 3402 and 3414 cm^{-1}. These absorptions were attributed to the O-O stretching, HOO bending, and H-O stretching vibrations, respectively. The spectrum has been confirmed by Ogilvie[39] in an argon-neon matrix at 4°K, but his low frequency assignments are reversed.

The transient ultraviolet absorption spectrum of HO_2 has been observed following the pulsed electron irradiation of oxygenated aqueous solutions

by Czapski and Dorfman.[40] The spectrum of the radical in solution begins at approximately 3000 A and has a maximum at 2300 A with a molar extinction coefficient $\alpha = 1150\ M^{-1}cm^{-1}$.

Only one report of a direct measurement of the HO_2-HO_2 disproportionation rate constant in the gas phase exists in the literature. In a review article, Foner and Hudson[41] mention some work of theirs which, by direct mass spectrometric observation of HO_2, gives a rate constant of 3×10^{-12} cm^3/molecule·sec. This rate constant is less than the estimate of Burgess and Robb[18] by a factor of 100 but greater than that of Lewis and von Elbe[15] by a factor of 10^5.

C. Structure of HO_2

Very little is known of the structure of the hydroperoxyl radical. Several theroretical studies of this molecule have been made, but there is no agreement. Green and Linnett[42] predict a bond angle between 55 and 70°; Boyd[43] carried out theoretical calculations which give a bond angle of 47° with the H atom at the apex of an isosceles triangle. In contrast, Walsh[44] predicts that the bond of HO_2 should lie between 90 and 180° and should be slightly less than the bond angle of HNO. The bond angle of HNO in the ground state has been found to be 108.5°.[45] Milligan and Jacox's[38] spectral work demonstrates that the O atoms of HO_2 are not equivalent which rules out an isosceles triangular structure. Considering the success of Walsh's theory in predicting the structure of HCO and HNO, the HO_2 molecule is probably nonlinear with a bond angle of about 108°.

II. EXPERIMENTAL

A. Methods

The detection and study of free radical intermediates in photochemical reactions at ordinary (moderate) light intensities present several problems. Radical concentrations are very small, on the order of 10^{10} to 10^{13} molecules/cm^3. Spectroscopic signals are likewise very small, so small in fact, that the noise inherent in photo-detectors is many times larger than the signals themselves. Second the reactants and products are in much greater concentrations than the radicals, typically by a factor of 10^3 to 10^4. In conventional spectroscopy any spectral overlap of reactant or product on a radical band would swamp the radical signal. The molecular modulation technique was devised to cope with these problems and, at the same time, provide information about radical reaction rates.

The technique is, in concept, similar to the phase-shift method of obtaining fluorescence life-times. A photolytic lamp is turned on and off so that the lamp output is a square wave. The frequency of the square wave is chosen to permit the radical concentration to reach approximately a steady value while the lamp is on and to decay to a near-zero value while the lamp is off. Thus the radical concentration and spectroscopic signal are given an A.C. component which can be extracted from the noise by using lock-in amplifiers with long time-constants. The flashing lamp also gives A.C. components to reactant and product concentrations. These components are generally less than one percent of the total concentration, mitigating to some extent the effect of spectral overlap. A flow system is used to make the periodic variations in reactant and product concentrations oscillate about stable D.C. levels.

The various species in a photo-chemical reaction not only have components at the frequency of the flashing lamp; they also have a rich harmonic content (see below). The harmonics which determine the wave shape (square, triangular, saw-tooth, etc.) are functions of the chemical kinetics. For example, a "first-order" radical, which decays by a process first order in the concentration of that radical, has no harmonics not present in the lamp flash. On the other hand, a "second-order" radical, which decays by a process second order in the radical concentration, has even harmonics not present in the lamp flash. A lock-in amplifier tuned to the frequency of the flashing lamp extracts the fundamental frequency, a fraction of the odd harmonics, and rejects all of the even harmonics (see Appendix A). Since the phase shift of the fundamental frequency is a strong function of chemical species and radical life-time, the necessary kinetic information can be obtained from just the fundamental frequency.

B. Mathematical Basis for the Method

The reaction scheme below illustrates the important types of chemical species in a modulation experiment. The species A through F are stable molecules; and X, Y, and Z are free radicals. The modulation of each species is a function of the type of species and of the elementary reaction rates.

$$A + h\nu \rightarrow 2X \qquad \text{(I)}$$

$$X + B \xrightarrow{k_1} Y + C \qquad \text{(II)}$$

$$Y + D \xrightarrow{k_2} Z + E \qquad \text{(III)}$$

$$Z + Z \xrightarrow{k_r} F \qquad \text{(IV)}$$

Since the concentrations of the species in the chemical system vary periodically in time, they can be represented by a Fourier expansion of the form

$$f(\omega t) = \sum_n a_n \sin(n\omega t) + b_n \cos(n\omega t) + b_o$$

where ω is the fundamental angular frequency of the wave obtained from the period T by the relation $\omega = 2\pi/T$. An alternative form of the Fourier expansion is:

$$f(\omega t) = \sum_n c_n \sin(n\omega t + \delta_n) + c_o.$$

The two are related by:

$$c_n = (a_n^2 + b_n^2)^{1/2} \text{ and } \delta_n = \tan^{-1}(b_n/a_n).$$

The coefficients c_n are amplitudes; the quantities δ_n are phase shifts. In the following analysis, the photolytic lamp is represented by an expansion involving sine terms only, i.e. all $b_n = 0$. Hence all $\delta_n = 0$. For any chemical species, then, δ_n is its phase shift relative to the photolytic lamp.

1. Reactant Decomposed by Light

The differential equation for A is:

$$\frac{d[A]}{dt} = \frac{f'}{V}[A]_o - \sigma[A]\left[\frac{I_o}{2} + \frac{2I_o}{\pi}\sum_{n,\text{odd}}\frac{1}{n}\sin(n\omega t)\right] - \frac{f'}{V}[A] \quad (1)$$

where f' is the flow rate into and out of the cell in liters/sec.

V is the volume of the cell in liters

$[A]_o$ is the concentration of A entering the cell in molecules/cm^3

I_o is the photon flux in photons/$cm^2 \cdot$sec

σ is the absorption cross-section of the reactant in cm^2/molecule

[a] is the concentration of A

ω is the flashing frequency in radians/sec

t is the time in sec

Since $\omega = 2\pi/T = 2\pi f$ where f is the flashing frequency in cycles/sec., we can write $\theta = \omega t = 2\pi f t$ from which we get $d\theta/dt = 2\pi f$ or $dt = d\theta/2\pi f$,

giving

$$\frac{d[A]}{d\theta} = \frac{1}{2\pi f} \frac{f'}{V}[A]_o - \sigma[A]\left(\frac{I_o}{2} + \frac{2I_o}{\pi} \sum_{n,odd} \frac{1}{n} \sin(n\theta)\right) - \frac{f'}{V}[A] \quad (2)$$

When the change in concentration over a flashing period is small compared to the total concentration ($\Delta[A] < 10^{-2}[A]$), [A] on the right side of the differential equation may be regarded as a constant. Collecting the D.C. terms gives

$$\frac{d[A]}{d\theta} = \frac{1}{2\pi f}\left(\frac{f'}{V}[A]_o - (\frac{\sigma I_o}{2} + \frac{f'}{V})[A] - \frac{2\sigma I_o[A]}{\pi} \sum_{n,odd} \frac{1}{n} \sin(n\theta)\right).$$

The requirement of a stable D.C. concentration means

$$\frac{f'}{V}[A]_o - (\frac{\sigma I_o}{2} + \frac{f'}{V})[A] = 0$$

which gives the following simplified differential equation

$$\frac{d[A]}{d\theta} = -\frac{2\sigma I_o[A]}{2\pi^2 f} \sum_{n,odd} \frac{1}{n} \sin(n\theta).$$

As long as the concentration modulation, $\Delta[A]$, is much smaller than the total concentration, [A], the equation is linear and is easily integrated[45] giving the concentration modulation

$$[A]_{mod} = \frac{\sigma I_o[A]}{\pi^2 f} \sum_{n,odd} \frac{1}{n^2} \cos(n\theta). \quad (3)$$

From the definition of phase shift, we see that the reactant concentration modulation has a phase shift of +90° with respect to the flashing lamp. The modulation of A is seen to be a triangular wave whose amplitude is inversely proportional to the flashing frequency.

2. Radical Formed by the Initial Photo-dissociative Step and Decaying by a Process First-order in Radical Concentration

The differential equation describing the radical concentration [X] in terms of the previously defined quantities σ,[A],ω, and I_o and the concentration of reactant B, is:

$$\frac{d[X]}{dt} = 2\sigma[A]\left(\frac{I_o}{2} + \frac{2I_o}{\pi}\sum_{n,odd}\frac{1}{n}\sin(n\omega t)\right) - k_1[B][X]^* \quad . \tag{4}$$

This can be solved in a straight forward manner like the previous case to yield:

$$[X] = \frac{2\sigma I_o[A]}{\pi^2 f}\sum_{n,odd}\left(\frac{k_1[B]}{2\pi f}\frac{1}{n}\sin(n\theta) - \cos(n\theta)\right)/\left(\left(\frac{k_1}{2}\frac{[B]}{\pi f}\right)^2 + n^2\right) + \frac{\sigma I_o[A]}{k_1[B]} \quad . \tag{5}$$

When this equation for [X], the radical concentration, is taken to its low frequency limit we get:

$$\lim_{f\to 0}[X] = \frac{4\sigma I_o[A]}{\pi k_1[B]}\sum_{n,odd}\frac{1}{n}\sin(n\theta) + \frac{\sigma I_o[A]}{k_1[B]} \quad . \tag{6}$$

This is the equation of a square wave with an amplitude of $\sigma I_o[A]/k_1[B]$ oscillating about a D.C. level of $\sigma I_o[A]/k_1[B]$. Thus the radical concentration has a maximum of $2\sigma I_o[A]/k_1[B]$ -- the radical concentration one obtains from the "steady-state" approximation for [X]. Note also that the phase shift of the radical concentration is 0°. At high frequencies we have:

$$\lim_{f\to\infty}[X] = \frac{2\sigma I_o[A]}{\pi^2 f}\sum_{n,odd} -\frac{1}{n^2}\cos(n\theta) + \frac{\sigma I_o[A]}{k_1[B]} \tag{7}$$

So [X] becomes a triangular wave with vanishing amplitude oscillating about a D.C. level equal to one-half the "steady-state" concentration. The phase shift is -90°.

It is convenient to define the "life-time" of the radical, X, to be

$$\tau_1 = \frac{1}{k_1 B}$$

* Strictly speaking the decay process includes a flow out term $(f'/V)[X]$, but usually $f'/V \ll k_1[B]$. If $f'/V \sim k_1[B]$, no real problem exists for $k_1[B]$ in the above equations can be replaced by $k_1[B] + (f'/V)$.

which is the time required for the concentration to drop by a factor of e. The behavior of the fundamental of [X] at intermediate flashing frequencies is plotted in Figure 1 as a function of the ratio of the flashing period (T=1/f) to the radical life-time.

The phase shift of the fundament of [X] is given by:

$$\delta = \tan^{-1}(b_1/a_1) = \tan^{-1}(-1/(K_1[B]/2\pi f)).$$

So

$$k_1[B] = \frac{-2\pi f}{\tan\delta} \quad .$$

Thus the radical life-time can be found from just one phase shift measurement at one frequency if the radical species is known to be formed in the initial step and to decay by a process first-order in radical concentration.

3. Radical Formed by a Radical-Molecule Reaction and Decaying by a Process First-Order in Radical Concentration

When a radical is formed by the reaction of a preceding radical, X, with a molecule, B, and is destroyed by reaction with another molecule, D, the differential equation describing the concentration of the new radical, Y, is:

$$\frac{d[Y]}{dt} = k_1[B]\,[X] - k_2[D]\,[Y] \quad . \qquad (8)$$

Integration of this equation after changing the variable from t to θ and substituting Eq. (5) for [X] gives

$$[Y] = \frac{\sigma I_o[A]}{k_2[D]} + \frac{2\sigma I_o[A]}{\pi^2 f}\,\frac{k_1[B]}{2\pi f}\sum_{n,\text{odd}}\left(\frac{k_1[B]k_2[D]-(2\pi fn)^2}{(2\pi f)^2 n^2((k_1[B]/2\pi f)^2+n^2}\sin(n\theta)\right.$$

$$\left. - \frac{k_2 D + k_1[B]}{2\pi f((k_1[B]/2\pi f)^2+n^2)}\cos(n\theta)\right)/((k_2[D]/2\pi f)^2+n^2 \quad . \qquad (9)$$

Since the coefficients b_n are always negative and the coefficients a_n may be either positive or negative depending on the sign of $k_1[B]k_2[D]-(2\pi fn)^2$, the phase shift of the fundamental of [Y] may lie anywhere between 0° and -180° . The dependence of the concentration modulation of Y on flashing frequency is determined by $k_1[B]$, $k_2[D]$, and f. A convenient way of looking at the modulation of Y is to plot the amplitude and phase shift of the

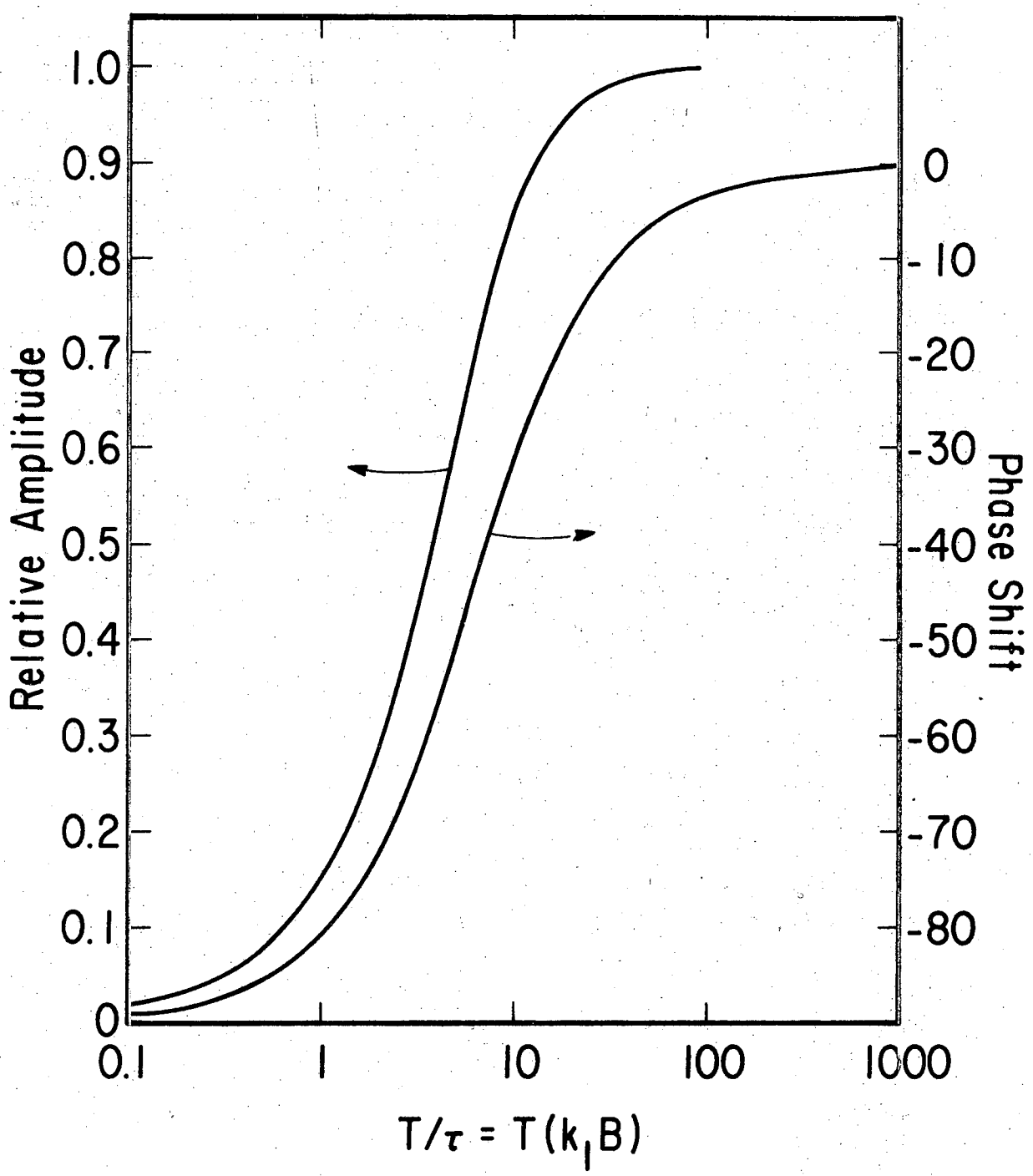

Figure 1. Dependence of the fundamental modulation frequency of a primary first-order radical on the ratio of flashing period to radical life-time. The amplitude is relative to the limiting amplitude as T/τ approaches infinity.

fundamental as a function of T/τ_1 for several values of τ_2/τ_1. This is done in Figures 2a and b. When τ_2/τ_1 is large, at frequencies where the primary radical X has a phase shift close to 0°, the secondary radical Y behaves like a primary radical. Under such conditions the life-time of Y can be easily obtained. When τ_2/τ_1 is small, however, determination of the life-time will be difficult because the phase shift of the secondary radical Y is determined, for the most part, by the phase shift of the preceding radical. At flashing frequencies high enough to impart a substantial phase shift to the secondary radical due to its own inherent life-time, the modulation amplitude of the preceding radical is very low. As a result, the modulation amplitude of the secondary radical is also very small making detection difficult.

4. Radical Which Decays by a Process Second-Order in Radical Concentration

The differential equation for the second-order radical Z is

$$\frac{d[Z]}{dt} = k_2[D][Y] - 2k_r[Z]^2. \qquad (10)$$

This equation is intractable because the equation is non-linear, and [Y] and [Z] are both functions of t. A numerical solution for [Z] can be readily obtained if the equation can be written in two parts, one corresponding to the lamp on and one to the lamp off, with [Y] a constant. This is the case when either the second-order radical is formed by the initial photo-dissociative step or by radical precursors that reach steady-state concentrations very quickly, i.e. their concentration modulations are square waves. Then the equations for [Z] are

$$\frac{d[Z]}{d\theta} = \frac{1}{2\pi f}\left(2\sigma I_o[A] - 2k_r[Z]^2\right) \quad \text{for } -\pi \leq \theta \leq 0 \qquad (11a)$$

and

$$\frac{d[Z]}{d\theta} = \frac{1}{2\pi f}\left(-2k_r[Z]^2\right) \quad \text{for } 0 \leq \theta \leq \pi \qquad (11b)$$

Each of these can be integrated giving

$$[Z]_\theta = \left(\frac{2\sigma I_o[A]}{2k_r}\right)^{1/2} \tanh \frac{(\theta+\pi)(2\sigma I_o[A]2k_r)^{1/2}}{2\pi f} \tan^{-1} \frac{[Z]_{-\pi}}{2\sigma I_o[A]/2k_r)^{1/2}} \qquad (12a)$$

when the lamp is on, and

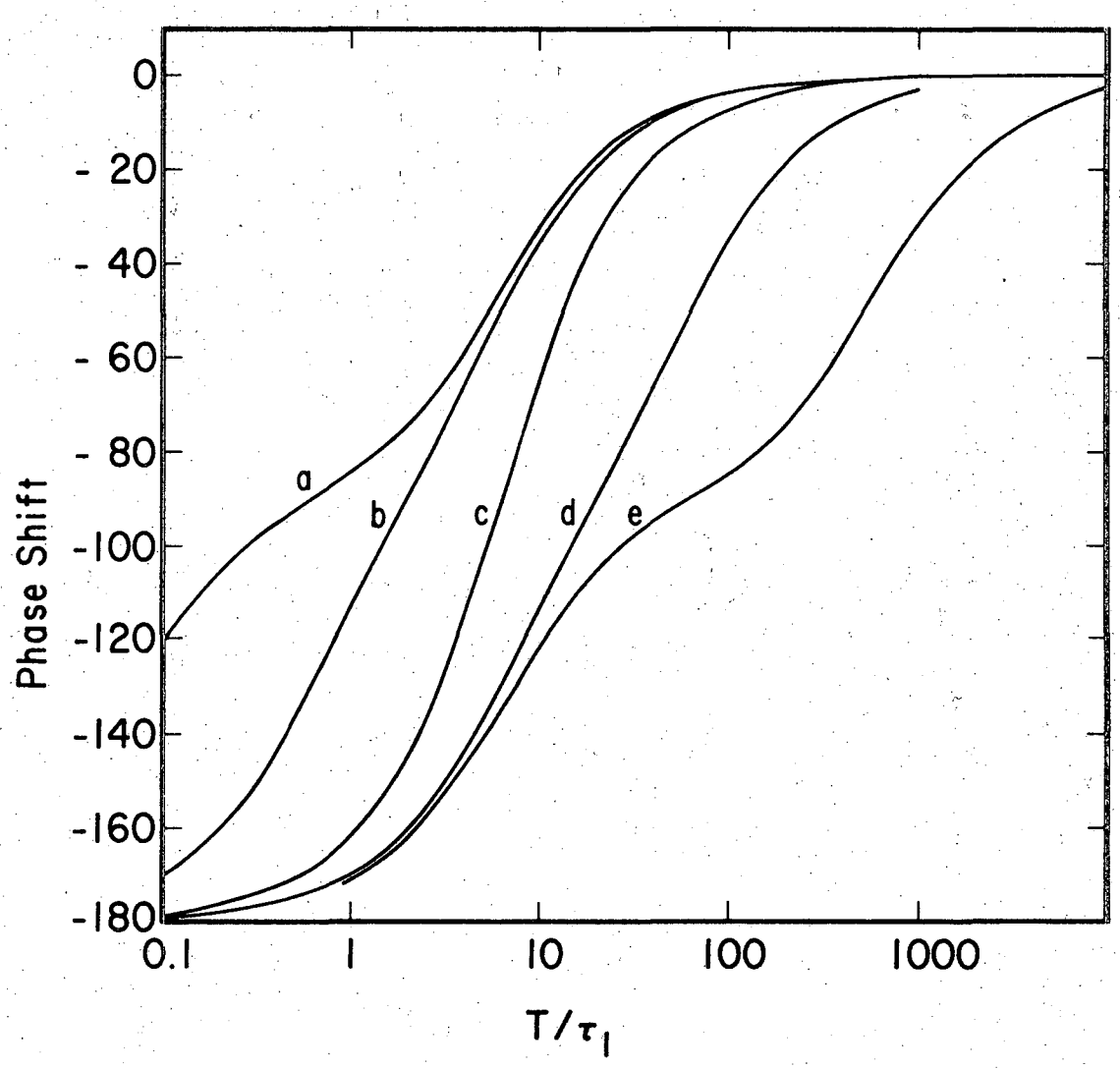

XBL 6910-5905

Figure 2a. The dependence of the modulation of a secondary radical on the ratio of its life-time to the life-time of the preceding radical.

a) $\tau_2/\tau_1 = 0.01$ b) $\tau_2/\tau_1 = 0.10$

c) $\tau_2/\tau_1 = 1.00$ d) $\tau_2/\tau_1 = 10$

e) $\tau_2/\tau_1 = 100$

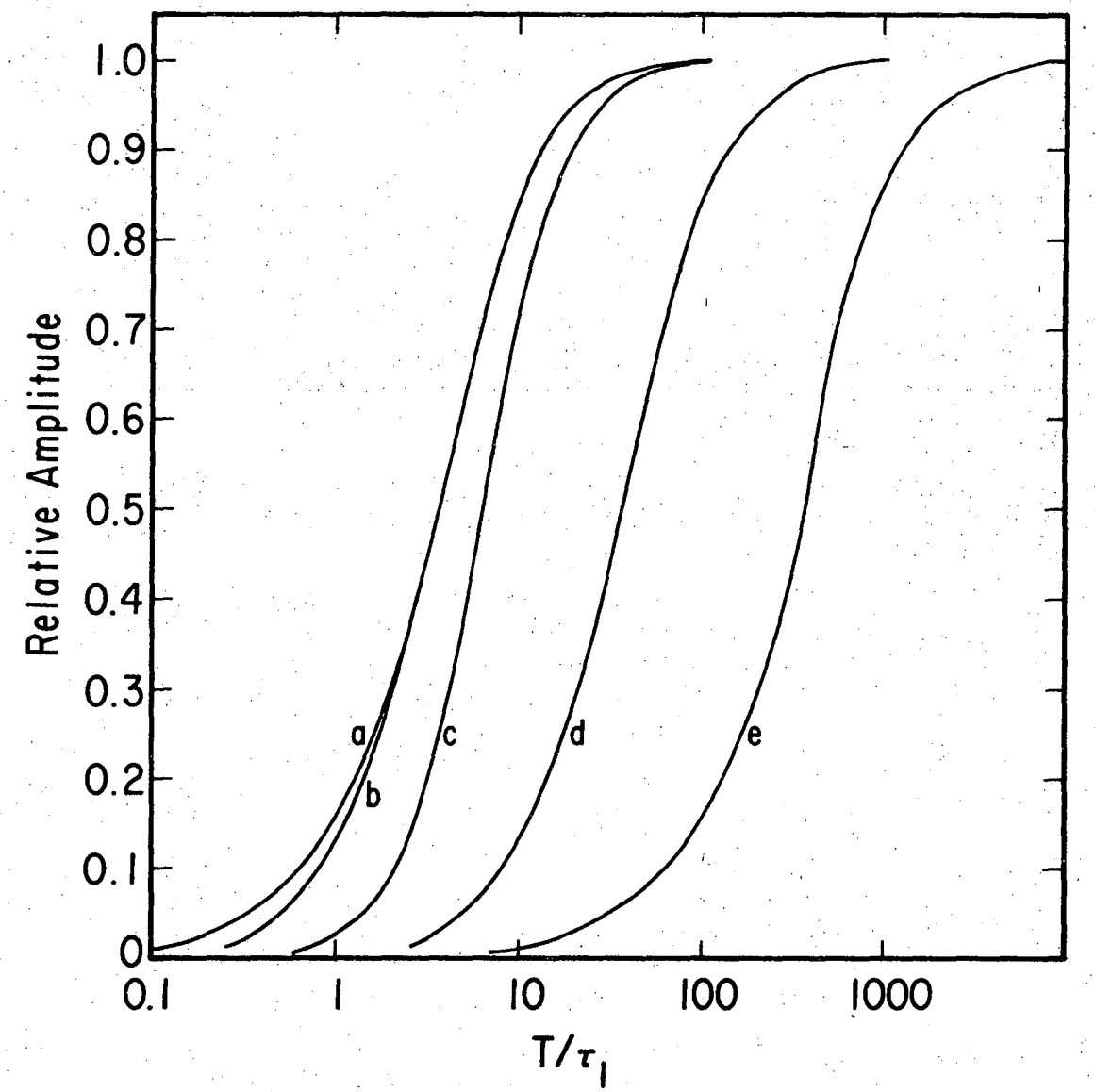

XBL 6910-5907

Figure 2b. Modulation amplitude relative to the limiting amplitude as T/τ_1 approaches infinity.

a) $\tau_2/\tau_1 = 0.01$ b) $\tau_2/\tau_1 = 0.10$

c) $\tau_2/\tau_1 = 1.00$ d) $\tau_2/\tau_1 = 10$

e) $\tau_2/\tau_1 = 100$

(12b) $$[Z]_\theta = \frac{2\pi f[Z]_0}{2\pi f + 2k_r\theta[Z]_0}$$ when the lamp is off.

Using these two equations, we may assume an initial value for $[Z]_{-\pi}$, calculate $[Z]_0$ and $[Z]_\pi$, set $[Z]_{-\pi} = [Z]_\pi$, and recalculate $[Z]_0$ and $[Z]_\pi$ until $[Z]_\pi = [Z]_{-\pi}$ within a desired degree of accuracy. Having found $[Z]_{-\pi}$, we then calculate [Z] for small increments of θ(e.g. $\Delta\theta = 2\pi/100$). The resulting table of $[Z]_\theta$ vs. θ provides the basis for the Fourier analysis of [Z]. For the periodic function

$$[Z] = \Sigma\, a_n \sin(n\theta) + b_n \cos(n\theta) + b_o/2 \qquad (13)$$

the coefficients a_n and b_n can be found by the numerical integrations

$$a_n = \frac{1}{\pi} \sum_{i=1}^{m} [Z]_{\theta_i} \sin(n\theta_i)\Delta\theta \qquad (14a)$$

$$b_n = \frac{1}{\pi} \sum_{i=1}^{m} [Z]_{\theta_i} \cos(n\theta_i)\Delta\theta \qquad (14b)$$

where m is the number of increments of θ. Such an analysis has been done over a wide range of flashing frequencies. The amplitude and phase shift behavior of the fundamental as a function of the ratio of flashing period to radical life-time is shown in Figure 3. Because the life-time of a second-order species depends on concentration, we define "the radical life-time" to be the half-life of the radical from its steady-state concentration. The steady-state concentration of the radical Z is

$$[Z]_{ss} = \left(\frac{2\sigma I_o[A]}{2k_r}\right)^{1/2} \qquad (15)$$

and the life-time becomes

$$\tau = \frac{1}{2k_r[Z]_{ss}} \quad . \qquad (16)$$

For convenience let us define the rate of radical formation P by

$$P = 2\sigma I_o[A]$$

and the rate constant of radical decay Q by

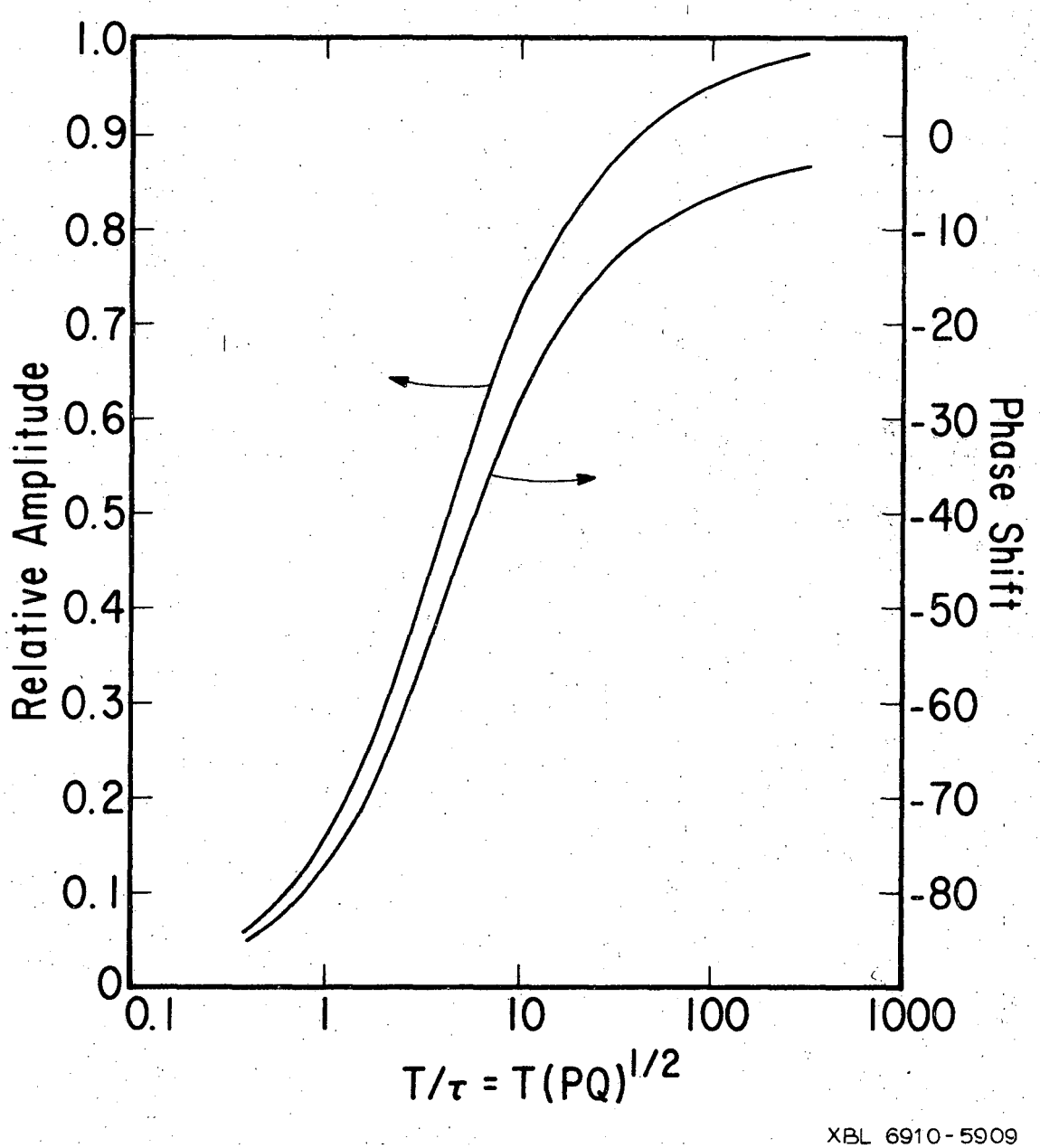

Figure 3. Concentration modulation of a record-order radical as a function of the ratio of flashing period to radical life-time. The amplitude is relative to the limiting amplitude as T/τ approaches infinity.

$$Q = 2k_r \tag{18}$$

Then

$$\tau = \frac{1}{(PQ)^{1/2}} \tag{19}$$

Comparison of the life-time formulae for the first- and second-order radicals indicated how these kinetically different radicals can be distinguished experimentally. The life-time of a first-order radical, given by

$$\tau = 1/k_1[B] \quad , \tag{20}$$

is independent of radical formation rate and inversely proportional to the concentration of a reactant involved in the radical's decay. The life-time of a second-order radical given by

$$\tau = 1/(PQ)^{1/2} \quad , \tag{21}$$

is inversely proportional to the square-root of the radical formation rate. Changes in reactant concentration affect the life-time only by affecting the radical formation rate. Thus varying reactant concentrations and the photolytic light intensity can provide the information necessary to determine whether the radical decay reaction is first or second order in radical concentration.

5. Products of Radical Reactions

The differential equations describing the behavior of the products C, E, and F all have the same general form:

$$\frac{dJ}{d\theta} = \frac{k'}{2\pi f}\left(G + H \Sigma \alpha_n \sin(n\theta) + \beta_n \cos(n\theta)\right) - \frac{f'}{V} J \tag{22}$$

where $J = [C]$, $[E]$, or $[F]$

$k' = k_1[B]$, $k_2[D]$, or k_r

G = the D.C. level of $[X]$, $[Y]$, or $[Z]^2$

and H = the modulation amplitude of $[X]$, $[Y]$, or $[Z]^2$.

The solution to this equation is

$$J = k'G\frac{V}{f'} + \frac{k'H}{2\pi f}\sum_{n,\text{odd}}\left\{[(\alpha_n\frac{f'}{2\pi fV} - n\beta_n)\sin(n\theta) + (\beta_n\frac{f'}{2\pi fV} + \alpha_n)\cos(n\theta)]/[(f'/2\pi fV)^2 + n^2]\right\}. \quad (23)$$

From this equation it is apparent that if $f'/2\pi fV \ll 1$, the product fundamental lags the radical fundamental by 90°. Note also the inverse dependence of the product modulation amplitude on flashing frequency. This means that a product amplitude falls off faster with increases in flashing frequency than does that for a radical. The amplitude and phase shift behavior of the product of a second-order radical is presented in Figure 4.

6. Reactant Attacked by a Radical

The differential equation for a reactant B which is attacked by a radical if of the same form as the equation in Sec. 5 with two minor differences: there is a flow-in term $(f'/V)[B]_o$ and a change in sign because molecules are being lost through reaction. The solution shows that the reactant modulation leads the radical by 90°. Also the reactant amplitude has the same frequency dependence as a product, i.e., it falls off faster than a radical with increases in flashing frequency.

All of the above results are summarized in plots of modulation amplitude and phase shift on polar coordinates (Figure 5). The ratio of radical life-time to flashing period is implicit in the plots; the only explicit notation is "fast" and "slow" indicating the rate of radical reactions relative to the flashing frequency. This picture is useful for the identification of species responsible for an observed modulation because it recapitulates the general results: the concentration modulation of primary radicals always lies in the fourth quadrant; the modulation of secondary radicals may lie in either the fourth or the third quadrant,

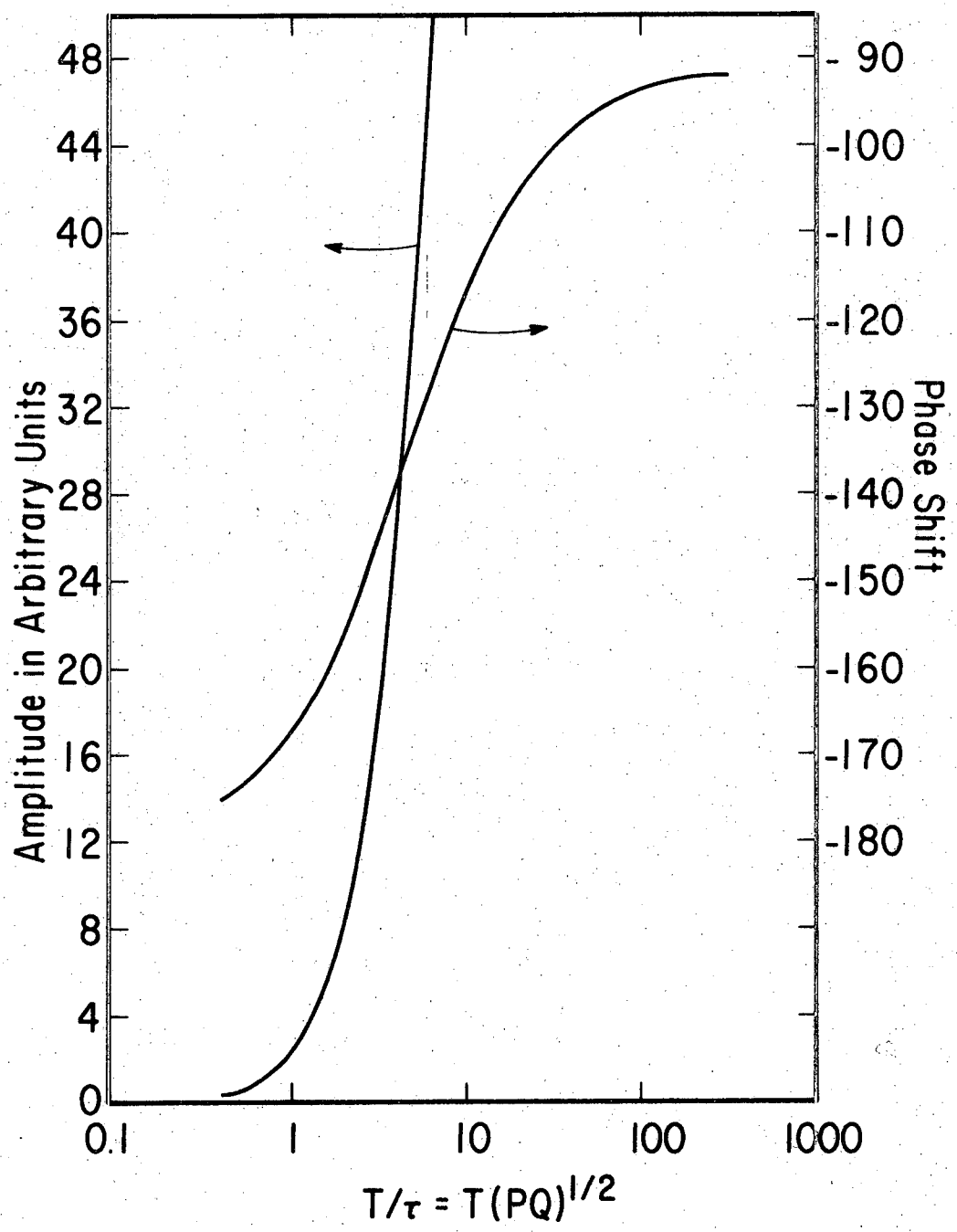

Figure 4. Concentration modulation of the product of a second-order radical as a function of the ratio of the flashing period to life-time of the radical forming the product. Note the strong dependence of amplitude on T/τ.

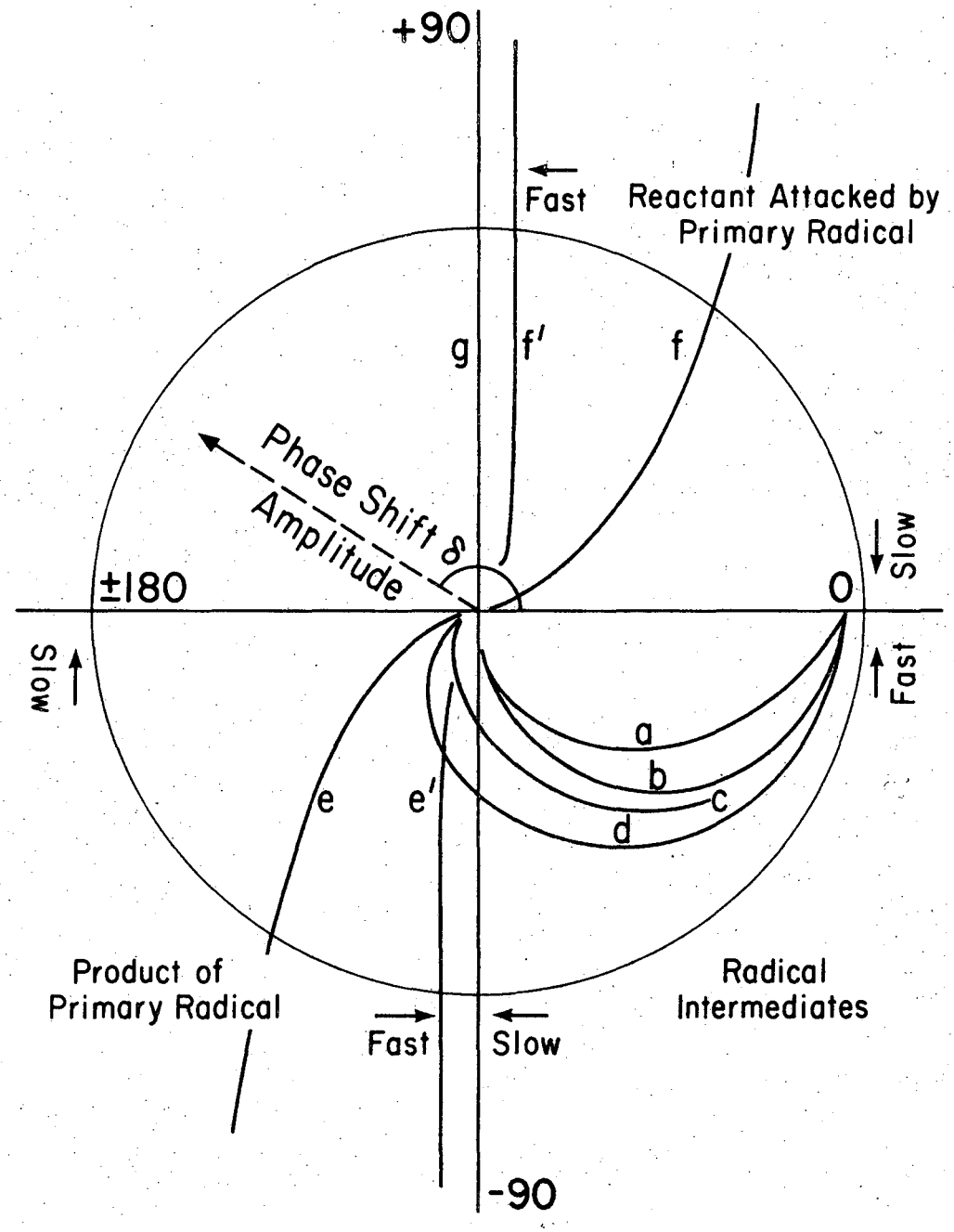

XBL 6910-5894

Figure 5. Summary of the amplitude and phase shift behavior of the species examined in this section. a) Primary first-order radical; b) Primary second-order radical: c) Secondary first-order radical, $\tau_2/\tau_1 = 1.0$: d) Secondary first-order radical, $\tau_2/\tau_1 = 10$: e) Product of a primary second-order radical: e') Product of a primary second-order radical, amplitude of product multiplied by 0.1: f) Reactant attacked by primary first-order radical: f') Reactant attacked by a primary first-order radical, amplitude of reaction multiplied by 0.1: g) Reactant decomposed by absorption of light.

products lag their radical precursors by 90°, and reactants attacked by radicals lead the radicals by 90°. There are other possible, but less general, cases (not shown) such as a reactant which is destroyed by the light and regenerated by subsequent radical reactions or a reactant which is destroyed by both light and radical attack. In a later section the first of these possibilities is treated quantitatively for a specific mechanism in which a reactant that is also a product has a concentration modulation lying in the second quadrant. The utility of Figure 5 is limited to qualitive interpretation of modulation features, for the figure lacks the detail necessary for extraction of rate constants. For this latter purpose, it is necessary to use the earlier graphs of amplitude and phase shift as functions of T/τ.

C. Apparatus

The two molecular modulation spectrometers used in this work are complex. The spectrometer used in the ultraviolet has been described by Morris.[11] Only two points need to be made about this apparatus. One, the photolysis lamps he used were replaced by mercury resonance lamps made by General Electric, Model G64T6. Second, all flashing frequencies refered to in the ultraviolet work are nominal; the true frequencies are 1.22 times the nominal frequencies.

The infrared modulation spectrometer is diagramed in Figure 6. The basic spectrometer is a Beckman IR-7 equipped with an external detector attachment. The detectors are: mercury doped germanium cooled to liquid helium temperature (4°K) for use from 800 to 3000 cm^{-1} and lead sulfide cooled to acetone-dry-ice temperature (193°K) for use between 3000 and 4000 cm^{-1}. Both detectors were obtained from Santa Barbara Research Center, Goleta, Calif.

The detector dewars were designed in this laboratory to facilitate interchange of detectors and to provide control over the field of view of the mercury-germanium detector. Restriction of the amount of background radiation striking the detector is important in optimizing the detectivity. With our optics we were able to restrict the field of view of the detector to 20° by a liquid nitrogen cooled heat shield, and thereby gain a factor of 2.5 in detectivity over the unshielded detector which had a field of view of 60°. Even with this reduction in background radiation, the major source of noise in our system is either internal noise in the detector or shot noise in the background.

The reaction cell is two meters long and about forty cm. in diameter,

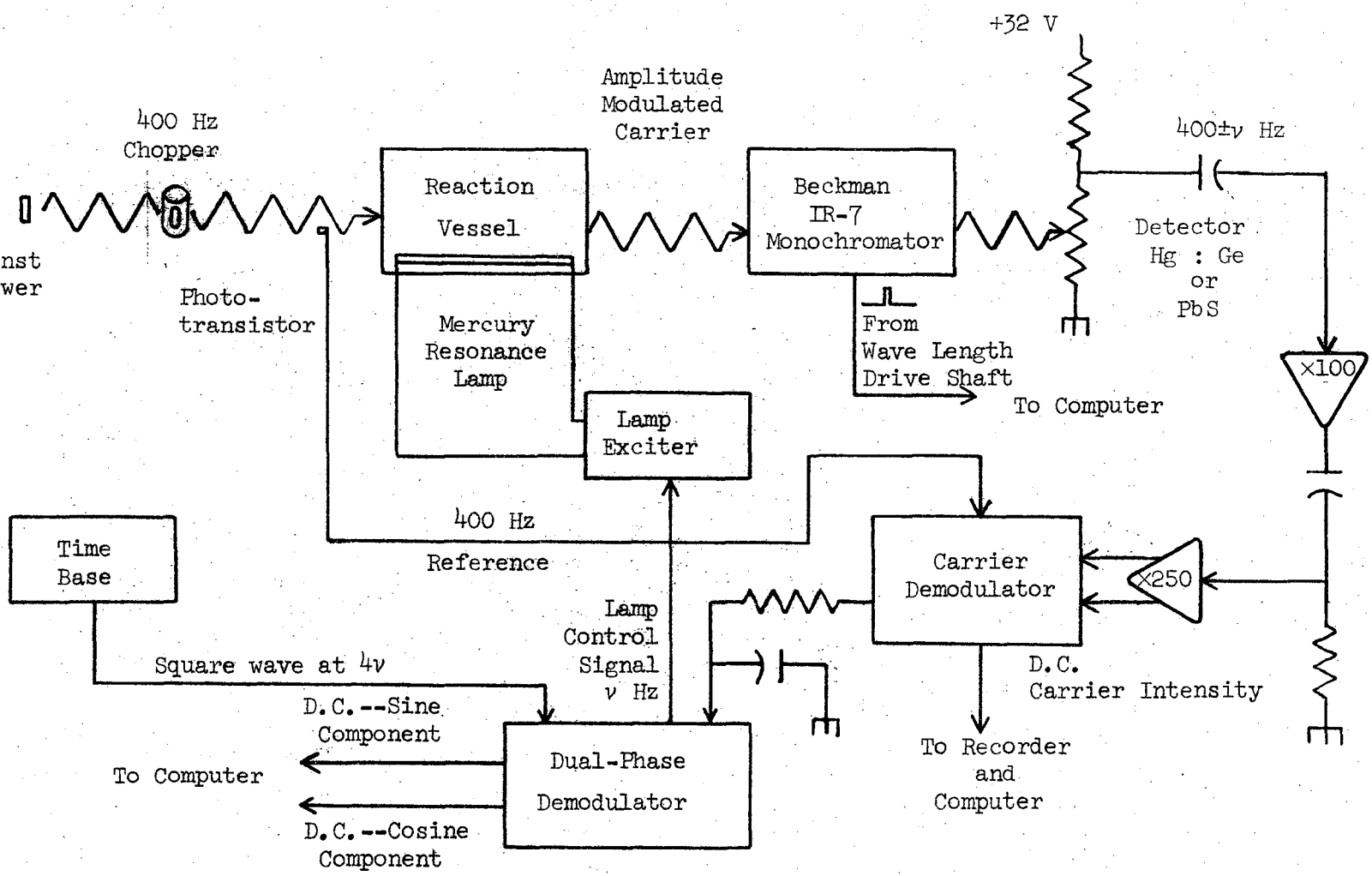

Figure 6a. Block diagram of apparatus.

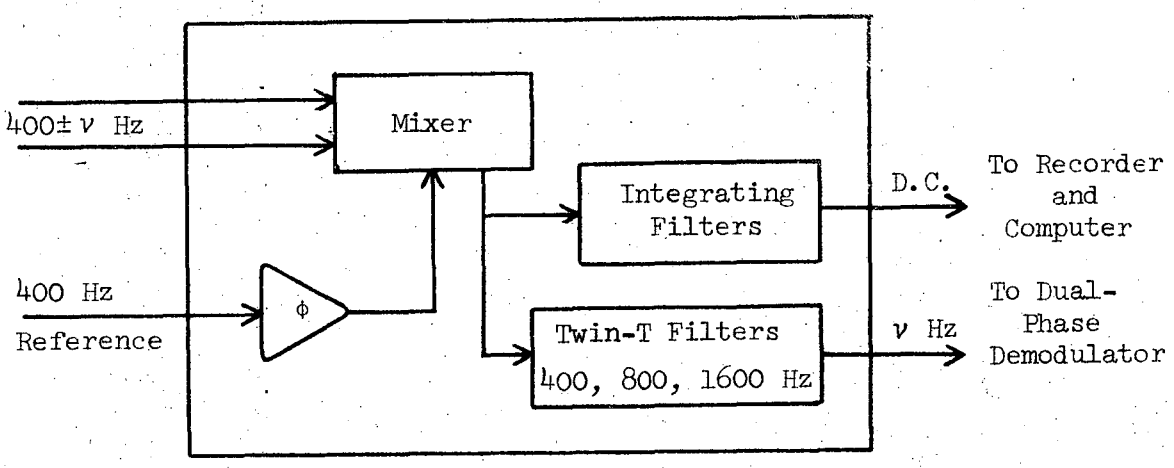

Figure 6b. Carrier demodulator.

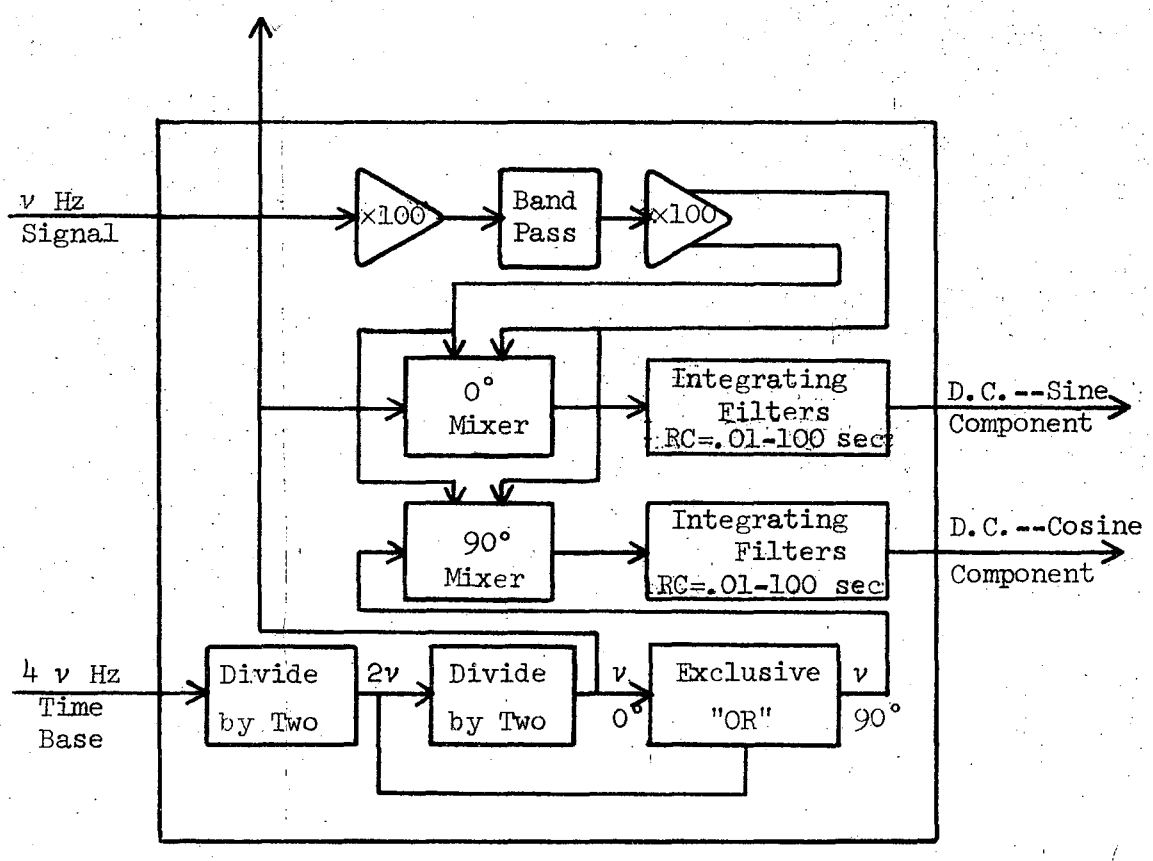

Figure 6c. Dual-phase demodulator.

having a capacity of 270 liters. The cell is equipped with gold multiple reflection mirrors to give an optical path variable from 8 to 80 meters. The path length was adjusted to give maximum signal for radicals. The conditions for optimization can be found from Beer's Law which relates the transmitted light intensity I through a cell containing radiation absorbers to the beam intensity I_o transmitted by the empty cell, the concentration of absorbers n, the path length l, and the cross-section for absorption σ. That is

$$I = I_o e^{-\sigma n l}. \tag{24}$$

When the concentration is small enough for the quantity (σnl) to be much less than one, the equation becomes

$$I = I_o(1 - \sigma n l) \tag{25a}$$

and

$$I \cong I_o. \tag{25b}$$

For changes in concentration Δn, the transmission varies from I to I'. Application of Beer's Law gives

$$\frac{I'}{I} = e^{-\sigma \Delta n l} \tag{26}$$

and since $\sigma \Delta n l << 1$

$$\frac{I'}{I} = 1 - \sigma \Delta n l. \tag{27}$$

Rearrangement provides the result

$$\sigma \Delta n l = \frac{I - I'}{I} = \frac{\Delta I}{I} \tag{28}$$

and

$$\Delta I = I(\sigma \Delta n l) \cong I_o(\sigma \Delta n l) \tag{29}$$

Thus the maximum ΔI for a given Δn occurs when $I_o \cdot l$, the light transmitted by the empty cell multiplied by the optical path, is maximized. This

condition is met at a path length of 48 meters.

Inside the reaction cell there is a low-pressure mercury resonance lamp manufactured by General Electric, Model G64T6. The lamp draws a nominal 64 watts of power, and the manufacturer claims an output of 44% of the input power concentrated in the 2537 A° mercury resonance line. This amount of power gives an intensity at the middle of the cell of approximately 5×10^{15} photons/$cm^2 \cdot$sec. The lamp is turned on and off by an electronic switch that puts 650 volts across the electrodes of the lamp. This voltage is sufficient to fire the lamp within one milli-second after it is applied, making the time asymmetry of the lamp's output less than 1%.

The infrared beam is chopped by a rotating cylindrical chopper at 400Hz before entering the reaction cell. A photo-transistor monitors the chopped I.R. beam and provides a phase-locked 400 Hz reference. As the beam passes through the cell, its intensity is modulated by absorption by the species whose concentrations are varying in response to the flashing lamp. The beam emerging from the cell passes through the Beckman monochromator before impinging on the detector. The signal produced at the detector consists of a 400 Hz voltage with a small amount of amplitude modulation at the flashing frequency. The amplitude of the 400 Hz carrier is proportional to the average I.R. intensity while the modulation amplitude is proportional to the changes in intensity due to concentration modulations. Since the amplitude modulation introduces side bands at $400 \pm \nu$ Hz, information about a chemical process occurring at a low frequency of less than ten cycles/sec. is carried at frequencies near 400 Hz --well beyond the point where the 1/f noise in electronic components is serious and far removed from any false signals which might arise from

the lamp flasher and associated electronics.

From the detector the signal passes through several stages of amplification and high-pass R-C filters. Then the 400 Hz carrier and its sidebands are mixed with the 400 Hz reference in the Carrier Demodulator producing a D.C. voltage proportional to the average infrared energy striking the detector and an A.C. voltage at the flashing frequency proportional to the concentration modulation.

The low-frequency voltage is still very small, less than one millivolt, and is submerged in noise. It passes through more filters-- primarily to discriminate against the odd harmonics-- and receives additional amplification. A pair of mixers operating 90° apart in the Dual-Phase Demodulator rectify the signal and extract the sine and cosine components of the fundamental frequency. These D.C. voltages go through R.C. integrating filters with ten second time constants to reduce noise fluctuations, but even under favorable conditions this is insufficient. At this point signal-to-noise ratios are approximately 1:1, and more integration time is needed.

The reference voltages driving the two mixers should be very symmetrical with respect to time and they must be exactly 90° apart. These conditions are met by frequency-dividing a square wave at four times the flashing frequency (4ν) in two steps. The resulting square waves at 2ν and ν are perfectly symmetrical. The square wave at frequency ν provides the reference for the "in-phase" mixer and is used to switch the photolytic lamp. The quadrature reference is derived from an "exclusive or" circuit operating on square waves at 2ν and ν, and thus is forced to be perfectly symmetrical and exactly 90° out of phase with the "in-phase"

reference.

D. Computer Coupling

In order to increase the integration time beyond 30 seconds or so, it is desirable to use some form of digital recording. One technique is to couple a digital computer to the experiment and have the computer perform the digitizing and averaging functions.

The Department of Chemistry owns an SDS 910 computer which is especially designed for connection with an experimental apparatus. It has provision for: (1) reading analog voltages and storing the digital equivalent, (2) converting a number to an analog voltage, (3) testing for certain conditions in the laboratory, and (4) sending pulses to the laboratory to set switches or otherwise direct the apparatus. All of these functions plus the standard computational facilities of a digital computer are available upon demand from an experimental apparatus. A demand for service is made by generating a pulse in some manner by the apparatus. The response is fast and usually within a couple of milliseconds the computer has performed the functions requested of it. Because of the potential for interplay implicit in the above four special functions, the degree of interaction between the experiment and the computer is limited only by the ingenuity of the experimenter.

The system used in this experiment consists of the hardware connections between the apparatus and the computer and the program which directs the computer's operations. The hardware connections include three analog lines which tie the carrier Demodulator and Dual-Phase Demodulator to the analog-to-digital converter of the computer, two lines connecting the computer's digital-to-analog converter to a pair of strip-chart recorders

in the laboratory, seven switches to direct the execution of the program, and the priority-interrupt line. A flow chart indicating the main features of the program is shown in Figure 7.

Access to the computer is gained by a pulse generated by a cam and micro-switch assembly on the wave-length drive shaft of the spectrometer. In the normal mode of operation the service pulse originating at the spectrometer causes the computer to read and store the three D.C. voltages presented by the Dual-Phase Demodulator and the Carrier Demodulator. Since the service pulses are generated by the wave-length drive shaft, the computer regularly samples the signals as the spectrometer scans and constructs a spectrum in digital form. One of the switches in the laboratory, when set, directs the computer to prepare to read in another spectrum and add it to the one just obtained. In this way several spectra can be averaged together to improve the signal-to-noise ratio. The noise is reduced by the square root of the number of scans in the average.

The process of averaging many scans is very time consuming and no more spectra should be taken than are necessary to characterize the spectrum. Therefore, the program has provision to calculate averaged amplitude and phase shift spectra and convert them to analog voltages for display on a strip chart recorder in the laboratory. Another program, very similar to the first permits a long-time average to be made with the spectrometer set to one infrared frequency. In this mode of operation, the computer calculates a cumulative average of the data after each new data point is read. The average is continuously displayed on the recorder in the laboratory. This second program is used for the kinetic analysis of absorption bands identified in the spectra.

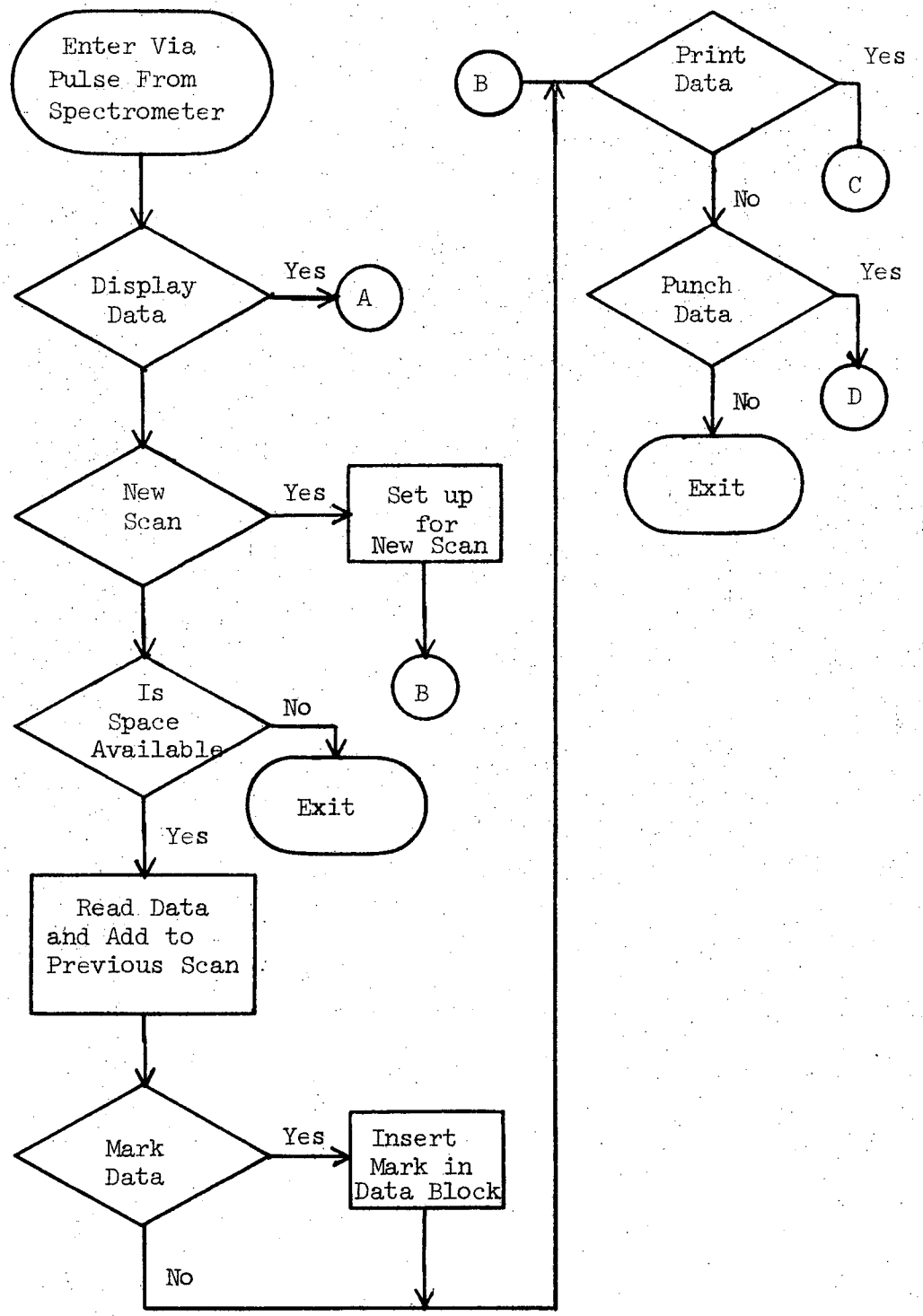

Figure 7. Flow diagram of data acquisition program.

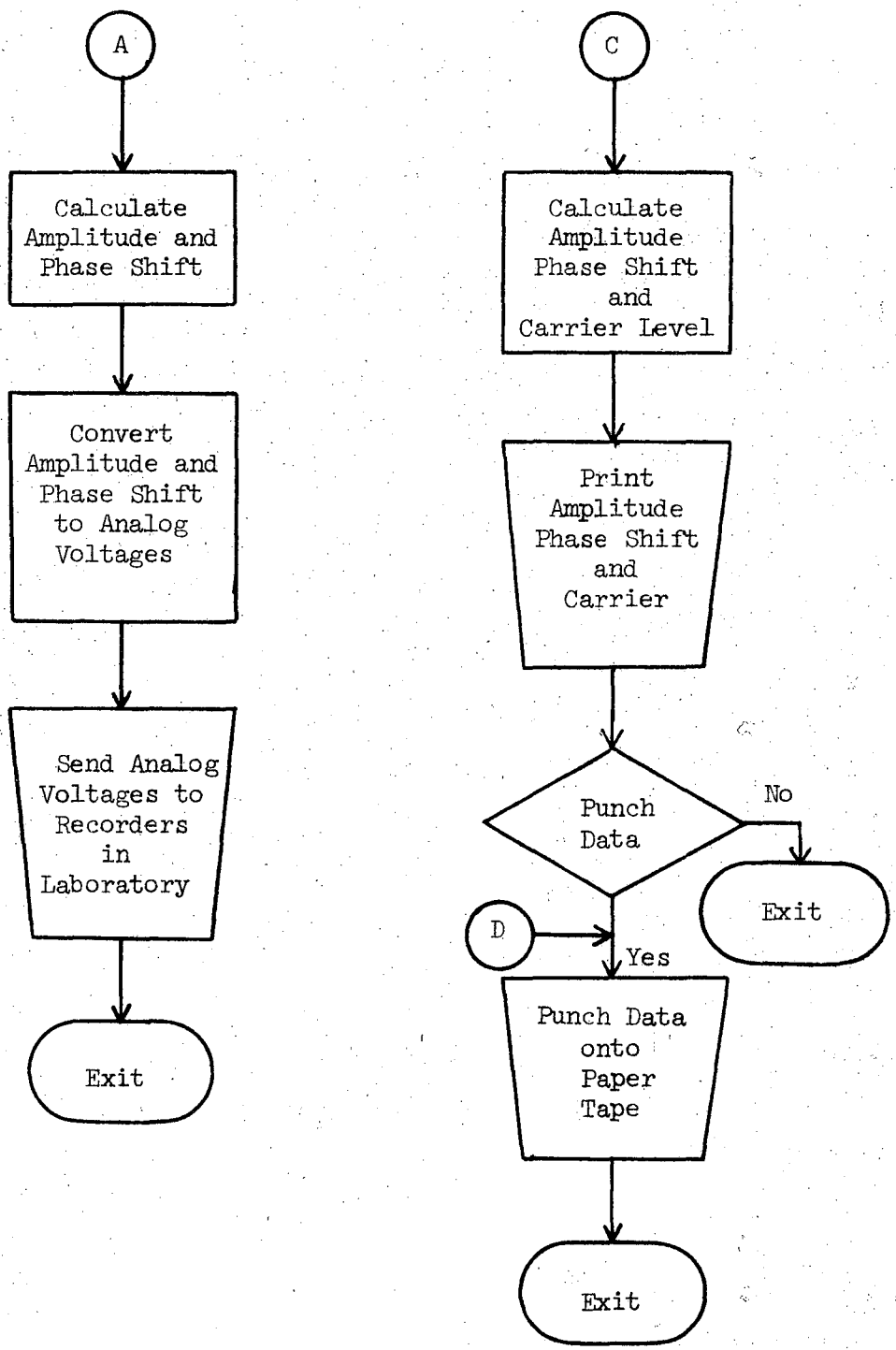

Figure 7. (continued)

E. Noise Reduction by Curve Smoothing

It has been pointed out by Sevitzky and Golay[47] that time independent data taken from basically continuous physical experiments are not truly independent by virtue of the continuity of the physical property being measured. This fact can be used to further reduce noise without unduly degrading the underlying information. The technique, basically, is to average points on either side of a data point together with the data point to derive a new value for the data at that point. As a consequence of the averaging procedure, noise is reduced. Some degradation of information may also occur. The amount of noise reduction and information loss depends on the averaging function employed and on the number of points included in the average. The simplest of this kind of procedure is the moving average, in which an odd number of the original data points, weighted equally, are added together and the sum is divided by the number of points in the sum. The average value is taken to be the new ordinate of the center point. The process is repeated advancing the central point one point. For this technique to work, the data must, of course, be taken at equal intervals.

More elegant averaging functions may be used by weighting the points in the average differently according to their positions relative to the center point. Sevitzky[47] has derived the weights for quadratic, cubic, and quartic averaging functions. The higher order averaging functions degrade the information less, but also reduce the noise less. Brubaker and Stevens[48] have derived the noise reduction factors to be expected for various averaging functions depending on the order of the function and the number of points included in the average. Their results clearly show the superiority of the moving averaging for noise reduction.

Care must be exercised in using the moving average, however. If the number of points in the average is too large, signal as well as noise will be reduced. For this reason, the number of points in our work was kept small. In regions of the spectrum where nine or more data points were taken per spectral slit width, no more than five points were included in the average. In regions where there were less than nine data points per slit width, the number of points in the average was restricted to three.

The degradation of information can best be evaluated by considering the effect of the curve smooth on the spectral slit width. An ideal slit function is triangular, and a moving average curve smooth will round off the top. The spectral spread at half-height is widened, but as long as the number of points in the curve smooth is less than the number of points per slit width the widening effect is less than twenty percent. (See appendix D for details.) Since a real slit function has a rounded peak, the effect of the curve smooth on peak height is less. The small loss in resolution is compensated by an improvement in the signal-to-noise ratio. The noise is reduced by the square root of the number of points in the average.

F. Calibration of the Instruments

1. Infrared System

Since the low frequency signals leaving the Carrier Demodulator pass through filters to reject harmonics, some phase shift and attenuation of the fundamental frequency is inevitable. Consequently, it was necessary to calibrate the system using modulation signals of known amplitude and phase shift. An electronic modulator was used to introduce a known amount of amplitude modulation to a 400 Hz square wave. This simulated

signal was then processed exactly like a signal arising in the detector. The phase shift and the relative amplitude response of the system at the various flashing frequencies was determined from the D.C. voltages presented by the Dual-Phase Demodulator.

The absolute gain of the system need be measured at only one frequency. It is related to the degree of modulation and the observed D.C. voltages by the equation:

$$\frac{\Delta I}{I} = \frac{\pi(V_{m,P}^2 + V_{m,Q}^2)^{1/2}}{V_c g} \qquad (30)$$

where $V_{m,P}$, $V_{m,Q}$, and V_c are the D.C. voltages presented by the "in-phase" and quadrature channels of the Dual-Phase Demodulator and the Carrier Demodulator; g is the system gain; and $\Delta I/I$ is the degree of modulation. (This formula is derived in Appendix A.) When $\Delta I/I$ is known and the D.C. voltages have been measured, the gain is easily acquired. At 1 Hz it is 4.7×10^3.

2. Ultraviolet System

The calibration of the ultraviolet system was accomplished in essentially the same manner. First of all, the relative response of the system at the various flashing frequencies was determined. All amplitudes in this paper are "frequency normalized" so that a square wave modulation of 2×10^{-3} produces an amplitude of 10,000 counts. Since the experimental apparatus extracts only the fundamental component of the square wave, it will be convenient to have an expression relating the amplitude (frequency normalized) to the modulation at the fundamental frequency.

All experiments were done at the same carrier level V_c and the same gain so the relation between the observed amplitude and the degree of

modulation can be written:

$$V_m = (V_{m,P}^2 + V_{m,Q}^2)^{1/2} = k \frac{\Delta I}{I} \qquad (31)$$

where k is a proportionality constant. This constant was evaluated by observing the amplitude V_m for a square wave modulation of 2×10^{-3}. Since the fundamental amplitude is larger than the square wave by a factor of $4/\pi$, the degree of modulation $\Delta I/I$ at the fundamental frequency is $8/\pi\times10^{-3}$. Since the amplitude V_m is 10,000 counts

$$k = \frac{10{,}000}{8/\pi\times10^{-3}} = 3.93\times10^{6}. \qquad (32)$$

G. Chemicals and Procedure

The chemicals used in these experiments were hydrogen peroxide, ozone, and helium. The liquid hydrogen peroxide was obtained from the Becco Chemical Division of FMC Corp. in 98% purity and was used without further purification.

Ozone was produced by an electrical discharge through oxygen. The oxygen had been purified by passing over hot copper turnings to oxidize any hydrocarbon impurities; an ascarite trap removed CO_2; and finally the oxygen was dried by a trap cooled by Dry-Ice and by a P_2O_5 column. The ozone in the oxygen stream was about 1%. The separation of ozone and oxygen was accomplished by adsorption of ozone on silica gel. Cook et al.[48] have described measurements of the adsorption of ozone on silica gel over a wide range of temperatures and ozone pressures. Safety tests showed ozone to be quite stable at temperatures lower than -78°C. Our experience confirms this; no safety problems were encountered as long as the ozone was kept at Dry-Ice temperature. At higher temperatures explosions are possible.

The silica gel was 6-12 mesh chromatographic gel obtained from Matheson, Coleman and Bell. The helium used as a carrier gas in these experiments came from Air Reduction Co. in purity exceeding 99.995%.

The reactants were carried into the cell by a stream of helium gas. Helium passed over liquid hydrogen peroxide in a saturator at a flow rate of 8400 cm^3/min. The temperature of the saturator was maintained at 25°C; saturation was very nearly complete as evidenced by slight condensation in the flow lines at room temperature, approximately 22°. When ozone was also used, it was carried by a slow stream of helium joining the main stream just before the entrance to the cell. Maintaining a stable ozone concentration in the cell proved to be difficult and required frequent adjustment of the flow rate of the helium picking up the ozone. The concentration of hydrogen peroxide was set by its vapor pressure and the rate of decomposition in the cell and at the walls of the cell and glass lines leading to the cell.

After about 45 minutes of flowing the reactants into the cell and illuminating the mixture with the flashing lamp, the reactants had reached fairly stable concentrations, and the measurements were begun.

The measurements were of two kinds: scan experiments and kinetic experiments. During the scan experiments, repetitive sweeps through an infrared region were averaged to reduce the noise to a level permitting the identification of absorption bands. These sweeps were carried out with the scan speed of the spectrometer set so that one data point was read every ten seconds, and the time constants of the integrating filters at the output of Dual-Phase Demodulator were set to ten seconds. Sampling the signal once each time constant results in data points that

are not completely independent in time, and some R-C tracking error is introduced. This error affects both peak height and peak position; its magnitude can be calculated by methods described in the Beckman IR-7 operations manual. Under our conditions tracking distortion does not exceed 4% in peak height and 2 cm^{-1} in peak position. Absorption bands which are wider than the resolution of the instrument are distorted less. As long as R-C filters are used on the outputs of the Dual-Phase Demodulator, the tracking error can be reduced only at the expense of integration time. In this experiment integration time is far more important so the error is tolerated.

After the absorption bands have been located, it is possible to study them kinetically. This done by setting the spectrometer to the peak of an absorption band and measuring the modulation signal as a function of flashing frequency. The signal at any combination of infrared frequency and flashing frequency can be averaged for long time, up to 40 minutes, to enhance the signal. The flashing frequency range 1/4 Hz to 4 Hz can be covered. The high frequency limit is imposed by low signal levels; the low frequency limit by the difficulty in making electronic circuits operate correctly.

The procedure in using the ultraviolet molecular modulation spectrometer is slightly different. Since the volume of the cell is only 30 liters the time required to attain stable reactant concentrations is reduced by almost a factor of ten. The higher photolytic light intensity permits the extension of the frequency range to 16 Hz. The spectra were obtained incrementally at 50 A° intervals instead of continuous sweeps.

H. Hydrogen Peroxide Concentrations During the Kinetic Experiments

1. Measurements in the Infrared Cell

The concentration of hydrogen peroxide was obtained from absorbance measurements in our cell and the coefficient of absorption reported by Giguere.[50] Giguere's work was done at five, ten, and fifteen millimeters pressure of H_2O_2 with a slit width of 13 cm^{-1}. Our measurements were done with less than one millimeter pressure of H_2O_2 in an atmosphere of helium in a flow system. The slit width of our spectrometer during these measurements was 20 cm^{-1}, the path length was 72 meters. Visual inspection of our spectra (Figure 8) compares well with the spectrum published by Giguere.

The infrared spectra of hydrogen peroxide and water were obtained in the region 3000 to 4000 cm^{-1} under the conditions of the kinetic experiments. From the transmission curves and the background intensity, the absorbance was calculated at 3600 and 3865 cm^{-1}. The absorption at 3600 cm^{-1} is primarily due to hydrogen peroxide, but there is some water contribution. The water contribution was determined from the absorbance of water at 3865 cm^{-1} and the ratio of absorption by water at 3600 cm^{-1} to that at 3865 cm^{-1} found from the water spectrum in Figure 8. Table I summarizes the data. The hydrogen peroxide concentration, calculated from Beer's law and the coefficient of absorption reported by Giguere was $5 \pm 2 \times 10^{15}$ molecules/cm^3.

2. Measurements in the Ultraviolet Cell

After each kinetic experiment the spectrometer was set to 2000 A , the transmitted light intensity I was noted, and the cell was closed and the lamp(s) turned on until all of the peroxide was decomposed. The final

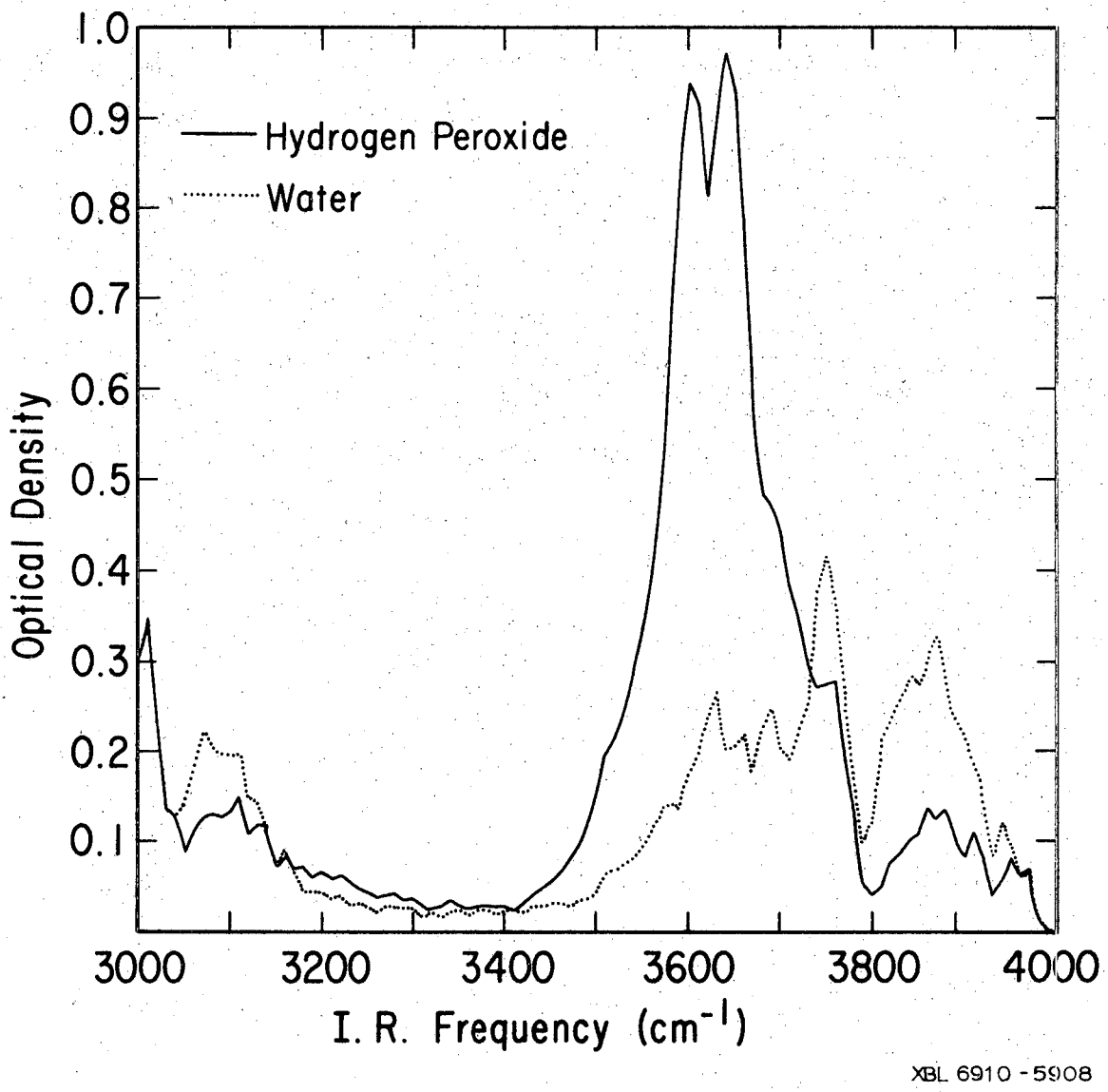

Figure 8. Absorption spectra of hydrogen peroxide and of water obtained in this Laboratory by conventional spectroscopy.

light intensity I_o through the cell was recorded. The hydrogen peroxide concentration was calculated from the absorbance and the absorption coefficient reported by Holt et al.[51] The value of the absorption coefficient-- 52.1×10^{-20} cm^2/molecule-- was read from their graph. The concentration during the one-lamp experiment was 1.13×10^{16} molecules/cm^3; during the two-lamp experiment it was 8.5×10^{15} molecules/cm^3.

TABLE I. Data Used for the Determination of the Hydrogen Peroxide Concentration in the Infrared Cell

Run	3600 cm^{-1} I_o	I	$\ln I_o/I$	3865 cm^{-1} I_o	I	$\ln I_o/I$	Corrected $\ln I_o/I$ at 3500 cm^{-1}	$[H_2O_2]$ molecules/cc
1	54.2	7.4	1.993	19.5	13.4	0.375	1.782	8.4×10^{15}
2	44.5	12.5	1.270	14.7	10.1	0.375	1.059	4.9×10^{15}
3	37.2	9.6	1.357	12.4	12.2	0.031	1.34	6.2×10^{15}
4	38.0	17.9	0.751	10.8	12.5	-0.162	0.842	3.9×10^{15}
5	40.5	10.3	1.351	14.8	10.9	0.305	1.18	5.5×10^{15}
6	36.2	15.9	.82 4	14.2	10.5	0.301	0.655	3.0×10^{15}

Average H_2O_2 concentration = $5.3 \pm 2 \times 10^{15}$ molecules/cc.

$a = 3.0 \times 10^{-20}$ cm^2/molecule to the base e.

III. RESULTS

A. The Infrared Spectrum

Molecular modulation absorption spectra were recorded while an ozone-hydrogen peroxide mixture in helium was being illuminated by the photolytic lamp flashing at 1.4 Hz. The ozone concentration was about 5×10^{14} molecules/cc; the peroxide concentration about 5×10^{15} molecules/cc. The two reactants were diluted by helium at atmospheric pressure. The total flow rate of gas through the cell was 8.4 l/min. The spectrometer slits were set to 6 mm which corresponds to an average resolution of 12 cm^{-1}. The spectrometer scanned at a rate of 1.4 cm^{-1}/min while the computer recorded data every 60 sec. The R.C. time constant during this run was 100 sec. The spectrum of the region 1050 to 1150 cm^{-1} shown in Figure 9 is the result of one scan; no repetitive scanning was done. Figure 9 shows the modulated absorption of ozone from 1050 to 1075 cm^{-1}; the phase shift of the ozone modulation is +85°, which is in the quadrant proper to a reactant destroyed by both the photolytic light and radical attack. Absorption by a second species displays a maximum at 1127 cm^{-1}. The phase shift of the second species is -35° which is proper for a radical intermediate. The breadth of the region with radical phase shift (1080 to 1140 cm^{-1}) indicates that the absorption by the second species is quite broad and may well extend below 1080 cm^{-1}, but the ozone absoption is so intense that it obscures all else.

The photolysis of ozone and hydrogen peroxide at 1.4 Hz under the same chemical conditions as above was studied in the infrared region 1340 to 1500 cm^{-1}. The resolution in this region with the slits opened to six mm is about 12 cm^{-1}. The scan speed of the spectrometer was 10.7 cm^{-1}/min,

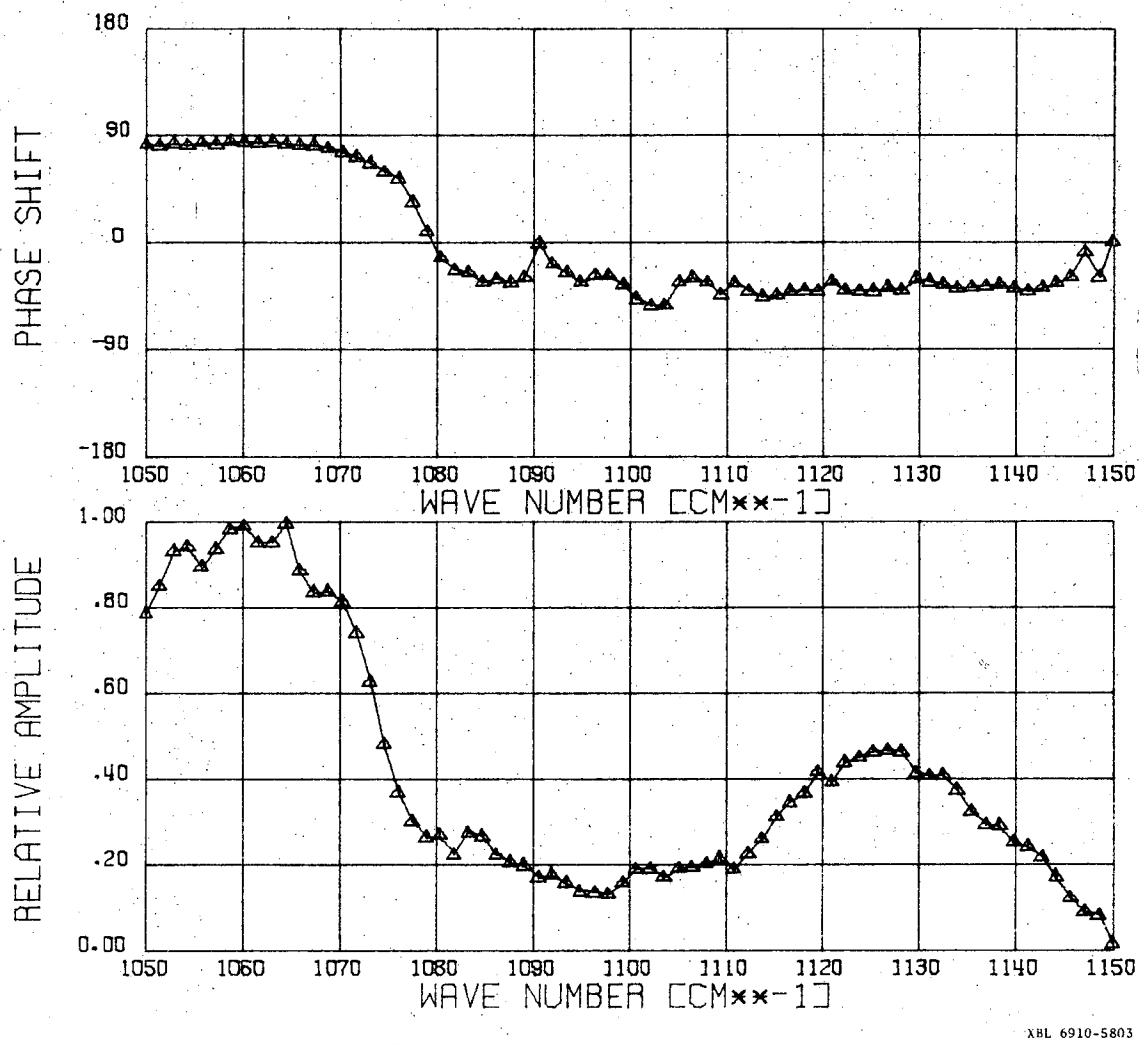

Figure 9. The modulated absorption spectrum of the infrared region 1050 to 1150 cm^{-1} obtained during the photolysis of ozone in the presence of hydrogen peroxide.

and the computer read data every 10 sec giving 1.78 cm^{-1}/datum. The R.C. time constant of the Dual-Phase demodulator was 10 sec. Repetitive scanning was employed and the average of six spectra is the modulation spectrum in Figure 10a. Another spectrum of this region, obtained under a resolution of 8 cm^{-1}, is shown in Figure 10b. In this figure there are 1.65 cm^{-1}/datum. Both spectra show a strong absorption with a radical phase shift between 1350 and 1440 cm^{-1}. An absorbance minimum occurs at 1390 cm^{-1}. The sharp peaks at 1408 and 1425 cm^{-1} in Figure 10a and at 1368, 1378, and 1425 cm^{-1} in Figure 12a and at 1368, 1378, and 1425 cm^{-1} in Figure 10b are narrower than the resolution of the spectrometer and cannot be regarded as spectral features. The spectrum in this region then consists of a pair of peaks centered at 1390 cm^{-1} and separated by about 42 cm^{-1}.

The last region in the infrared which shows modulated absorption is between 3300 and 3605 cm^{-1}. This region was studied under the same chemical conditions as the previous two at a flashing frequency of 1.4 Hz. The resolution in this region varied from 18 to 25 cm^{-1}; the scan speed employed was 24 cm^{-1}/min. Data were read every 10 sec; the Dual-Phase Demodulator had a time constant of 10 sec. The modulated absorption spectrum shown in Figure 11 is the result of sixteen scans and a three point curve smooth. The absorption maximum at 3600 cm^{-1} is very similar to the hydrogen peroxide peak in Figure 8 and has a +90° phase shift so it is due primarily to hydrogen peroxide. At lower infrared frequencies new absorption peaks are evident which cannot be assigned to either hydrogen peroxide or water because the new absorption is strongest where both water and peroxide absorption is weak, i.e., between 3350 and 3450 cm^{-1}. Furthermore the phase shift of the new absorption is moving rapidly toward the radical

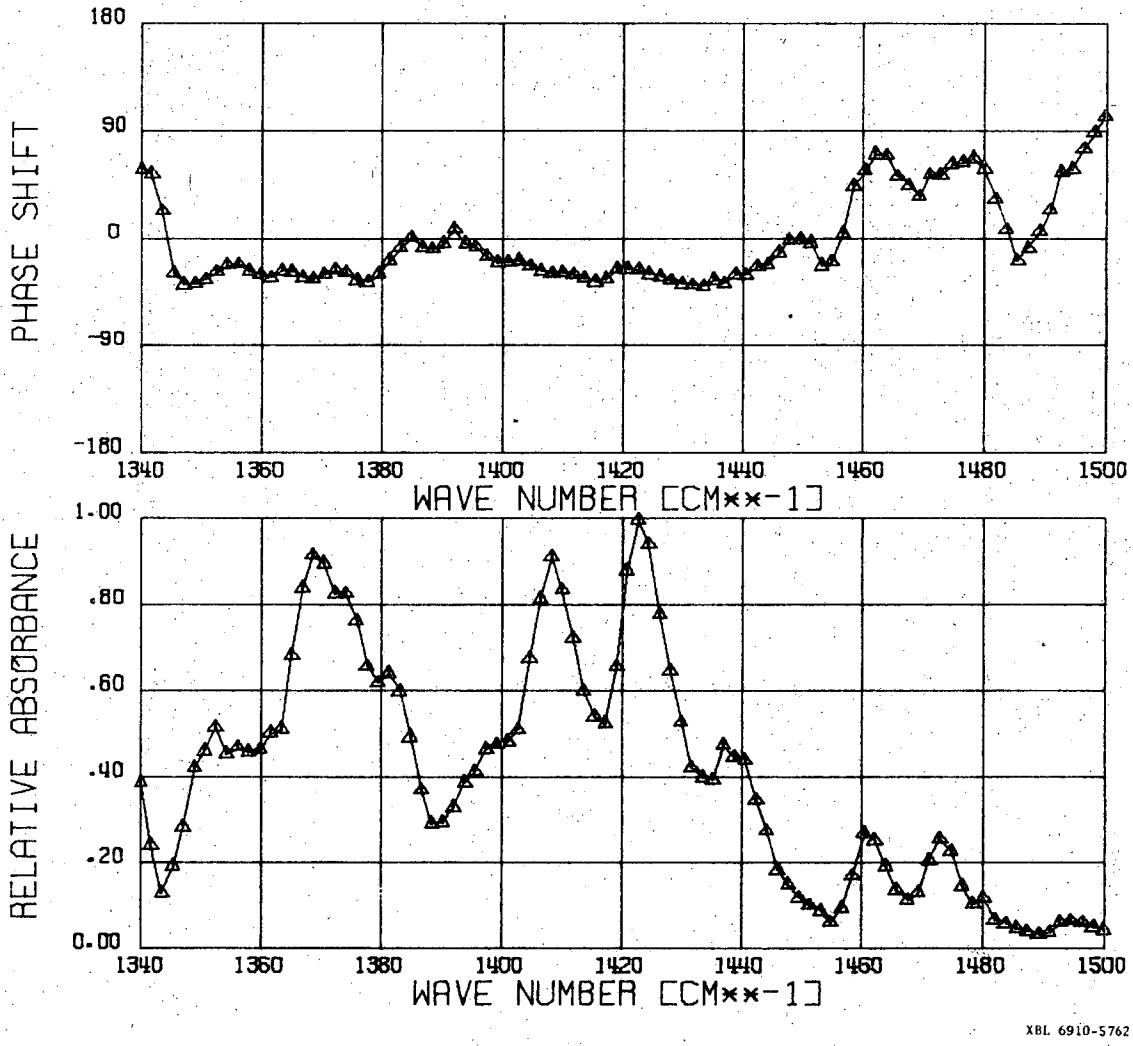

Figure 10a. The modulated absorption spectrum obtained during the photolysis of ozone in the presence of hydrogen peroxide at 1.4 Hz. Six repetitive scans at 12 cm^{-1} resolution and a three-point curve smooth.

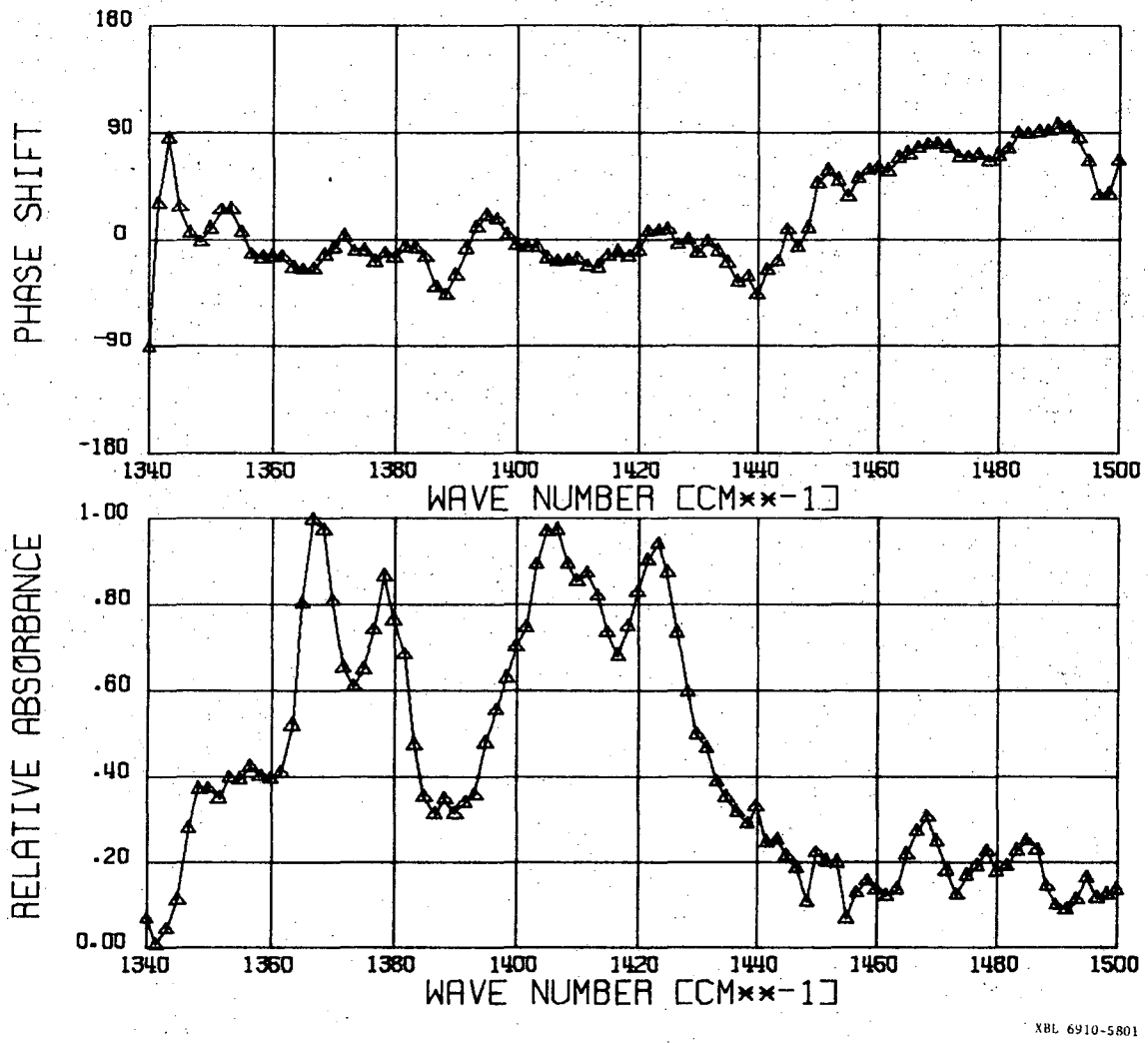

Figure 10b. The modulated absorption spectrum obtained during the photolysis of ozone in the presence of hydrogen peroxide at 1.4 Hz. Eleven repetitive scans at 8 cm^{-1} resolution and a three-point curve smooth.

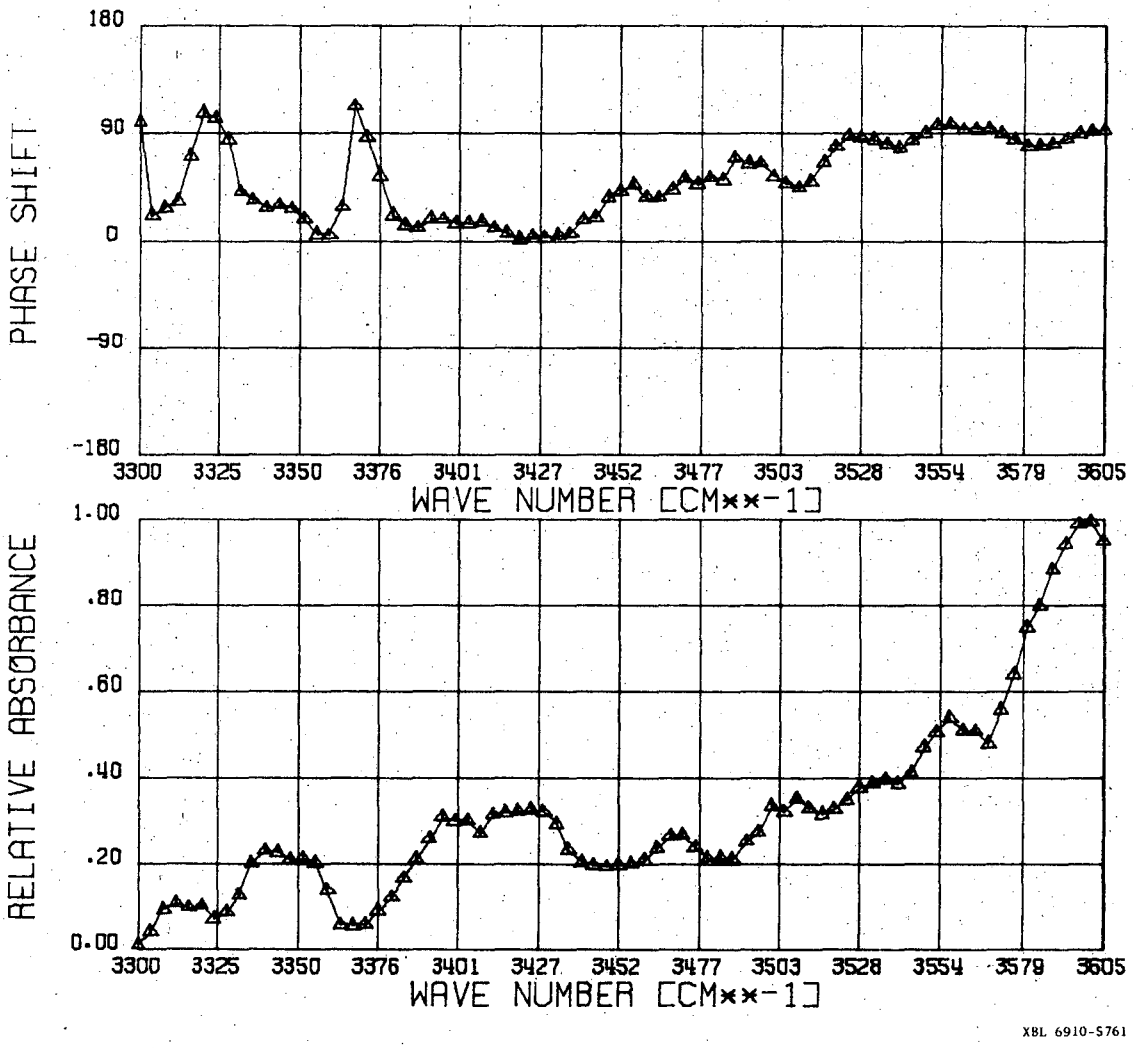

Figure 11. The modulated absorption spectrum obtained during the photolysis of ozone in the presence of hydrogen peroxide at 1.4 Hz. The spectrum is the average of sixteen sweeps and a three-point curve smooth.

quadrant, but the phase shift never reaches a constant value typical of single species absorption so there must still be some peroxide component in the signal.

In addition to the main peak which extends from 3380 to 3440 cm^{-1}, there are several smaller peaks at 3550, 3505, 3470, 3345, and 3312 cm^{-1}. These peaks are not present in the spectrum of water or hydrogen peroxide. The pattern of peaks does not fit the positions of Q and P branch lines of the OH radical which is known to be present in this chemical system. From the molecular structure of OH,[52] the locations of the lines can be calculated from the formula

$$\nu = \nu_o + (B_{v'} + B_{v''})m + (B_{v'} - B_{v''})m^2$$

where ν is the frequency of the rotation-vibration transition

ν_o is the band origin

$B_{v''}$ is the rotational constant in the ground vibrational state

$B_{v'}$ is the rotational constant of the first excited vibrational state

and m is a running number that takes -1, -2, etc. for the P branch and is 0 for the Q branch. The structural parameters of OH are: $\nu_o = 3570\ cm^{-1}$, $B_{v''} = 18.514\ cm^{-1}$, and $B_{v'} = 17.800\ cm^{-1}$ leading to: one, a Q branch at 3570 cm^{-1}, and two, P branch lines at 3553, 3494, 3454, 3413, and 3371 cm^{-1}. The observed peaks do not fit this pattern at all. Furthermore the intensity maximum of the P branch can be found from the rotational population as specified by the Boltzmann distribution law. This maximum should occur at 3494 cm^{-1}. In the observed spectrum there is nothing to indicate the presence of this line. It is reasonable, then, to regard the smaller peaks as

due to the same species that absorbs strongly at 3415 cm^{-1}. Later it will be shown that these peaks are consistent with the best current estimates of the structure of HO_2.

Another series of experiments were carried out photolyzing hydrogen peroxide in helium with no ozone. The hydrogen peroxide concentration during these experiments was 5×10^{15} molecules/cm^3 in one atmosphere of helium. The total flow rate of gas through the cell was 8.4 l/min. The photolytic lamp was flashed at 1 Hz. The spectrometer scanned at the rate 8 cm^{-1}/min. The time constant was 10 sec. Data was read every 1.1 cm^{-1}. The spectra obtained in the region 1000 to 1150 cm^{-1} were quite noisy so six separate spectra each the result of from four to nine multiple sweeps and five-point curve smoothing are presented in Figure 12. The observed phase shifts from 1065 to 1135 cm^{-1} lie predominately in the radical quadrant. An absorption maximum occurs at approximately 1120 cm^{-1}--very close to the maximum observed in the ozone-peroxide system (Figure 9). A second absorption maximum in Figure 12 is evident at 1075 cm^{-1}, and a minimum occurs between 1090 and 1100 cm^{-1}.

When the photolysis of hydrogen peroxide under the same conditions was studied in the region 1350 to 1520 cm^{-1}, the spectrum presented in Figure 13 was obtained. This spectrum includes twelve scans and a five-point curve smooth. A pair of peaks separated by 45 cm^{-1} and centered at 1395 cm^{-1} dominates the spectrum. The phase shift of these two peaks is near -45°. The progressive enhancement of this band by multiple-scanning and curve smoothing techniques is shown in Figure 14.

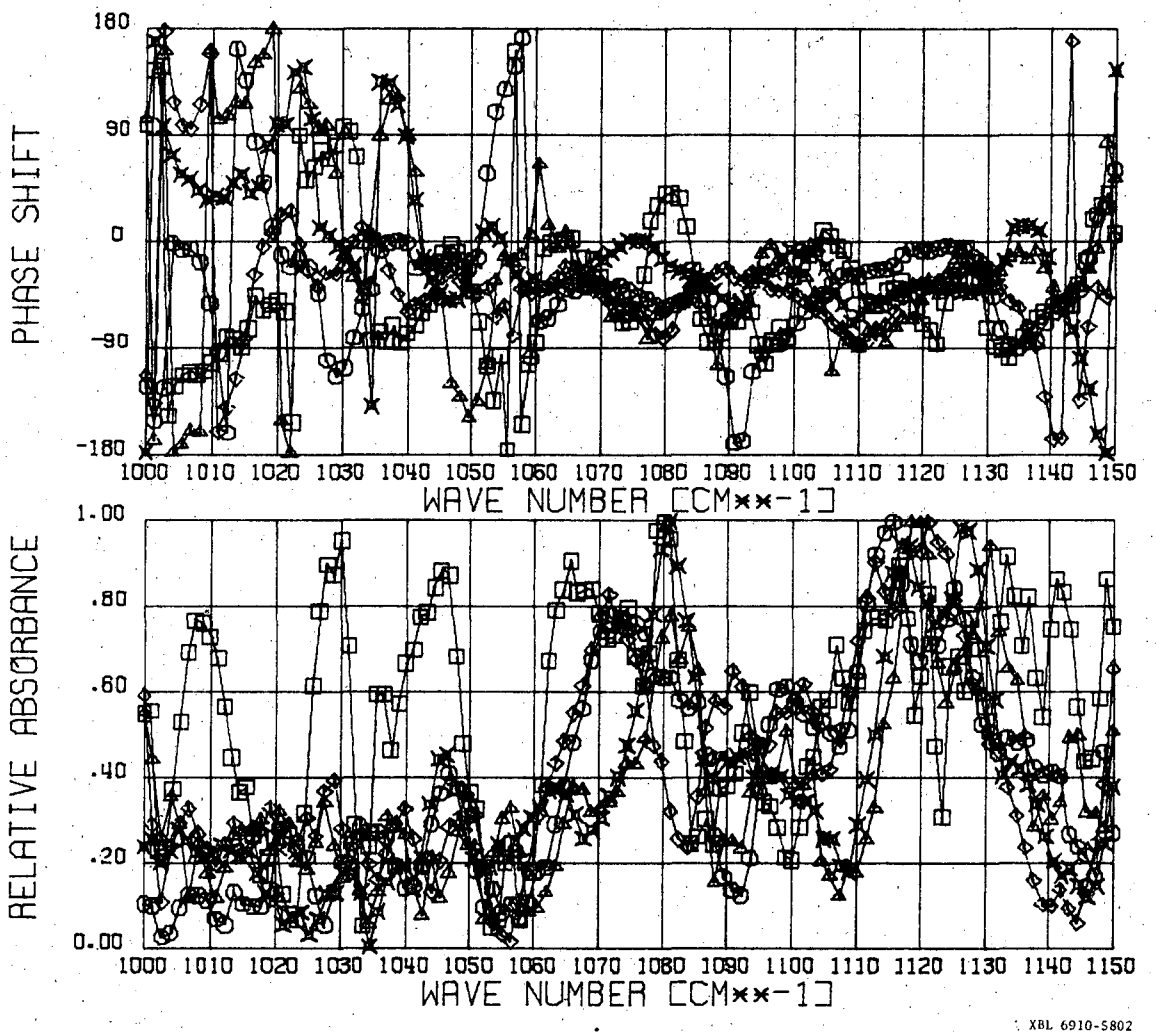

Figure 12. Infrared spectra from 1000 to 1150 cm^{-1} obtained during the photolysis of hydrogen peroxide at 1 Hz.

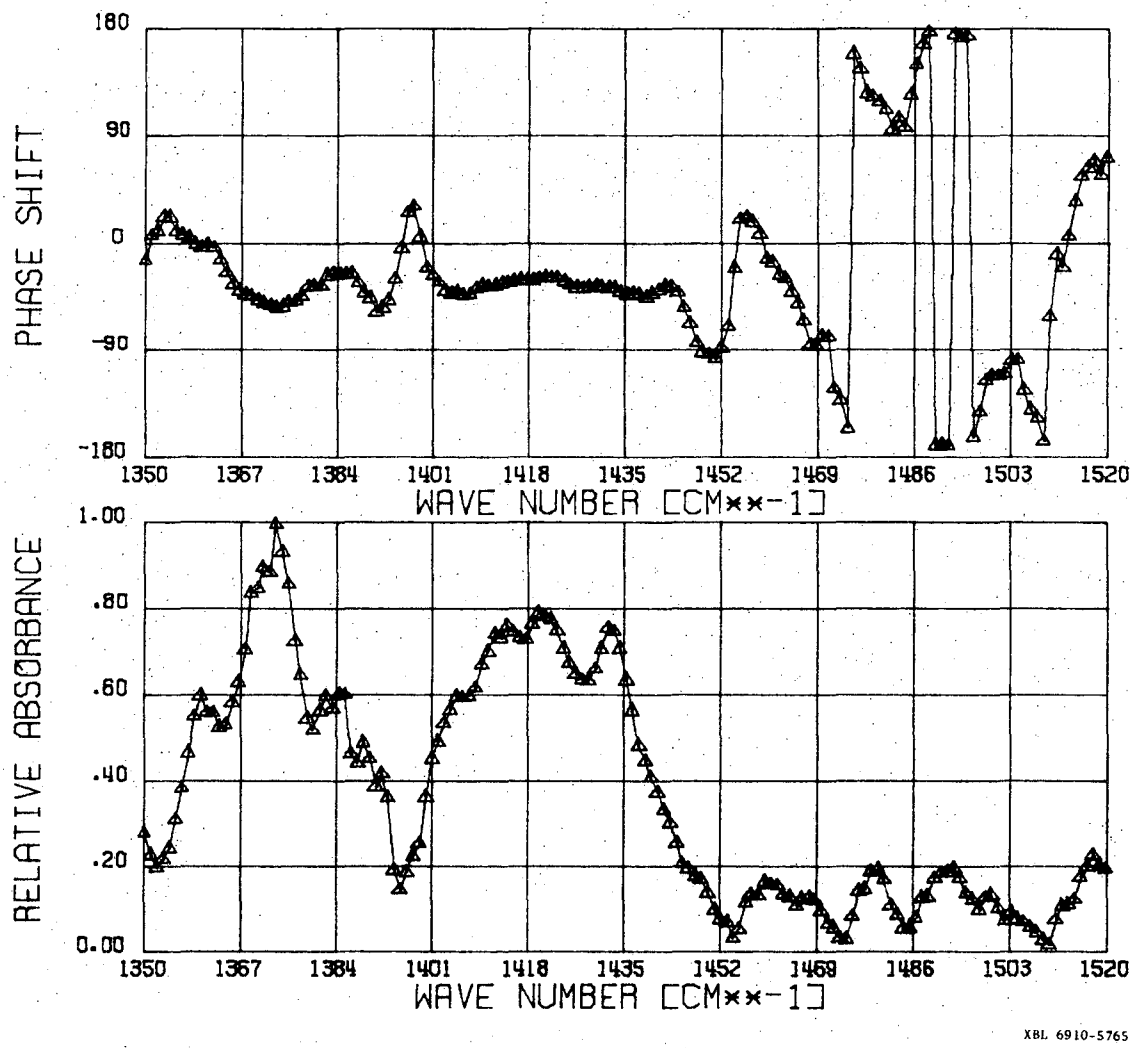

Figure 13. The modulated infrared absorption between 1350 and 1520 cm^{-1} obtained during the photolysis of hydrogen peroxide at 1 Hz. The spectrum is the average of 12 scans and a five-point curve smooth.

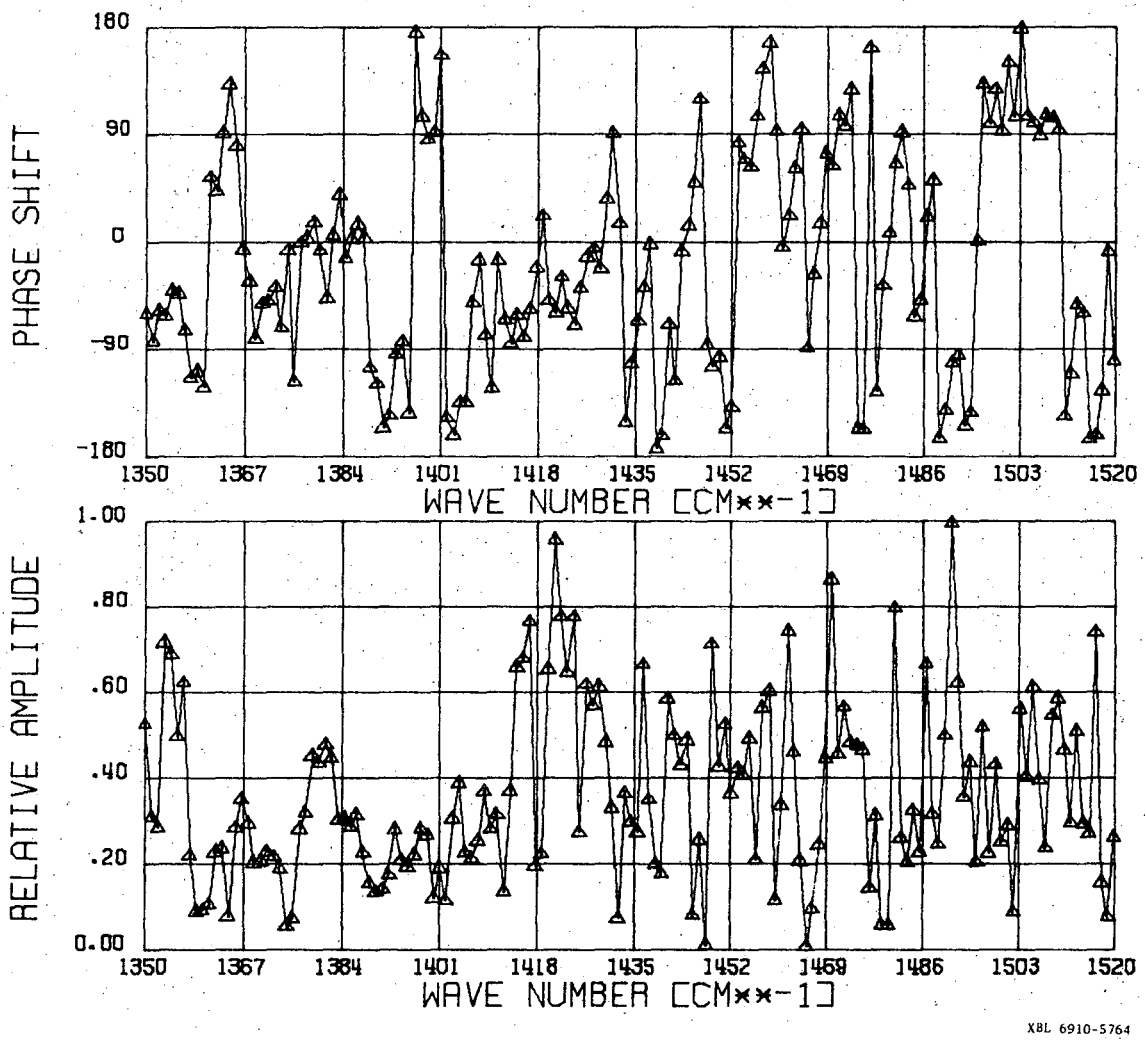

Figure 14. The progressive enhancement of the spectrum in Fig. 13 resulting from repetitive sweeps and curve smoothing.

A. One scan; no curve smooth
B. Seven scans; no curve smooth
C. Twelve scans; no curve smooth
D. Twelve scans; five-point curve smooth

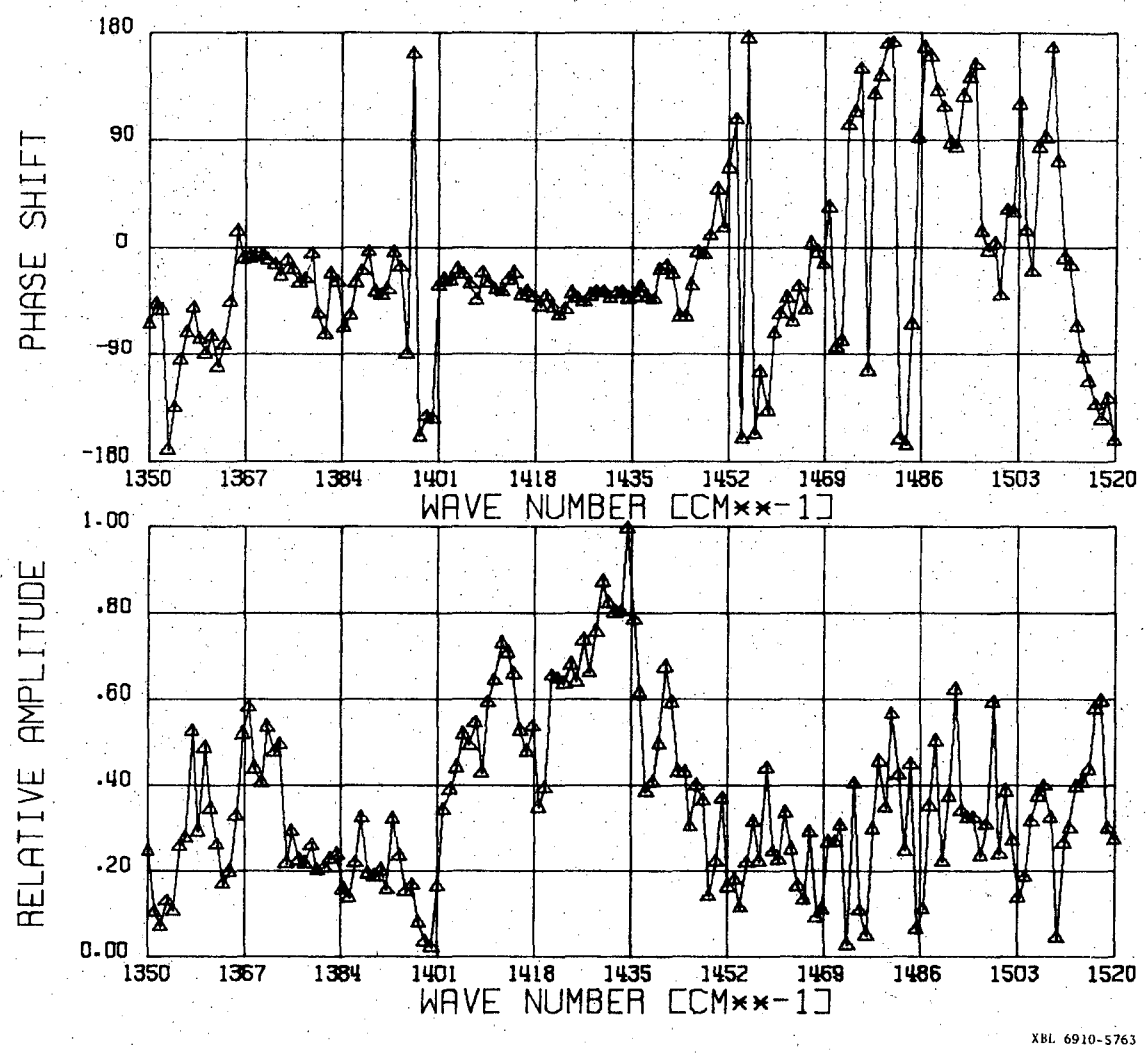
PHASE SHIFT
180
90
0
-90
-180
1350
1367
1384
1401
1418
1435
1452
1469
1486
1503
1520
WAVE NUMBER [CM**-1]
RELATIVE AMPLITUDE
1.00
.80
.60
.40
.20
0.00
1350
1367
1384
1401
1418
1435
1452
1469
1486
1503
1520
WAVE NUMBER [CM**-1]
XBL 6910-5763

Figure 14 B.

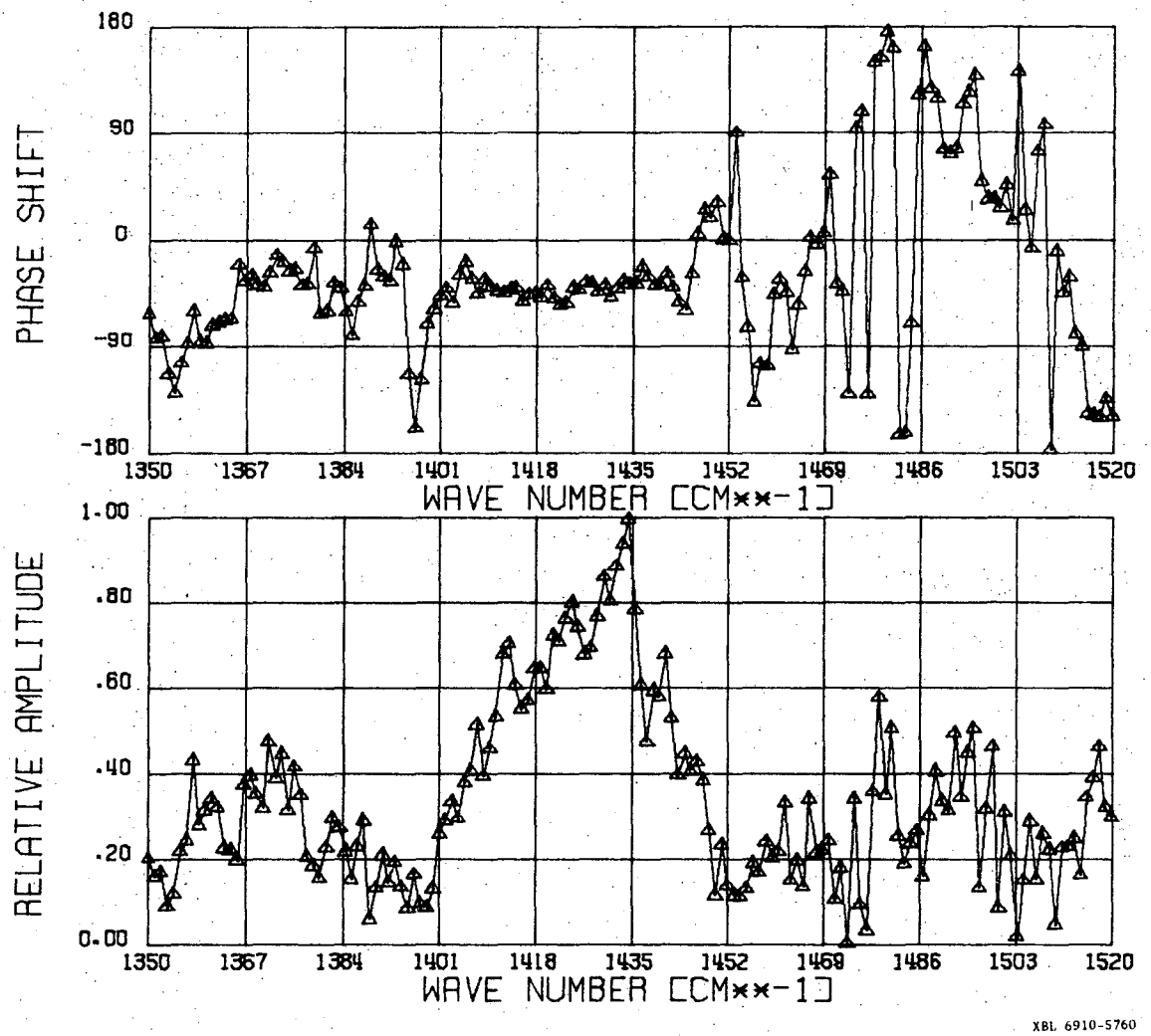
PHASE SHIFT
180
90
0
-90
-180
1350
1367
1384
1401
1418
1435
1452
1469
1486
1503
1520
WAVE NUMBER [CM**-1]
RELATIVE AMPLITUDE
1.00
.80
.60
.40
.20
0.00
1350
1367
1384
1401
1418
1435
1452
1469
1486
1503
1520
WAVE NUMBER [CM**-1]
XBL 6910-5760

Figure 14 C.

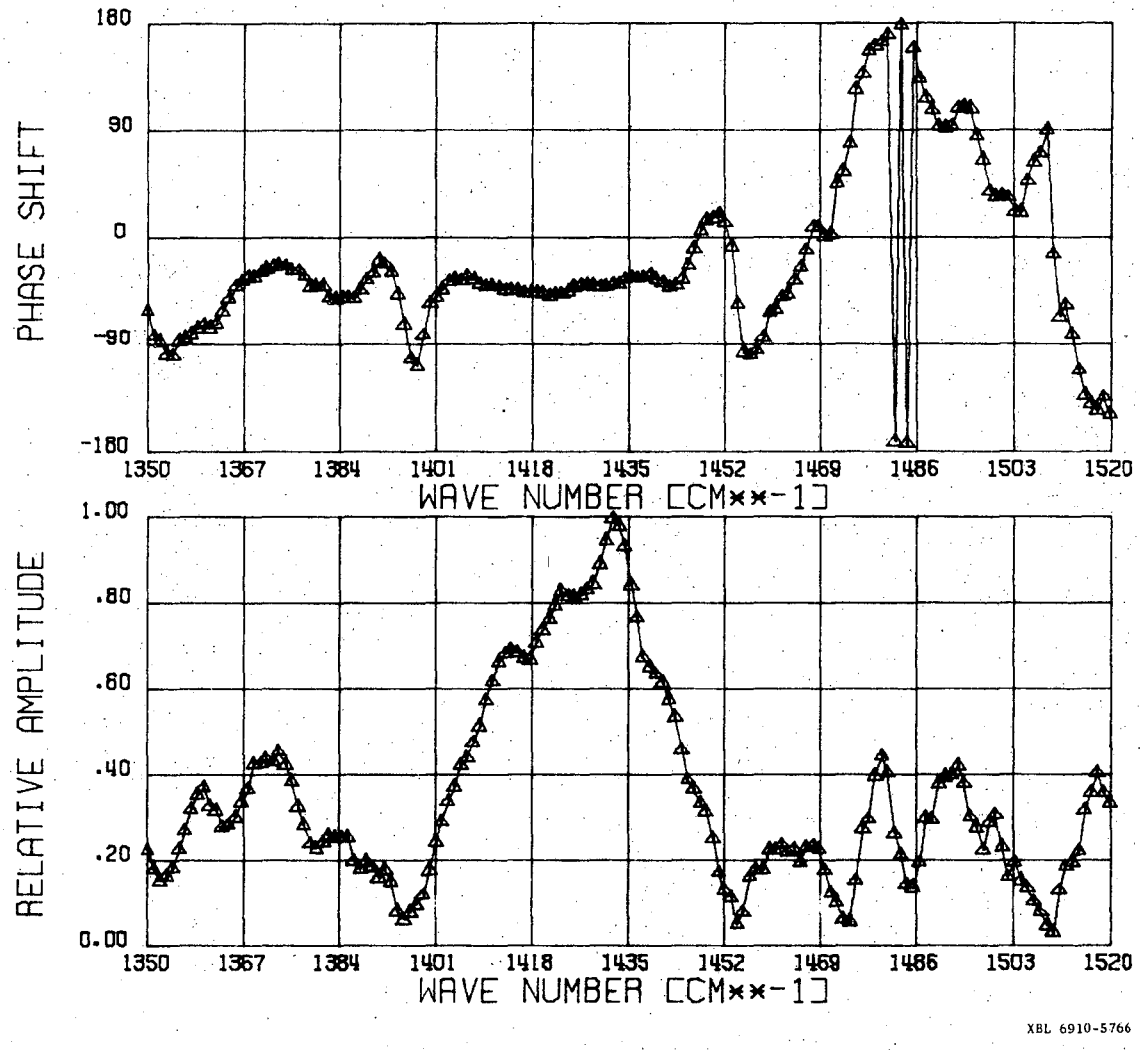
PHASE SHIFT
180
90
0
-90
-180
1350
1367
1384
1401
1418
1435
1452
1469
1486
1503
1520
WAVE NUMBER [CM**-1]
RELATIVE AMPLITUDE
1.00
.80
.60
.40
.20
0.00
1350
1367
1384
1401
1418
1435
1452
1469
1486
1503
1520
WAVE NUMBER [CM**-1]
XBL 6910-5766

Figure 14 D.

B. Kinetic Results

The dependence of the modulated absorption peaks at 1075, 1120, 1373, and 1420 cm^{-1} on flashing frequency was studied during the photolysis of hydrogen peroxide. In these experiments the infrared spectrometer was set at a fixed I.R. frequency and the modulation signal was recorded by the computer every 10 sec for a period of ten to thirty min. The hydrogen peroxide concentration, determined by the method explained in Sec. II-H, was 5×10^{15} molecules/cm^3. The helium carrier gas at a pressure of one atmosphere flowed through the cell at 8.4 l/min. The spectrometer slits were set at six mm which corresponds to 12 cm^{-1} slit width at the four infrared frequencies studied. Room temperature during these runs was 22°C. Flashing frequency was varied from 1/4 Hz to 4 Hz.

The observed phase shifts, each the result of from ten to thirty min of averaging, are plotted in Figure 15 and are tabulated in Table II. The average phase shift at each flashing frequency is indicated in Figure 18 by an arrow. The solid curve in the figure is the calculated curve for a second-order radical described in Sec. II-B-4. The position of the calculated curve on the time axis gives the quantity $(PQ)^{1/2}$; it is 5.55 sec^{-1}.

C. The Ultraviolet Spectrum

A molecular modulation absorption spectrum was obtained from 2450 to 2000 A during the photolysis of hydrogen peroxide at 1 Hz. The peroxide concentration was approximately 1×10^{16} molecules/cm^3 in one atmosphere of helium flowing through the cell at 8.4 l/min. The modulated absorption was measured at 50 A intervals with a spectral resolution of 13.3 A. The photolysis was initiated by only one mercury resonance lamp. The

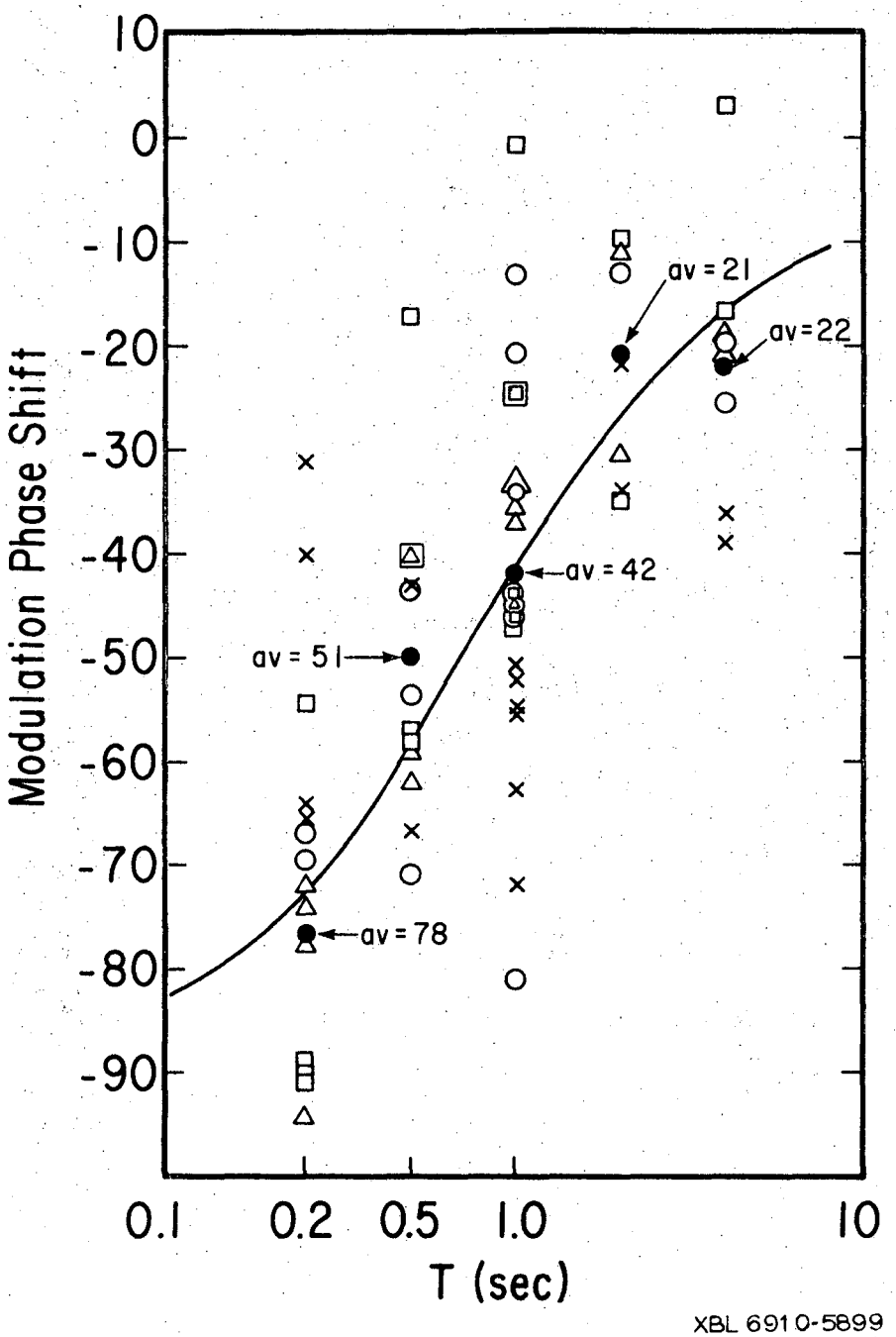

Figure 15. Phase shift of the infrared absorption peaks as a function of flashing period

× 1075 cm^{-1} △ 1420 cm^{-1}

○ 1120 cm^{-1} ● Average of all points

□ 1373 cm^{-1}

TABLE II Modulation Phase of the Radical Absorptions in the Infrared

Flashing Period (sec)	Infrared frequency (cm^{-1})	Modulation Phase Shift (0°)
4	1075	-38.9
4	1075	-35.9
4	1120	-25.6
4	1120	-20.4
4	1373	-16.2
4	1373	3.7
4	1420	-19.6
4	1420	-20.8
4	Average	-21±11
2	1075	-21.7
2	1075	-34.1
2	1120	-12.9
2	1373	- 9.7
2	1373	-35.1
2	1420	-10.7
2	1420	-30.4
2	Average	-22±9
1	1075	-55.1
1	1075	-50.9
1	1075	-55.6
1	1075	-52.6
1	1075	-72.2
1	1075	-62.7
1	1120	-81.6
1	1120	-20.4
1	1120	-12.9
1	1120	-34.0
1	1120	-45.7
1	1120	-44.6

TABLE II continued

Flashing Period (sec)	Infrared Frequency (cm^{-1})	Modulation Phase Shift (°)
1	1373	-45.7
1	1373	-32.9
1	1373	-43.9
1	1373	-24.4
1	1373	-24.8
1	1373	-47.3
1	1373	- 0.47
1	1420	-36.9
1	1420	-44.9
1	1420	-32.9
1	1420	-35.3
1	1420	-44.3
1	Average	-42±8
0.5	1075	-43.2
0.5	1075	-66.6
0.5	1120	-53.4
0.5	1120	-70.9
0.5	1120	-43.5
0.5	1373	-57.1
0.5	1373	-57.9
0.5	1373	39.9
0.5	1373	-16.8
0.5	1420	-40.1
0.5	1420	-59.2
0.5	1420	-62.5
0.5	Average	-51±9
0.25	1075	-39.9
0.25	1075	-65.6
0.25	1075	-31.1
0.25	1075	-117.3

TABLE II continued

Flashing Period (sec)	Infrared Frequency (cm^{-1})	Modulation Phase Shift (°)
0.25	1075	-64.3
0.25	1120	-68.6
0.25	1120	-66.9
0.25	1373	-119.8
0.25	1373	-89.2
0.25	1373	-89.6
0.25	1373	-54.4
0.25	1373	-90.6
0.25	1420	-71.8
0.25	1420	-94.3
0.25	1420	-117.2
0.25	1420	-77.5
0.25	1420	-73.8
0.25	Average	-78±13

spectrum in Figure 16 shows an absorption band with a peak at 2100 A. The phase shift of this modulation lies between -15.8 and -24.0° which indicates a radical species. There is a slight upward trend in the phase shift from 2150 to 2000 A suggesting presence of another species with a positive phase shift becoming important at shorter wave lengths. The same spectral region was examined at 1/4 Hz; the resulting modulation spectrum is presented in Figure 17. At this frequency the phase shift of the modulation displays a strong dependence on wave length, clearly indicating the presence of two species one of which is relatively more important at 1/4 Hz than at 1 Hz.

Since the phase shift at 1/4 Hz is in a reactant quadrant and since reactant amplitudes show a stronger dependence on flashing frequency than radical amplitudes, the species gaining importance at 1/4 Hz must be the reactant hydrogen peroxide. The shape of the hydrogen peroxide absorption spectrum is well-known[51,53] and agrees closely with the spectrum obtained in our laboratory (Figure 18). It is evident that hydrogen peroxide could be contributing to the modulated spectrum.

D. Dependence of the UV Spectrum on Flashing Frequency

The response of the modulated absorption at 2200 A to variations in flashing frequency was studied from 1/4 to 32 Hz. The conditions of the experiment were set as closely as possible to the conditions under which the spectrum was obtained; the hydrogen peroxide concentration determined by the method described in Sec. II-H was 1.13×10^{16} molecules/cm^3. The experimental data is presented in Table III. The phase shift is also plotted against log T where T is flashing period in Figure 19; the theoretical second-order radical curve is included in the figure for comparison with the observed

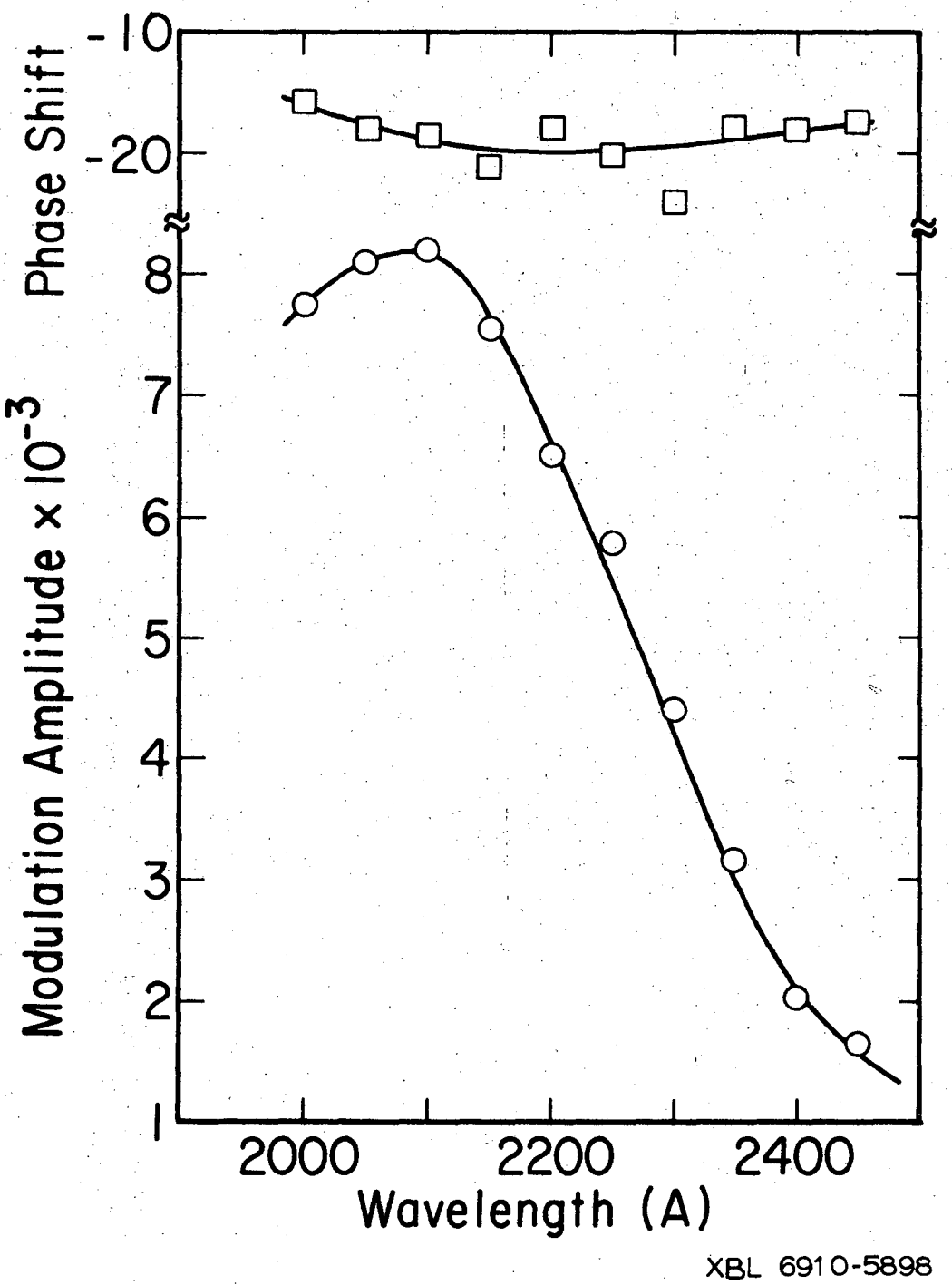

Figure 16. The modulated ultraviolet absorption spectrum observed during the photolysis of hydrogen peroxide by one photolytic lamp at 1 Hz.

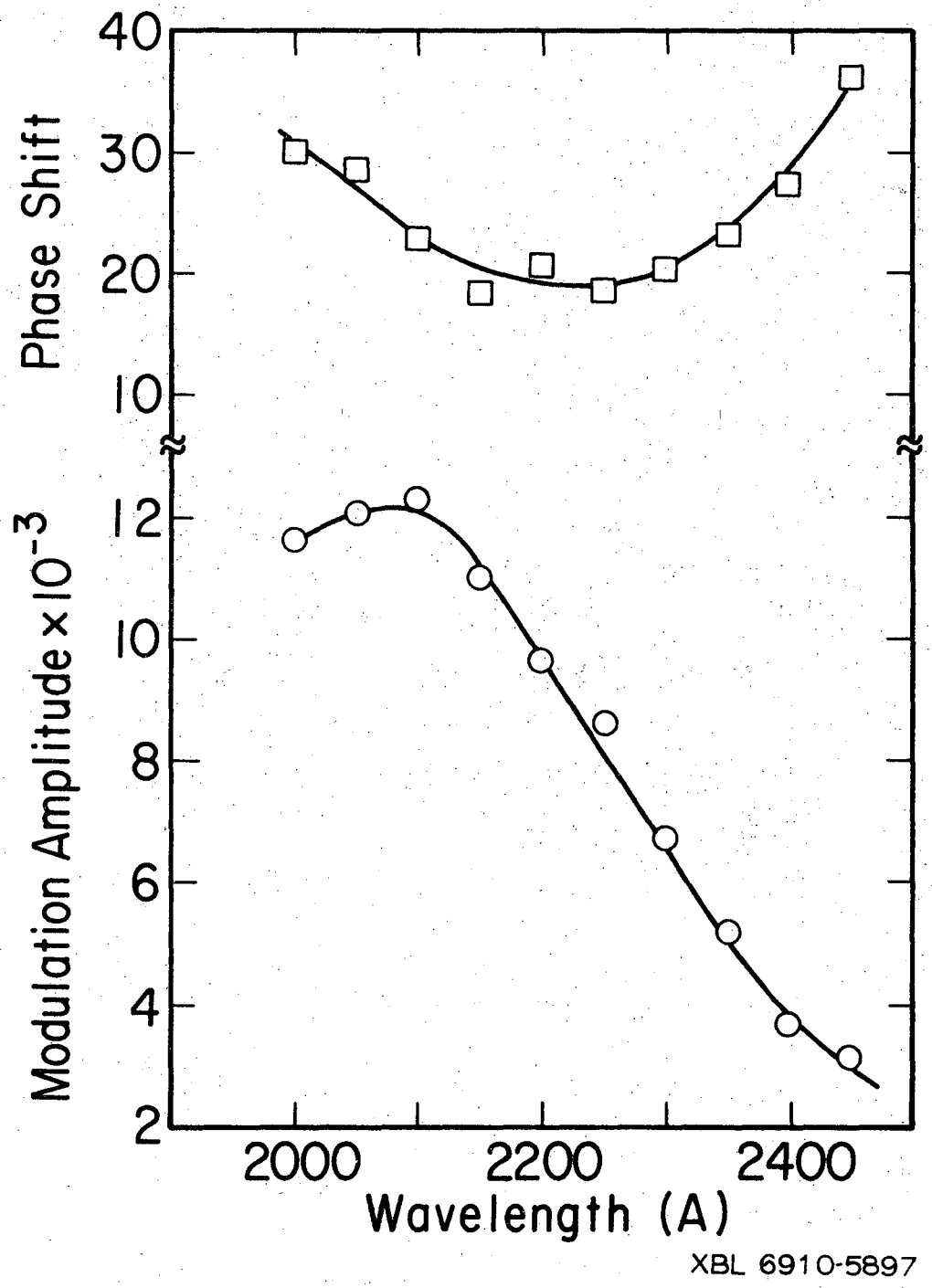

Figure 17. The modulated ultraviolet absorption spectrum obtained during the photolysis of hydrogen peroxide by one lamp at 1/4 Hz.

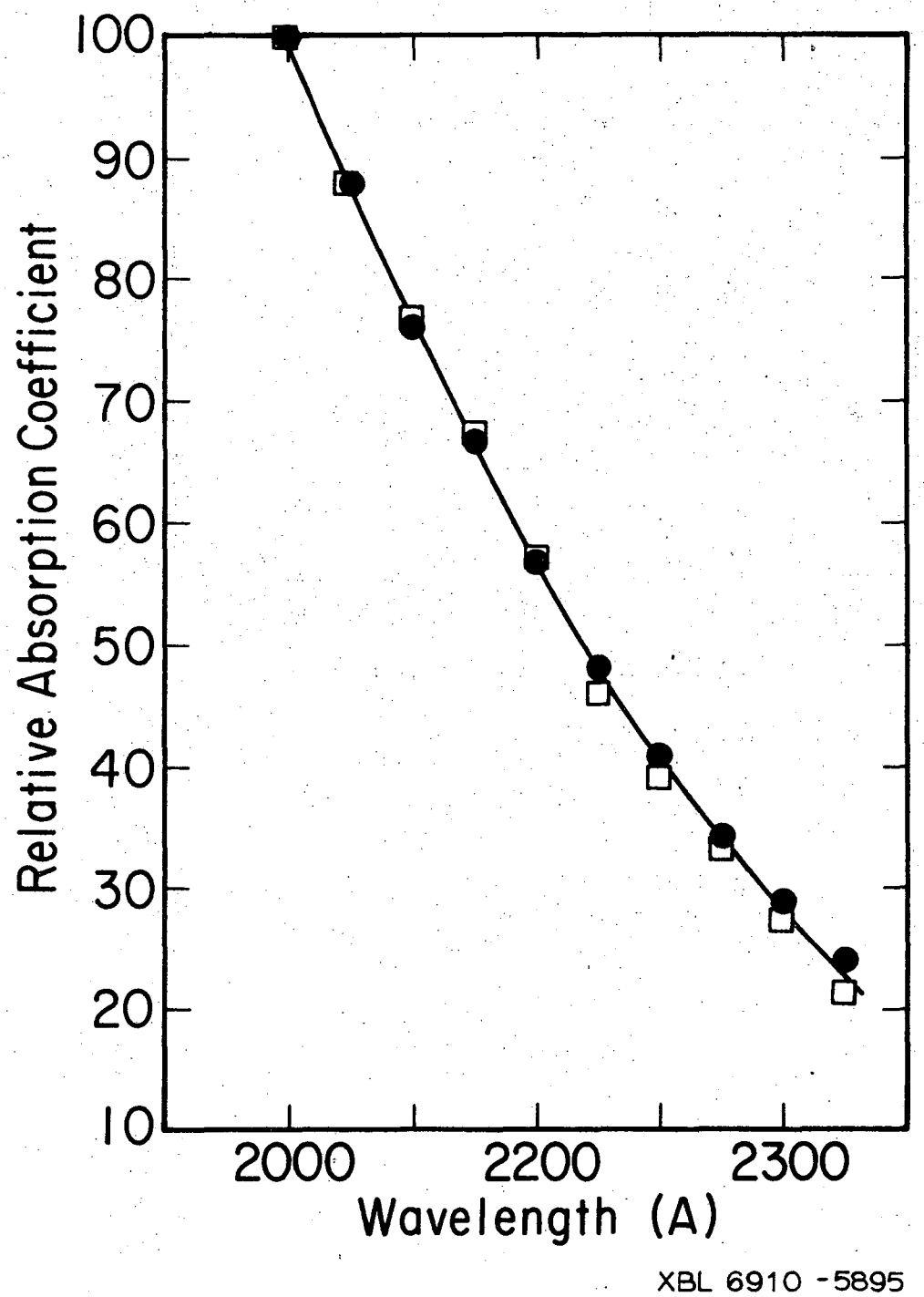

Figure 18. The absorption spectrum of hydrogen peroxide

● Literature (Refs. 51 and 53)

□ This laboratory by standard spectroscopic techniques

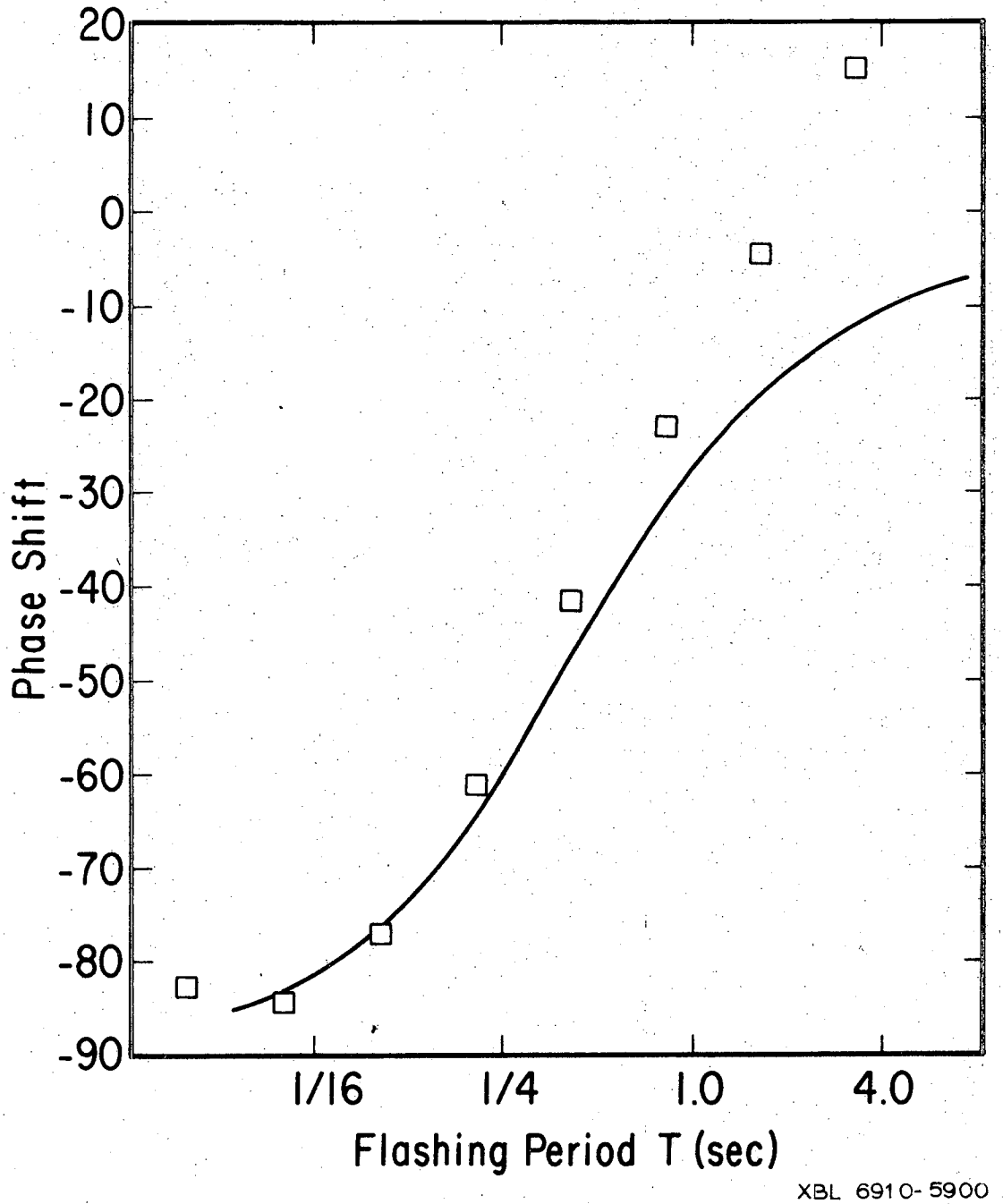

Figure 19. The dependence of the phase shift of the modulation at 2200 A on flashing period. The curve is the calculated curve for a primary second-order radical. Only one photolysis lamp was used.

TABLE III. Resolution of Modulation at 2200A into Radical and Reactant Components

Flashing Frequency (Hz)	Experimental Phase Shift(°)	Experimental Amplitude	Radical Phase Shift (°)	Reactant Phase Shift (°)	Radical Amplitude	Reactant Amplitude
1/4	15.3	8674	-12.0	95.4	8955	4169
1/2	- 4.3	7640	-20.0	98.6	8482	2355
1	-22.8	6186	-31.0	101.5	6931	1197
2	-41.5	4559	-47.5	101.9	5340	936
4	-61.1	2800	-64.0	98.8	3254	479
8	-77.0	1501	-76.5	95.2	1411	- 91
16	-84.3	816	-83.0	93.1	544	- 272
32	-82.8	363	-87.0	92.0	1884	1522

results. At low frequencies the observed phase shift is too positive for a pure radical signal. Apparently a reactant is becoming progressively more important as the flash period increases, agreeing completely with the previous results.

If this interpretation of the data is correct, it should be possible to break the signals down into radical and reactant components. Because the hydrogen peroxide is both a reactant and a product in this system, the actual modulation is a sum of reactant and product contributions. It is not, however, a simple vector sum, and it is easier and more straight forward to calculate the peroxide concentration profile from differential equations describing the mechanism and then to carry out a Fourier analysis of the concentration profile for the fundamental amplitude and phase shift. The details of the calculation are given in Appendix C. The results of the calculation are presented in Table IV which list the amplitudes and phase shifts of the reactant and radical as functions of T/τ_{ss}. The phase shift of the radical at each frequency can be found from the theoretical phase shifts are found from Table IV. The observed signals are then decomposed into components specified by the phase shifts. Table III shows the experimental data, the phase shifts, and the resulting amplitudes; all amplitudes in this table are frequently normalized as described in Sec. II-F-2. At flashing frequencies of 8 Hz and greater, the reactant amplitude is so small that noise can introduce negative amplitudes.

The above treatment is acceptable only if the amplitudes extracted from the data respond to variations in flashing frequency as expected from the mechanism. The amplitude behavior of the two species reactant and radical predicted by the mechanism and the measured amplitudes at

TABLE IV Modulation Amplitude and Phase-Shift of a Radical and a Reactant* as Function of T/τ_{ss}

T/τ_{ss}	Radical		Reactant	
	Amplitude†	Phase Shift	Amplitude (arbitrary units)	Phase Shift
333.3	.9846	-3.2	33,798	91.7
285.7	.9822	-3.4	28,978	91.8
250.0	.9798	-3.6	25,358	91.9
200.0	.9750	-4.0	20,295	92.0
166.7	.9704	-4.4	16,920	92.2
142.9	.9658	-4.8	14,510	92.4
125.0	.9614	-5.2	12,704	92.5
100.0	.9528	-6.0	10.176	92.8
83.33	.9446	-6.8	9,492	93.2
71.43	.9367	-7.5	7,290	93.5
62.50	.9291	-8.3	6,389	93.8
55.56	.9216	-9.0	5,690	94.0
50.00	.9145	-9.6	5,130	94.3
40.00	.8973	-11.2	4,125	95.0
33.33	.8812	-12.7	3,457	95.7
28.57	.8659	-14.1	2,982	96.3
25.00	.8514	-15.5	2,628	96.8
22.22	.8374	-16.8	2,350	97.3
20.00	.8241	-18.0	2,130	97.8
18.18	.8112	-19.2	1,950	98.3
16.67	.7988	-20.4	1,800	98.7
15.38	.7867	-21.5	1,674	99.1
14.29	.7750	-22.6	1,566	99.4
13.33	.7636	-23.7	1,472	99.8
12.50	.7526	-24.7	1,391	100.1
11.76	.7418	-25.8	1,319	100.4
11.11	.7314	-26.8	1,255	100.6

*Reactant obeys rate law $dR/dt = -3/2A + B/2X^2$ where X is a radical.

†Relative to the limiting amplitude as $T \rightarrow \infty$.

TABLE IV (continued)

T/τ_{ss}	Radical		Reactant	
	Amplitude	Phase Shift	Amplitude (arbitrary units)	Phase Shift
10.53	.7209	-27.7	1,197	100.8
10.00	.7109	-28.7	1,146	101.0
9.524	.7010	-29.6	1,099	101.2
9.090	.6913	-30.5	1,057	101.4
8.696	.6809	-31.5	1,018	101.5
8.333	.6726	-32.3	982.0	101.7
8.000	.6635	-33.2	949.1	101.8
7.692	.6545	-34.0	918.6	101.9
7.143	.6371	-35.6	864.0	102.0
6.667	.6203	-37.2	816.3	102.1
6.250	.6042	-38.7	774.2	102.2
5.882	.5885	-40.1	736.8	102.2
5.556	.5734	-41.5	703.2	102.2
5.263	.5589	-42.8	672.9	102.2
5.000	.5449	-44.1	645.3	102.1
4.762	.5313	-45.4	620.0	102.0
4.545	.5182	-46.5	596.8	101.9
4.348	.5056	-47.7	575.4	101.8
4.167	.4935	-48.7	555.6	101.7
4.000	.4818	-49.9	537.1	101.6
3.846	.4705	-50.8	519.9	101.5
3.704	.4596	-51.7	503.8	101.3
3.571	.4491	-52.7	488.7	101.2
3.448	.4389	-53.6	474.4	101.0
3.333	.4292	-54.4	461.1	100.9
3.226	.4198	-55.2	448.4	100.7
3.077	.4062	-56.4	430.7	100.5
2.941	.3934	-57.5	414.3	100.3
2.817	.3813	-58.5	399.2	100.1
2.703	.3698	-59.5	385.1	99.9

TABLE IV (continued)

T/τ_{ss}	Radical		Reactant	
	Amplitude	Phase Shift	Amplitude (arbitrary units)	Phase Shift
2.597	.3589	-60.5	372.0	99.6
2.500	.3485	-61.3	359.7	99.4
2.381	.3354	-62.4	344.5	99.2
2.273	.3232	-63.5	330.6	98.9
2.174	.3118	-64.4	317.7	98.7
2.083	.3011	-65.3	305.8	98.4
2.000	.2910	-66.2	294.7	98.2
1.905	.2792	-67.2	282.0	97.9
1.818	.2683	-68.1	270.2	97.7
1.739	.2582	-68.9	259.5	97.5
1.667	.2487	-69.7	249.5	97.2
1.562	.2349	-70.8	235.1	96.9
1.471	.2243	-71.9	222.2	96.6
1.389	.2112	-72.8	210.7	96.3
1.316	.2010	-73.7	200.3	96.1
1.250	.1916	-74.4	190.9	95.8
1.176	.1811	-75.3	180.4	95.5
1.111	.1717	-76.1	170.9	95.3
1.042	.1615	-76.9	160.8	95.1
.9524	.1483	-78.0	147.7	94.7
.8689	.1359	-79.0	135.5	94.4
.8000	.1254	-79.8	125.2	94.1
.7407	.1163	-80.6	116.4	93.9
.6667	.1049	-81.5	105.4	93.6
.5714	.0902	-82.7	91.16	93.2
.5000	.0791	-83.6	80.42	92.9
.4000	.0634	-84.9	65.35	92.4
.2500	-	-	42.65	91.8
.1250	-	-	23.67	91.2
.0500	-	-	12.27	90.9

1/4 Hz in Table V. Graphical comparison of the observed amplitude behavior with the expected behavior is provided in Figure 20. The agreement between experimental and predicted behavior is quite good and justifies the above treatment of the data. From the position of the phase shift curve on the time axis in Figure 19, we determine the quantity $(PQ)^{1/2}$ for the intermediate to be 11.09 sec^{-1}.

In another set of experiments, modulation spectra of the entire 2450 to 2000 A region were obtained at flashing frequencies from 1/4 to 16 Hz. The spectra were acquired at 50 A intervals with a resolution of 13.3 A. The hydrogen peroxide was again carried into the reaction cell by a stream of helium flowing at 8.4 l/min. Two photolysis lamps were used. Because of the greater light intensity, the hydrogen peroxide concentration was lower than in the previous experiment. The concentration of peroxide in the two-lamp experiment was 8.5×10^{15} molecules/cm^3.

The observed spectra acquired at the various flashing frequencies in this experiment are shown in Figures 21 and 22. The experimental data is listed in Table VI. Each spectrum has its most negative phase shift between 2150 and 2250 A usually at 2200 A. The phase shift at 2200 A is plotted against log T and the model curve is fitted to the high frequency data, i.e., 2, 4, and 8 Hz. The spectrum at 16 Hz is not used here because it is quite noisy. The model curve predicts a radical phase shift of -8.2° at 1/4 Hz. From Table IV the reactant phase shift should be 93.7° so the 1/4 Hz spectrum is decomposed into -8.2° and 93.7° components. The 93.7° component is fit by the method of least squares to the known hydrogen peroxide spectrum to obtain the amplitude of the peroxide modulation at 1/4 Hz. The phase shift and amplitude behavior of

TABLE V Radical and Reactant Amplitudes Predicted from Volman's Mechanism and the Amplitudes Measured at 1/4 Hz

Flashing Frequency (Hz)	Radical Amplitude*	Reactant Amplitude*
1/4	8955	4169
1/2	8080	2169
1	6840	1181
2	5122	718
4	3165	385
8	1638	193
16	907	96
32	-	48

*Frequency normalized

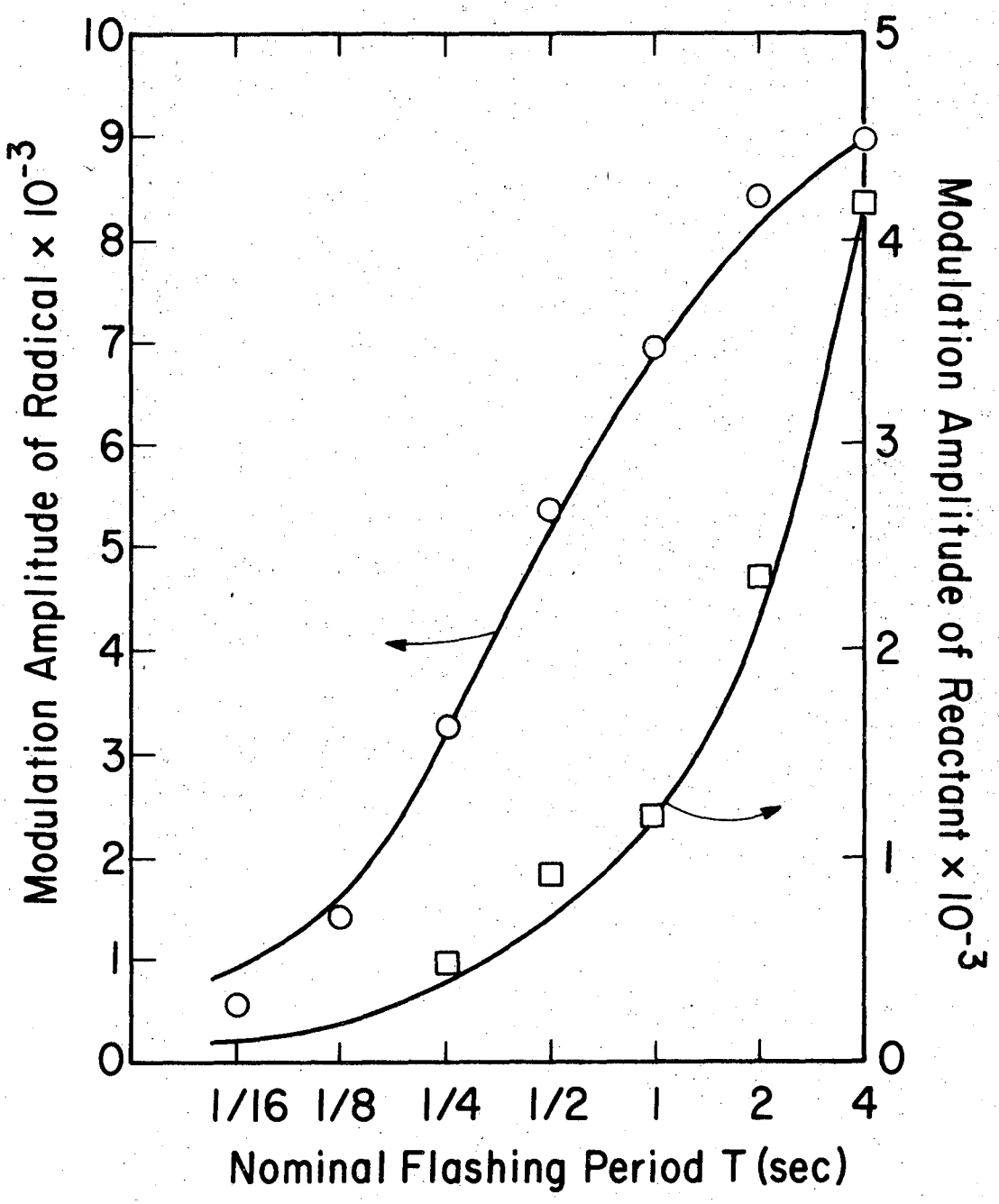

XBL 6910 - 5904

Figure 20. Comparison of radical and reactant amplitudes extracted from the data with the amplitudes predicted by the mechanism.

○ Radical amplitude

□ Reactant amplitude. Solid curves are the amplitudes predicted by the mechanism.

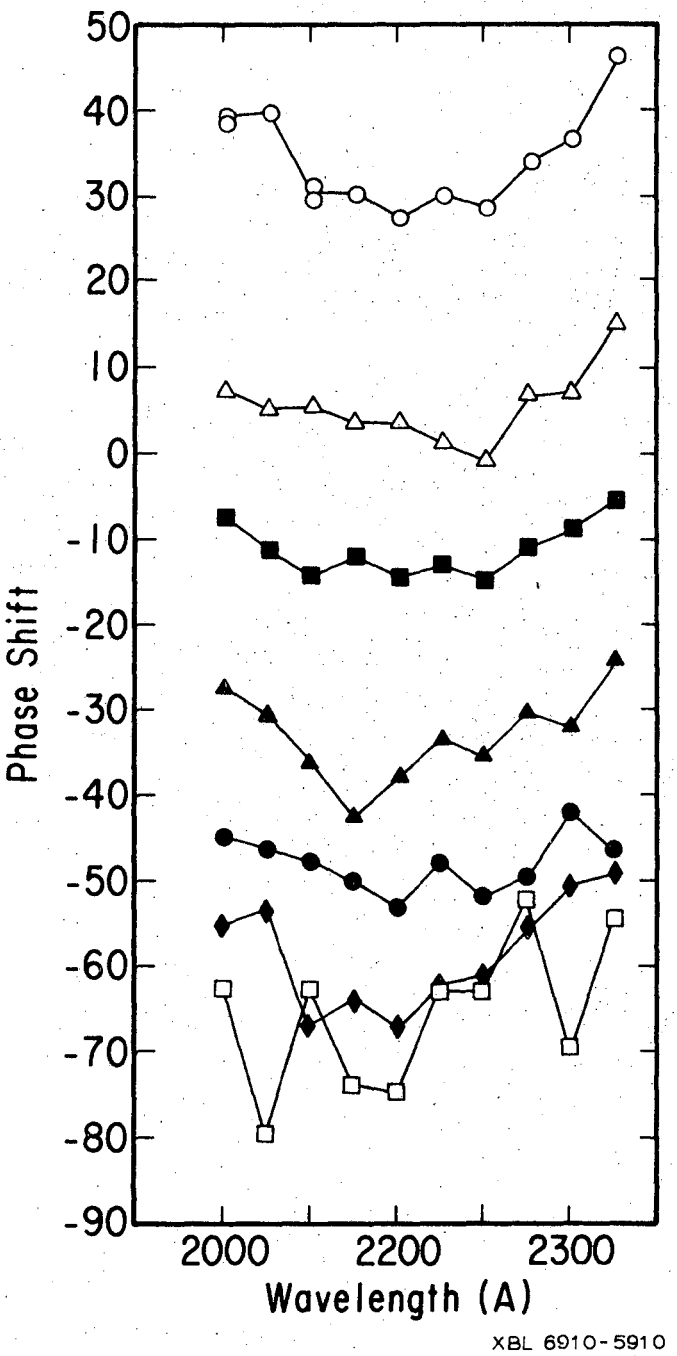

Figure 21. The modulated absorption phase shifts from 2450 to 2000 A obtained during the photolysis of hydrogen peroxide by two lamps.

○ 1/4 Hz, △ 1/2 Hz, ■ 1 Hz, ▲ 2 Hz,

● 4 Hz, ♦ 8 Hz, □ 16 Hz.

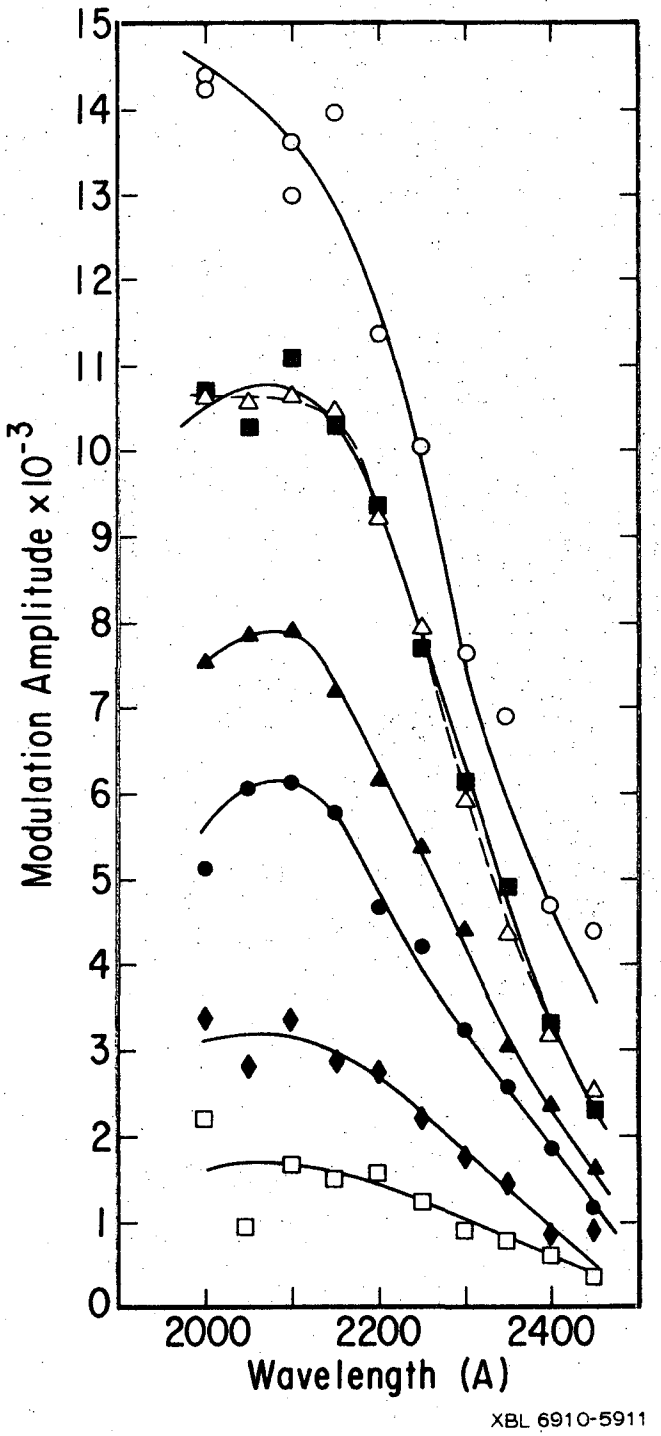

Figure 22. The modulated absorption amplitudes from 2450 to 2000 A obtained during the photolysis of hydrogen peroxide by two lamps.

○ 1/4 Hz, △ 1/2 Hz, ■ 1 Hz, ▲ 2 Hz,

● 4 Hz, ♦ 8 Hz, □ 16 Hz.

TABLE VI Modulation Spectra from 2450 to 2000A at Flashing Frequencies from 1/4 to 16 Hz Resulting from the Photolyses of Hydrogen Peroxide by Two Lamps

	2450	2400	2330	2300	2250	2200	2150	2100	2050	2000
1/4 Hz								17400		19151
Amplitude	5905	6238	9257	10228	14076	15234	18731	18276	21165	19316
Phase Shift	+46.3	+36.6	+34.0	+28.7	+30.0	+27.4	+30.3	+29.5 +31.1	+39.8	+38.6
1/2 Hz										
Amplitude	2895	3746	5026	6843	9135	10625	12019	12192	12188	12258
Phase Shift	+15.0	+7.2	+6.5	-0.9	+1.0	+3.7	+3.6	+5.4	+5.0	+7.2
1 Hz										
Amplitude	2612	3721	5532	6929	8695	10547	11630	12524	11604	12091
Phase Shift	-5.6	-8.9	-11.1	-14.8	-13.0	-14.4	-12.2	-14.3	-11.5	-7.4
2 Hz										
Amplitude	1677	2472	3190	4631	5631	6506	7571	8344	8274	7948
Phase Shift	-24.3	-31.9	-30.6	-35.6	-33.4	-37.9	-42.7	-36.2	-30.8	-27.2
4 Hz										
Amplitude	1178	1882	2621	3272	4258	4761	5883	6261	6178	5223
Phase Shift	-46.5	-42.1	-49.6	-52.0	-48.0	-53.5	-50.2	-47.9	-46.4	-44.9
8 Hz										
Amplitude	838	784	1352	1607	2100	2564	2709	3124	2660	3065
Phase Shift	-49.3	-50.6	-55.5	-61.2	-62.5	-67.1	-63.9	-67.3	-53.5	-55.3
16 Hz										
Amplitude	370	633	828	950	1284	1660	1574	1771	991	2330
Phase Shift	-54.5	-69.8	-52.1	-63.1	-62.8	-74.9	-73.9	-62.8	-79.9	-62.6

the reactant as a function of flashing frequency is known from the model, so the reactant contribution at each flashing frequency can be calculated and subtracted from the experimental data to get the modulation signal of the radical.

The phase shift of the radical vs. wavelength at the various flashing frequencies is plotted in Figure 23. Modulation of hydrogen peroxide does indeed account for the wave length dependence of the phase shift in the raw data. Furthermore, when the radical phase shifts at each flashing frequency are averaged together and the averages plotted against log T (Figure 24), a curve results that fits the second-order radical curve within the experimental error. The position of the curve gives a value of $(PQ)^{1/2}$ of 14.5 sec^{-1}.

E. Comparison of Hydrogen Peroxide Modulation as Extracted from the Kinetic Data with the Modulation as Calculated from the Photolytic Decay Rate

A reactant which is destroyed only by light and fast radicals and is regenerated only by fast radicals has a triangular concentration modulation. When the photolytic lamp is off, the concentration increases at the rate of net reactant flux (R_f) into the cell. When the lamp is on, the concentration decreases at the rate of photo-decay minus in-flux ($R=R_p-R_f$). Since the profile is triangular, $R = -R_f$. The situation can be represented vectorially by:

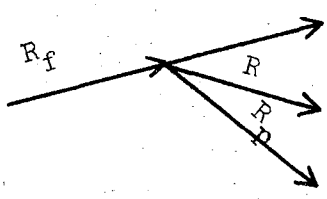

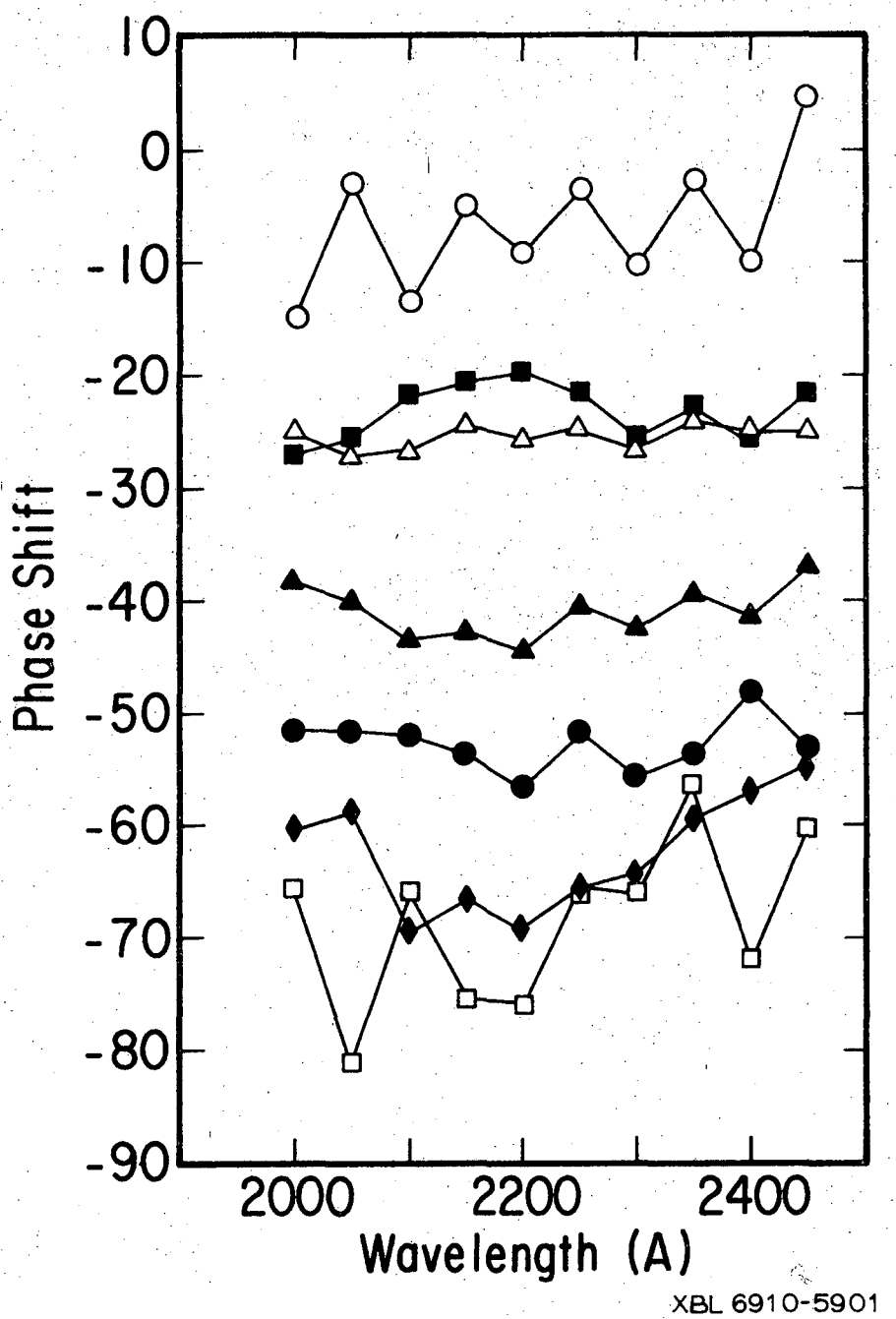

Figure 23. The phase shift of the radical spectrum vs ultraviolet wavelength at the flashing frequencies from 1/4 to 16 Hz.

○ 1/4 Hz, △ 1/2 Hz, ■ 1 Hz, ▲ 2 Hz,
● 4 Hz, ♦ 8 Hz, □ 16 Hz.

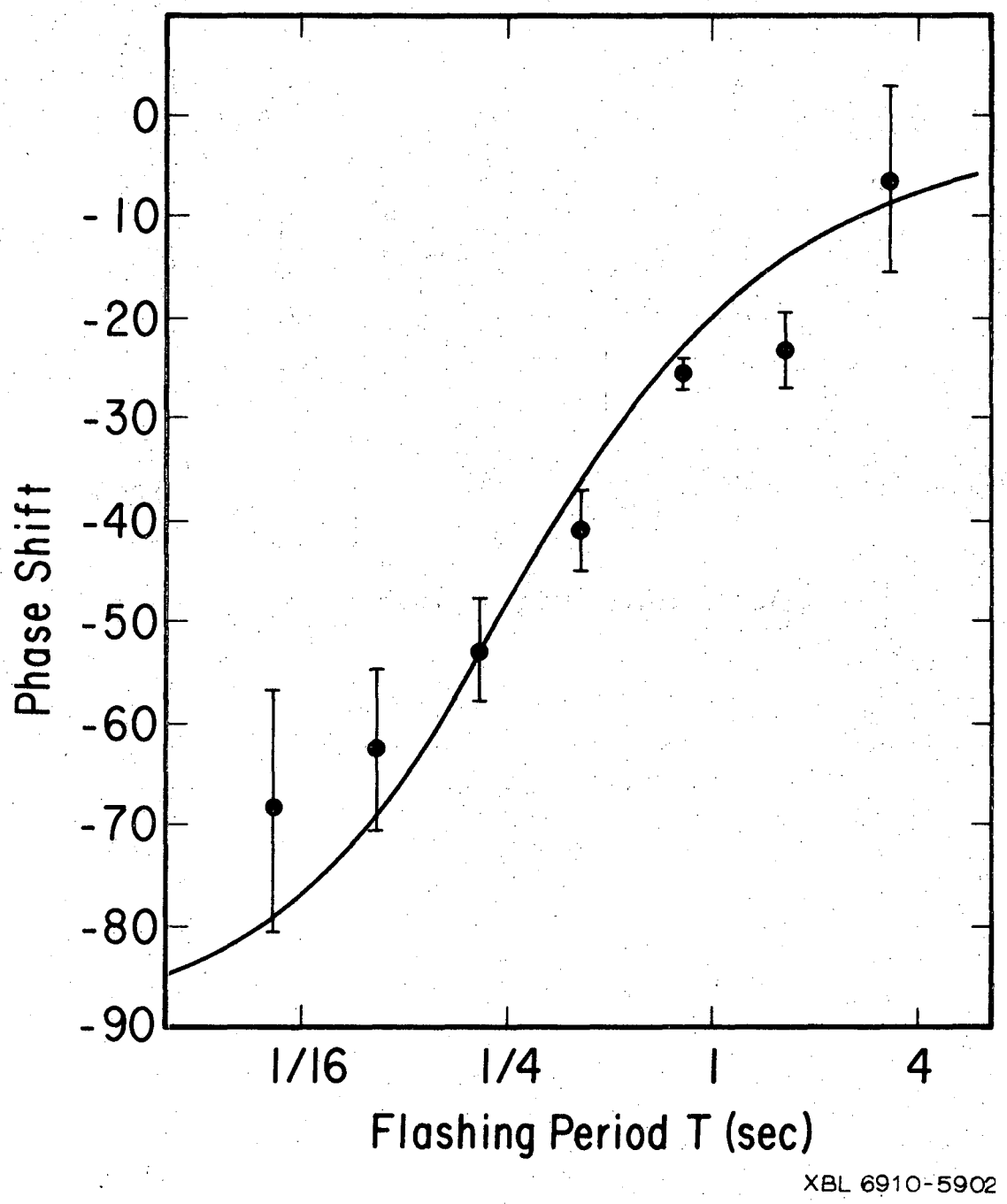

Figure 24. The phase shift of the radical vs the flashing period. The curve is the calculated curve for a primary second-order radical.

Since $R_f = -R = -R_p/2$, knowledge of R_p is sufficient to specify all the rates. R_p is given by

$$R_p = -2k_\sigma[H_2O_2]$$

so

$$R_f = k_\sigma[H_2O_2]$$

where k_σ is the rate constant of photon absorption. The change in peroxide concentration during a half-cycle is

$$\Delta[H_2O_2] = k_\sigma[H_2O_2]\Delta t$$

At the lowest frequency of observation--1/4 Hz--Δt is 1.64 sec. (1/4 Hz is the nominal frequency; the true frequency is 1.22 × 1/4 Hz). Thus the concentration modulation of hydrogen peroxide can be calculated once the rate constant of photon absorption k_σ is known.

1. Two-Lamp Experiment

In the experiment previously described in which hydrogen peroxide was photolyzed by two flashing photolytic lamps, the peroxide concentration was 8.5×10^{15} molecules/cm^3. The rate constant of photon absorption k_σ was found to be 1.65×10^{-3} sec^{-1} by the method described in the following section--Sec. F. Therefore

$$\Delta[H_2O_2] = 2.3 \times 10^{13} \text{ molecules/cm}^3$$

At 2000A where hydrogen peroxide has an extinction coefficient of 52.1×10^{-20} cm^2/molecule,[51] this change in concentration produces a change in absorbance

$$\Delta A = \sigma \Delta n l \qquad \text{where } l \text{ the path length is 380 cm}$$

$$= 4.55 \times 10^{-3}$$

This is the peak-to-peak amplitudes of a triangular modulation; the amplitude modulation at the fundamental frequency is smaller by a factor of $8/\pi^2$. Thus the change in absorbance at the fundamental frequency is

$$\Delta I/I = 3.69 \times 10^{-3}$$

From the calibration of the instrument (Sec. II-F) we know that

$$V_m = k \frac{\Delta I}{I} \qquad \text{and } k = 3.93 \times 10^6$$

Therefore the amplitude of the hydrogen peroxide signal calculated from the photolysis rate is 14,500 counts (arbitrary units); the peroxide amplitude extracted from the 1/4 Hz spectrum is 16,254 counts. The difference between the two is 11%.

2. One-Lamp Experiment

In the experiment in which the modulated absorption at 2200A was studied during the photolysis of hydrogen peroxide by one lamp at frequencies from 1/4 Hz to 32 Hz, the peroxide concentration was 1.13×10^{16} molecules/cm^3. The rate constant of photon absorption was found to be 0.825×10^{-3} sec^{-1} (Sec. F). The change in peroxide concentration at 1/4 Hz then is

$$\Delta[H_2O_2] = 1.53 \times 10^{13} \text{ molecules/cm}^3$$

At 2200A where the modulation was observed the extinction coefficient of hydrogen peroxide is 27.2×10^{-20} cm^2/molecule.[51] The change is absorbance where path length is 380 cm is

$$\Delta A = \sigma \Delta n l$$
$$= 1.58 \times 10^{-3}$$

At the fundamental frequency the modulation is

$$\frac{\Delta I}{I} = 1.58 \times 10^{-3} \quad \frac{8}{\pi 2} = 1.28 \quad 10^{-3}$$

from which we obtain

$$V_m = 5030 \text{ counts.}$$

The reactant amplitude extracted from the modulation data is 4169 counts. The difference is 19%. There are two factors which may explain the greater

discrepancy between the calculated and experimental amplitudes in the one-lamp experiment than in the two-lamp experiment. First the modulated absorption in the one-lamp experiment is smaller so that the signal-to-noise ratio is smaller than in the two-lamp experiment. Second, the data from the one-lamp experiment was obtained at only one observational wave length, but the data from the two-lamp experiment was obtained at ten observational points over the entire region 2450 to 2000 A. Hence considerably more data was used to extract the peroxide amplitude in the two-lamp experiment.

F. Extraction of the Disproportionation Rate Constant

In the previous section where the modulation behavior of the various kinds of species was analyzed it was shown that the lifetime, and hence the phase shift of first order radicals is independent of radical production rate. In contrast the lifetime of second order radicals depends on the square root of the radical production rate. Since the rate of radical production depends on photolytic light intensity, the variation of the quantity $(PQ)^{1/2}$ seen in Table VIII in the three different kinetic systems (one lamp in the I.R. cell, one lamp in the U.V. cell, and two lamps in the U.V. cell) is strong evidence of a second order radical. Quantitative correlation of the three systems requires knowledge of the rate of photon absorption of radical formation.

The rate of radical formation was obtained from the photolytic decay rate of hydrogen peroxide assuming the mechanism proposed by Volman. This is the mechanism successfully applied in the immediately preceding sections (Sec. II-D&E). The decay of hydrogen peroxide was followed in dark cells and in cells illuminated by the photolytic lamps. It was found that both

"dark" and "light" decay were first order in hydrogen peroxide concentration. The decay constants k_d for dark and k_l for light were obtained from the slopes of $\ln(D_o/D)$ plotted against time, where D_o is the initial optical density and D is the optical density at time t. Table VII lists the decay constants and also k_p the photolytic decay constant which is $k_p = k_l - k_d$. Because the rate of peroxide decomposition in the dark u.v. cell is of the same magnitude as the photolytic decay, there is a large degree of uncertainty. Within experimental error, the one and two lamp photolytic rate constants differ by a factor of two.

Since Volman's mechanism predicts a quantum yield of two for peroxide decomposition, the rate constant of photon absorption $k_\sigma = k_p/2$. The rate of photon absorption then is $k_\sigma[H_2O_2]$ and the rate of radical production is $P = 2k_\sigma[H_2O_2]$. Now the disproportionation rate constant can be found from

$$k_r = Q/2 = \frac{PQ}{2P} \quad .$$

Table VIII lists the appropriate data and the rate constant.

G. Absorption Coefficients of the Hydroperoxyl Radical

The absorption coefficient σ is defined by the equation $\Delta I/I = \sigma \Delta n l$ for small changes in the transmitted light intensity through an absorbing medium of length l caused by small changes in the concentration of the absorbers Δn. In our spectroscopic systems, the optical path length is known and the modulated absorbance $\Delta I/I$ is measured. Evaluation of the concentration modulation Δn would permit the determination of the absorption cross-section σ.

Application of the steady-state approximation to the equations of a second-order radical gives the concentration modulation in the low frequency limit in terms of the experimentally available quantities P and Q,

TABLE VII Evaluation of the Photodecay Constants of Hydrogen Peroxide in the Three Kinetically Different Systems

Decay Constants (sec^{-1})	Infrared Cell		Ultraviolet Cell one lamp	Ultraviolet Cell two lamps
$k_1 \times 10^3$	1.17	2.21	4.03	5.98
$k_d \times 10^3$	0.404	1.27	2.70	2.70
$k_p \times 10^3$	0.77	0.94	1.33	3.18

TABEL VIII Quantities Used Evaluation of k_r, the HO_2 - HO_2 Disproportionation Rate Constant

System	$(PQ)^{1/2}$ (sec^{-1})	k_σ (sec^{-1})	$[H_2O_2]$ $\left(\frac{molecules}{cm^3}\right)$	P $\left(\frac{molecules}{cm^3\ sec}\right)$	PQ (sec^{-2})	Q $\left(\frac{cm^3}{molecule\ sec}\right)$
Infrared System	5.55	0.425×10^{-3}	5.3×10^{15}	0.45×10^{13}	30.8	6.8×10^{-12}
Ultraviolet One Lamp	11.09	0.8×10^{-3}	1.13×10^{16}	1.8×10^{13}	123.0	6.8×10^{-12}
Ultraviolet Two Lamps	14.5	1.6×10^{-3}	8.5×10^{15}	2.7×10^{13}	210.2	7.8×10^{-12}

$$k_r = Q/2 = 3.6 \pm 0.5 \times 10^{-12}\ cm^3/molecule.sec$$

$$\Delta n = (P/Q)^{1/2}$$

where P is the rate of radical formation rate and Q is the empirical rate constant for radical decay.

The absorbance $\Delta I/I$ is measured at finite flashing frequencies and must be corrected to the low frequency limit. The observed phase shift and the model second-order radical curves specify the ratio of measured absorbance at each flashing frequency to the absorbance at the low frequency limit.

The experiments in the ultraviolet cell provide a considerable body of data from which to calculate the cross-section for absorption. From the two-lamp experiment the spectra obtained at 1/4, 1, 2, and 4 Hz were used to determine the absorption coefficient. (The amplitude of the spectrum at 1/2 Hz is not used because it is abnormally small.) Both the spectra at 1/4 and 1 Hz obtained from one-lamp experiments were used for another determination of the absorption coefficient. The appropriate data and the results of this calculation are given in Table IX. At the absorption peak of the hydroperoxyl radical its absorption coefficient is to the base e: 4.5×10^{-18} cm^2/molecule; to the base ten: 2.0×10^{-18} cm^2/molecule. The absorption coefficient of this radical at its peak has been found in aqueous solution[40] to be (base 10): 1.9×10^{-18} cm^2/molecule.

The infrared absorption of HO_2 is strongest at 1420 cm^{-1} where $\Delta I/I$ is observed to be 1.56×10^{-4} under conditions which give the radical a phase shift of approximately -40°. In the low frequency limit $\Delta I/I = 2 \times 10^{-4}$. The concentration modulation of HO_2 in the low frequency limit is

TABLE IX Evaluation of the Absorption Cross-Section of HO_2 at its Absorption Maximum in the Ultraviolet

f (sec^{-1})	Frequency Normalized Amplitudes Observed 2000	2050	2100	Limit as f→0 2000	2050	2100	$\Delta I/I$ f→0	P $\frac{molecules}{cm^3\ sec}$	Q $\frac{cm^3}{molecule.sec}$	$\Delta[H_2O_2]$ $\frac{molecules}{cm^2}$	σ $cm^2/molecules$ Base e	Base 10
Two Photolytic Lamps												
1/4	16519	17201	16391	17480	18202	17345						
1	14081	13550	14285	18725	18021	18996	3.39×10^{-3}	2.7×10^{13}	7.1×10^{-12}	1.95×10^{12}	4.6×10^{-18}	2.0×10^{-18}
2	9606	9798	9745	16010	16330	16242						
4	6373	7196	7146	14162	15991	15880						
One Photolytic Lamp												
1/4	11117	11653	12306	12491	13093	13827						
1	9392	9542	9625	13612	13892	13950	2.65×10^{-3}	1.8×10^{13}	7.1×10^{-12}	1.59×10^{12}	4.4×10^{18}	1.9×10^{-18}

$$\Delta[HO_2] = (P/Q)^{1/2}$$

$$= \left(\frac{4.5 \quad 10^{12} \text{ molecules/cm}^3 \cdot \text{sec}}{7.1 \quad 10^{-12} \text{cm}^3/\text{molecules} \cdot \text{sec}} \right)^{1/2}$$

$$= 8 \times 10^{11} \text{ molecules/cm}^3$$

The optical path is 48 meters; the absorption coefficient to the base e is 5×10^{-20} cm^2/molecule. Because of uncertainties in the hydrogen peroxide concentration when the spectra was obtained, this figure may be in error by as much as a factor of two.

H. Discussion

1. The Infrared Spectrum

The most notable difference between the infrared spectrum of HO_2 in the gas phase obtained by molecular modulation and the spectrum acquired by matrix isolation is the presence of multiple peaks. The gas phase spectrum should, if the resolution is good enough, display rotation-vibration features unobtainable in the matrix.

The nature of such features is dependent on the structure of the molecule and at present the structure of HO_2 is largely unknown. Walsh[44] has predicted that HO_2 should have a bent configuration with a slightly smaller bond angle than HNO and that both molecules should have bond angles greater than 90°. His model for HNO was found to be correct by Dalby[45] who determined the bond angle to be 108.5° in the ground state and 116.2° in the first excited state. In view of Walsh's success with HNO, it is reasonable to accept his conclusions regarding HO_2. As a lower limit on the HO_2 bond angle, we may take the H-O-O angle in hydrogen peroxide which is 94.8°. The HO_2 bond angle, then, is probably near 108°, but is surely within the range 95-116°.

The bond lengths of the hydroperoxyl radical present less of a problem. The O-H bond in the molecules H_2O_2, H_2O, and OH is 0.96 ± 0.01 A,[52,54,55] so a bond length of 0.96 A is reasonable for HO_2. The O-O bond length is less certain, but must lie between 1.21 A--the O-O bond distance in O_2--and 1.45 A--the O-O distance in H_2O_2. The O-O bond in ozone is 1.28 A and the bond in HO_2 is probably close to that, as the O-O bonds in both molecules have a bond order of 1 1/2. Boyd[43] used 1.3 A in her apriori calculations on HO_2. The precise value in this case is not important, however, as the calculations show that the only rotational constant large enough to be seen in our system is relatively insensitive to the O-O bond length.

The rotational constants calculated for this model of HO_2 are presented in Table X. The molecule has one large rotational constant and two small and nearly equal ones. Thus the symmetric rotor approximation is appropriate. The allowed rotational transitions for a symmetric top are: for a parallel band $\Delta J = 0, \pm 1$ and $\Delta K = 0$ for $K \neq 0$ and $\Delta J = \pm 1$ and $\Delta K = 0$ for $K = 0$; for a perpendicular band $\Delta J = 0, \pm 1$ and $\Delta K = \pm 1$.[56] These selection rules give rise to the parallel and perpendicular rotation-vibration band structure of a symmetric top. If the asymmetric rotor has only a small degree of asymmetry, its rotation-vibration band structure will be a hybrid of parallel and perpendicular components.

A parallel band consists of a superposition of a number of sub-bands, one for each value of K, having P, Q, and R branches. The complete parallel band, neglecting the interaction of rotation and vibration, has a strong Q branch flanked by P and R branches similar to a diatomic molecule.

A perpendicular transition leads to a band consisting of the superposition of a number of sub-bands, one for each value of K, having P, Q,

TABLE X Moments of Inertia and Rotational Constants for Various Geometrical Configurations of HO_2

Bond Lengths (A)		Bond Angle	Moments for Inertia ($\times 10^{40}$ g-cm^2)			Rotational Constants (cm^{-1})		
H-O	O-O	(°)	I_A	I_B	I_C	A	B	C
0.96	1.30	115	1.21	22.5	23.8	23.15	1.24	1.18
0.96	1.30	110	1.29	22.6	23.9	21.61	1.24	1.17
0.96	1.30	105	1.36	22.7	24.1	20.54	1.23	1.16
0.96	1.30	100	1.41	22.8	24.3	19.87	1.22	1.15
0.96	1.30	95	1.43	23.0	24.4	19.55	1.22	1.15
0.96	1.27	105	1.36	21.7	23.0	20.53	1.29	1.21
0.96	1.45	105	1.36	28.3	29.7	20.57	0.99	0.94

and R branches. Because of the change in the quantum number K ($\Delta K = \pm 1$), the sub-bands do not coincide so that the spectrum shows the individual Q branches on top of a diffuse unresolved background.

Since HO_2 is only slightly asymmetric, we can construct a general picture of its parallel and perpendicular bands using A = 20 cm^{-1} and B = 1.2 cm^{-1}--the average of the two minor rotational constants. The parallel Q branches will occur at ν_o, the vibrational frequency. The P and R branch separation found from the room temperature population distribution is 42 cm^{-1}. The perpendicular Q branches are positioned at:

$$\nu_Q = \nu_o + (A-B) + 2(A-B)K \quad K = 0,1,2,\ldots$$

and

$$\nu_Q = \nu_o + (A-B) - 2(A-B)K \quad K = 1,2,3,\ldots$$

Thus the Q branches would be positioned at

$$\nu_o \pm 19 \text{ cm}^{-1}$$

$$\nu_o \pm 57 \text{ cm}^{-1}$$

$$\nu_o \pm 95 \text{ cm}^{-1}$$

$$\nu_o \pm 143 \text{ cm}^{-1}$$

Taking ν_o to be 3410 cm^{-1}, the perpendicular band would have Q branches at 3429, 3467, 3505, 3553, 3391, 3353, and 3312 cm^{-1}. If the spectrum were a hybrid of the two types of bands, the parallel band with its Q branch at 3410 cm^{-1} and its P and R branches peaking at about 3431 and 3389 cm^{-1} could merge with the perpendicular Q branches at 3429 and 3391 cm^{-1} forming one broad intense peak, a likely possibility in low resolution work such as this. The observed peaks (Figure 13) at 3312, 3345, 3470, and 3505 cm^{-1} and a broad peak from 3380 to 3440 cm^{-1} fit well with the calculated peak positions.

The low frequency absorptions at 1395 cm^{-1} and 1100 cm^{-1} display a simpler structure. Each band has a pair of peaks separated by about 45 cm^{-1}, very close to the P-R separation expected from a parallel band. Neither band gives any evidence of a Q branch. This is in accordance with the predictions of Gerhard and Dennison[57] who show that the intensity of the Q branch of a parallel band relative to the P and R branches becomes small as I_A/I_B becomes small. From the calculated moments of inertia of HO_2 given in Table X the ratio of I_A/I_B is about 16.5. This leads to a ratio of Q branch intensity to P + R branch intensity of less than 0.1.

The infrared absorption frequencies observed in the gas phase are compared with the frequencies of the molecule isolated in a low temperature matrix in Table XI. None of our data permits a positive assignment of the observed frequencies to vibrational modes. The assignments of Milligan and Jacox of the 1101 cm^{-1} band to the O-O stretching vibration and their 1389 cm^{-1} band to the bending vibration seem more reasonable than the reverse assignments by Ogilvie. An O-O stretching vibration at 1110 cm^{-1} is consistent with the stretching frequencies of ozone at 1110 cm^{-1} and 1048 cm^{-1},[58] and a bending vibration near 1390 cm^{-1} agrees with an estimate of 1380 cm^{-1} for the H-O-O symmetric bending vibration of H_2O_2 by Redington et al.[54]

2. The Ultraviolet Spectrum

The ultraviolet absorption spectrum of HO_2 obtained in this laboratory has its peak intensity near 2100 A, but the spectrum reported by Czapski and Dorfman in aqueous solution has its maximum at 2300 A. Because of this discrepancy Morris photolyzed chlorine in the presence of hydrogen peroxide at 3600 A and obtained a modulated absorption spectrum from 2450 to 1950 A. (A brief description of his experiment is given in

TABLE XI Infrared Absorption Frequencies of the Hydroperoxyl Radical

Workers	Phase	Absorption Frequencies cm^{-1}			Assignments
Milligan and Jacox	Argon Matrix at 4°K	3414	1389.5	1101	$\nu_1\nu_2\nu_3$
J.F.Ogilvie	Argon-Neon Matrix at 4°K	3412	1395	1104	$\nu_1\nu_3\nu_2$
Present Results	Gas Phase at 295°K	3410	1390	1095	see text

Appendix E.) At 3600 A the absorption coefficient of hydrogen peroxide is very small, less than 2×10^{-21} cm^2/molecule.[59] The absorption coefficient of chlorine--averaged over the output of the lamp--was found by Morris[11] to be 9.2×10^{-20} cm^2/molecule. The hydroperoxyl radical is expected from the reaction of a chlorine atom with hydrogen peroxide.

$$Cl + H_2O_2 \rightarrow HCl + HO_2$$

The modulated absorption spectrum obtained from this system is compared with the radical spectrum obtained from the photolysis of hydrogen peroxide in Figure 25. The radical spectrum in this figure is an average of the radical spectra extracted from all the ultraviolet data presented in this work. The two spectra agree very well, providing strong evidence that the band is indeed due to HO_2 free radical.

It is well known that a solvent can have a profound effect on the wave length of maximum absorption in the electronic spectra of molecules.[60-66] The maximum may be shifted to either higher energies (blue shift) or to lower energies (red shift) depending on the solute, solvent, and the nature of the transition involved. A red shift implies stabilization of the excited state relative to the ground state by interaction with the solvent. Conversely, a blue shift implies stabilization of the ground state relative to the excited state. Numerous workers have attempted to correlate solvent effects with the dipole moment of the solute and the dielectric constant of the solvent,[60,61,65,67] the refractive index of the solvent,[60,61,65] molar volume of the solute or solvent,[61,62] and hydrogen bonding between solvent and solute molecules.[66]

The absorption maximum in the spectrum of HO_2 obtained in this laboratory is separated from the maximum in aqueous solution by 4100 cm^{-1}.

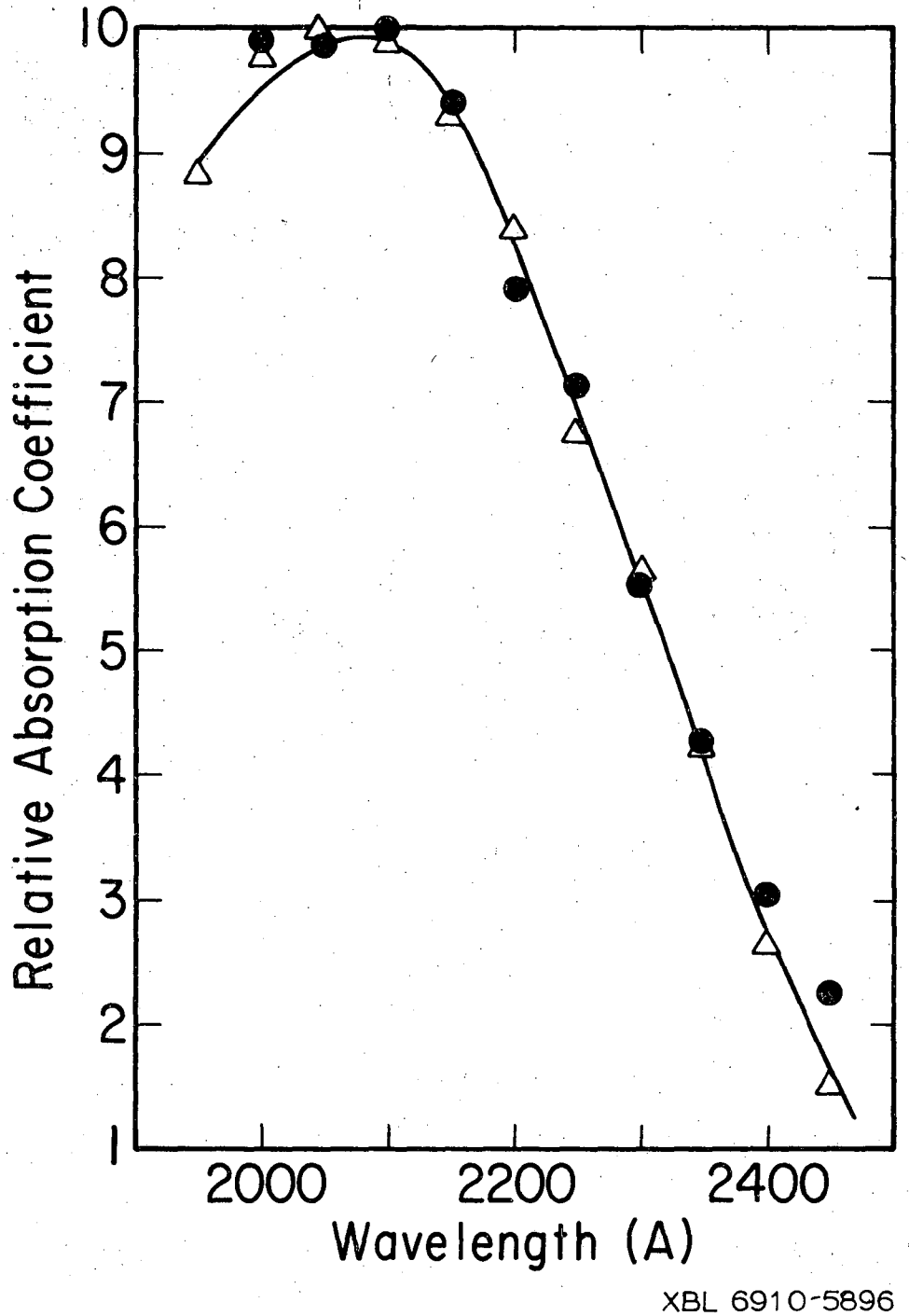

Figure 25. The ultraviolet spectrum of the hydroperoxyl radical.

● Average of all the ultraviolet spectra obtained from the photolysis of hydrogen peroxide at 2537 A

△ The spectrum from the photolysis of chlorine in the presence of hydrogen peroxide at 3600 A

The well-known correlation of a red shift in aqueous solution with molecules experiencing a $\pi \rightarrow \pi^*$ transition and capable of forming hydrogen bonds with water can be used to explain part of the shift we have here. The transfer of electron density from central regions of the molecule in the ground state to peripheral regions in the excited state can promote the formation of a hydrogen bond in the excited state. The magnitude of the resulting red shift depends on the strength of the hydrogen bond formed and is usually less than 2400 cm^{-1}.[66] The remaining part of the red shift may be due to some other interaction with the solvent or to a solvent induced change in the geometry of the HO_2 molecule.

The determination of the HO_2 - HO_2 disproportionation rate constant is based on the assumption that the reaction forming HO_2--OH + H_2O_2 → H_2O + HO_2--is fast, i.e., the OH concentration modulation is a square wave. The rate constant for this reaction at room temperature is 8.15×10^{-13} cm^3/molecule·sec.[68] The hydrogen peroxide concentration in our experiments was about 1×10^{16} molecules/cm^3. From these two quantities we can easily calculate the time required for the OH radical to reach its "steady-state" concentration or to decay to zero. This time is approximately 4τ where $\tau = 1/k[H_2O_2]$. The OH life-time τ is, then, about 10^{-4} sec, and the concentration modulation of OH is very nearly a square wave when the flashing period is greater than 10^{-2} sec. Most of our work was done at flashing periods greater than 10^{-1} sec.

The elementary rate constant for the reaction

$$HO_2 + HO \rightarrow H_2O_2 + O_2$$

has been found in this work to be $k_r = 3.6 \pm .5 \times 10^{-12}$ cm^3/molecule·sec. This compares well with the value obtained by Foner and Hudson[33] which is 3×10^{-12} cm^3/molecule·sec.

APPENDIX A

A Mathematical Treatment of Amplitude Modulation and the Demodulation Procedures used in this Laboratory

The 400 Hz carrier can be represented by a train of pulses of width τ, period T, and peak height E_p which is described by the following equation.

$$e(t) = E_p \frac{\tau}{T} + \sum_n \frac{2E_p}{n\pi} \sin\left(\frac{n\pi\tau}{T}\right) \cos\left(\frac{n2\pi t}{T}\right) \qquad \text{(A-1)}$$

where e(t) is the instantaneous voltage at time t. A modulating voltage at frequency w_m represented by

$$e_m(t) = E_m \sum_i a_i \sin(i\omega_m t) + b_i \cos(i\omega_m t) \qquad \text{(A-2)}$$

when mixed with the pulse train produces the amplitude modulated pulse train:

$$\begin{aligned} e'(t) = &\left(1 + \frac{E_m}{E_p} \sum_i a_i \sin(i\omega_m t) + b_i \cos(i\omega_m t)\right) \times \\ &\left(E_p \frac{\tau}{T} + \sum_n \frac{2E_p}{n\pi} \sin\left(\frac{n\pi\tau}{T}\right) \cos\left(\frac{n2\pi t}{T}\right)\right. \\ = &\ E_p \frac{\tau}{T} + \sum_n \frac{2E_p}{n\pi} \sin\left(\frac{n\pi\tau}{T}\right) \cos\left(\frac{n2\pi t}{T}\right) \\ &+ E_m \frac{\tau}{T} \sum_i a_i \sin(i\omega_m t) + b_i \cos(i\omega_m t) \\ &+ \sum_n \frac{2E_m}{n\pi} \sin\left(\frac{n\pi\tau}{T}\right) \cos\left(\frac{n2\pi t}{T}\right) \sum_i a_i \sin(i\omega_m t) + \cos(i\omega_m t) \end{aligned} \qquad \text{(A-3)}$$

The D.C. term $E_p \frac{\tau}{T}$ and the term at frequency ω_m are rejected by a high-pass filter. The following simplified expression describes the signal

received by the Carrier Demodulator:

$$e''(t) = \sum_n \frac{2E_p}{n\pi} \sin\left(\frac{n\pi\tau}{T}\right) \cos\left(\frac{n2\pi t}{T}\right) + \sum_n \frac{2E_m}{n\pi} \sin\left(\frac{n\pi\tau}{T}\right) \cos\left(\frac{n2\pi t}{T}\right) \sum_i a_i \sin(i\omega_m t) + b_i \cos(i\omega_m t) \tag{A-4}$$

The Carrier Demodulator has a switching type demodulator operating at the carrier frequency $\omega_c = \frac{2\pi}{T}$ which multiplies the signal by a square wave at the carrier frequency. The demodulated signal is:

$$e_j'' = e''(t) \sum_k \frac{4}{k\pi} \sin\left(\frac{k\pi}{2}\right) \cos\left(\frac{k2\pi t}{T}\right)$$

$$= \frac{8E_p}{\pi^2} \sum_n \frac{1}{n} \sin\left(\frac{n\pi\tau}{T}\right) \cos\left(\frac{n2\pi t}{T}\right) \sum_k \frac{1}{k} \sin\left(\frac{k\pi}{2}\right) \cos\left(\frac{k2\pi t}{T}\right)$$

$$+ \frac{8E_m}{\pi^2} \sum_n \frac{1}{n} \sin\left(\frac{n\pi\tau}{T}\right) \cos\left(\frac{n2\pi t}{T}\right) \sum_k \frac{1}{k} \sin\left(\frac{k\pi}{2}\right) \cos\left(\frac{k2\pi t}{T}\right) \tag{A-5}$$

$$\times \sum a_i \sin(i\omega_m t) + b_i \cos(i\omega_m t)$$

Let us examine the summation:

$$\sum_n \frac{1}{n} \sin\left(\frac{n\pi\tau}{T}\right) \cos\left(\frac{n2\pi t}{T}\right) \sum_k \frac{1}{k} \sin\left(\frac{k\pi}{2}\right) \cos\left(\frac{k2\pi t}{T}\right)$$

$$= \sum_n \frac{1}{n} \sin\left(\frac{n\pi\tau}{T}\right) \sum_k \frac{1}{k} \sin\left(\frac{k\pi}{2}\right) \cos\left(\frac{k2\cong t}{T}\right) \cos\left(\frac{n2\pi t}{T}\right)$$

$$= \sum_n \frac{1}{n} \sin\left(\frac{n\pi\tau}{T}\right) \sum_k \frac{1}{k} \sin\left(\frac{k\pi}{2}\right) \frac{1}{2} \left(\cos\left(\frac{(n+k)2\pi t}{T}\right) + \cos\left(\frac{(n-k)2\pi t}{T}\right)\right). \tag{A-6}$$

Only the D.C. term is of interest since all the harmonics of the carrier frequency are rejected by filters. Therefore we need consider only the case of k=n, and we get

$$\sum_n \frac{1}{n} \sin\left(\frac{n\tau\pi}{T}\right) \cdot \frac{1}{n} \sin\left(\frac{n\pi}{2}\right) \frac{1}{2}\left(\cos\left(\frac{n4\pi t}{T}\right) + 1\right) \tag{A-7}$$

The D.C. component of $e_d''(t)$ is, then, proportional to:

$$\sum_n \frac{1}{2n^2} \sin\left(\frac{n\pi\tau}{T}\right) \sin\left(\frac{n\pi}{2}\right). \tag{A-8}$$

Just as the first term $e_d''(t)$ leads to a D.C. term, the second leads to a low frequency term proportional to:

$$\sum_n \frac{1}{2n^2} \sin\left(\frac{n\pi\tau}{T}\right) \sin\left(\frac{n\pi}{2}\right) \sum_i a_i \sin(i\omega_m t) + b_i \cos(i\omega_m t) \tag{A-9}$$

The demodulated signal in its simplified form is then:

$$\begin{aligned} e_d''(t) = {} & \frac{8E_p}{\pi^2} \sum_n \frac{1}{2n^2} \sin\left(\frac{n\pi\tau}{T}\right) \sin\left(\frac{n\pi}{2}\right) \\ & + \frac{8E_m}{\pi^2} \sum_n \frac{1}{2n^2} \sin\left(\frac{n\pi\tau}{T}\right) \sin\left(\frac{n\pi}{2}\right) \sum_i a_i \sin(i\omega_m t) \\ & + b_i \cos(i\omega_m t). \end{aligned} \tag{A-10}$$

Then D.C. voltage proportional to carrier level is:

$$V_c = \frac{4E_p}{\pi^2} \sum_n \frac{1}{n^2} \sin\left(\frac{n\pi\tau}{T}\right) \sin\left(\frac{n\pi}{2}\right). \tag{A-11}$$

The low frequency voltage proportional to the modulating signal is:

$$\begin{aligned} e_m'(t) = {} & \frac{4E_m}{\pi^2} \sum_n \frac{1}{n^2} \sin\left(\frac{n\pi\tau}{T}\right) \sin\left(\frac{n\pi}{2}\right) \sum_i a_i \sin(i\omega_m t) \\ & + b_i \cos(i\omega_m t). \end{aligned} \tag{A-12}$$

The Dual-Phase Demodulator has two switching demodulators operating 90° apart at the fundamental modulating frequency. One mixer can be represented by a square wave expressed as a Fourier expansion of sine waves; the other by a Fourier expansion of cosine waves.

$$P = \sum_p \frac{2}{p\pi} (1 - \cos p\pi) \sin (p\omega_m t) \tag{A-13}$$

$$Q = \sum_q \frac{4}{q\pi} \sin \frac{q\pi}{2} \cos (q\omega_m t) \tag{A-14}$$

Multiplying $e'_m(t)$ by P gives:

$$e'_{m,p}(t) = A \sum_i a_i \sin (i\omega_m t) + b_i \cos (i\omega_m t) \sum_p \frac{2}{p\pi} \tag{A-15}$$

$$(1 - \cos) (p\pi)) \sin (p\omega_m t)$$

where $$A = \frac{4E_m}{\pi^2} \sum_n \frac{1}{n^2} \sin \left(\frac{n\pi\tau}{T}\right) \sin \left(\frac{n\pi}{2}\right)$$

$$e'_{m,p}(t) = \frac{2A}{\pi} \sum_p \frac{1}{p} (1 - \cos p\pi) \left\{ \sum_i a_i \sin (i\omega_m t) \sin (p\omega_m t) \right.$$

$$\left. + b_i \cos (i\omega_m t) \sin (p\omega_m t) \right\} \tag{A-16}$$

$$= \frac{2A}{\pi} \sum_p \frac{1}{p} (1 - \cos p\pi) \left\{ \sum_i \frac{a_i}{2} (\cos (i-p)\omega_m t - \cos(i+p)\omega_m t) \right.$$

$$\left. + \frac{b_i}{2} (\sin (i+p)\omega_m t + \sin (i-p)\omega_m t) \right\} \tag{A-17}$$

Again only the D.C. is of interest, so i=p

$$e'_{m,p}(t) = \frac{2A}{\pi} \sum_p \frac{1}{p} (1 - \cos p\pi) \left\{ \sum_p \frac{a_p}{2} (1 - \cos p\, 2\omega_m t) \right.$$

$$\left. + \frac{b_p}{2} \sin p\, 2\omega_m t \right\} \tag{A-18}$$

and the D.C. voltage is

$$V_{m,p} = \frac{2A}{\pi} \sum_p \frac{1}{p} (1 - \cos p\pi) \sum_p \frac{a_p}{2} \tag{A-19}$$

Now

$$1 - \cos p\pi = 0 \quad \text{if } p \text{ is even}$$

$$= 2 \quad \text{if } p \text{ is odd.}$$

Therefore all even harmonics of the original modulation are rejected, but a fraction of all odd harmonics comes through. Low pass filters used before the demodulation reject the odd harmonics of ω_m; i.e. $a_p \sim 0$ and $b_p \sim 0$ for $p > 1$. Hence only the fundamental is extracted giving:

$$V_{m,P} = \frac{4A}{\pi} \cdot \frac{a_1}{2}$$

$$= \frac{8 E_m a_1}{\pi^3} \sum_n \frac{1}{n^2} \sin\left(\frac{n\pi\tau}{T}\right) \sin\left(\frac{n\pi}{2}\right) \tag{A-20}$$

The other demodulator gives

$$V_{m,Q} = \frac{8E_m b_1}{\pi^3} \sum_n \frac{1}{n^2} \sin\left(\frac{m\pi\tau}{T}\right) \sin\left(\frac{n\pi}{2}\right) \tag{A-21}$$

The amplitude of the fundamental frequency as extrasted by the electronics is

$$V_m = \left(V_{m,P}^2 + V_{m,Q}^2\right)^{1/2} \tag{A-22}$$

$$= \frac{8E_m (a_1^2 + b_1^2)^{1/2}}{\pi^2} \sum_n \frac{1}{n^2} \sin\left(\frac{n\pi\tau}{T}\right) \sin\left(\frac{n\pi}{2}\right)$$

The modulation of the carrier by the fundamental modulating frequency ω_m is

$$\frac{\Delta E_p}{E_p} = \frac{2 E_m (a_1^2 + b_1^2)^{1/2}}{E_p} \tag{A-23}$$

In terms of the measured quantities V_c, $V_{m,p}$ and $V_{m,Q}$

$$\frac{\Delta E_p}{E_p} = \frac{\pi (V_{m,p}^2 + V_{m,Q}^2)^{1/2}}{V_c} \tag{A-24}$$

$$= \frac{\pi V_m}{V_c} \qquad \text{(A-25)}$$

This result makes possible the determination of absolute modulations $\Delta I/I$ by measurement of the experimental voltages $V_{m,P}$, $V_{m,Q}$, and V_c. Since the amplitude of the low frequency signal exiting the Carrier Demodulator is modified by filters and amplifers before it is rectified in the Dual Phase Demodulator, the expression relating $\Delta I/I$ to the D.C. voltage $V_{m,p}$, $V_{m,Q}$ and V_c must be modified to

$$\frac{\Delta I}{I} = \frac{\pi (V_{m,p}^2 + V_{m,Q}^2)^{1/2}}{V_c \cdot g} \qquad \text{(A-26)}$$

where g is net gain of all ampliers and filters operating on the low frequency signal.

APPENDIX B

Details of the Calculation of the Amplitude and Phase Shift Behavior of a Second-Order Radical

The integrated rate equations for a radical which decays by a process second order in its concentration have been shown to be (Sec. II-B-4):

$$[Z]_\theta = \left(\frac{2\sigma I_o[A]}{2k_r}\right)^{1/2} \tanh\left(\frac{(\theta+\pi)(2\sigma I_o[A]2k_r)^{1/2}}{2\pi f} + \tanh^{-1}\left(\frac{[Z]}{(2\sigma I_o[A]^{-\pi}/2k_r)^{1/2}}\right)\right) \quad \text{when the lamp is on} \tag{12a}$$

and $$[Z]_\theta = \frac{2\pi f[Z]_o}{2\pi f + 2k_r\theta[Z]_o} \quad \text{when the lamp is off.} \tag{12b}$$

In the following Fortran program ($2\sigma I_o[A]$) is represented by A and $2k_r$ is represented by B. The radical concentration at the beginning, middle, and end of a flashing cycle is calculated by an iterative procedure until the concentration at the beginning and the end are equal within 0.0001 times the radial concentration in the "steady-state." Then the radical concentration is calculated at angle increments of $2\pi/100$ and a Fourier analysis of the concentration modulation is carried out to determine the amplitude and phase shift of the fundamental frequency. The coefficients of the third and fifth harmonics are also obtained for magnitude comparisons with the coefficients of the fundamental, but the amplitude and phase shift are not calculated since our apparatus discriminates against the harmonics.

APPENDIX C

Reactant Behavior in any Chemical System Following the Mechanism of the Photolysis of Hydrogen Peroxide

The mechanism proposed by Volman to account for the photolysis of hydrogen peroxide is:

$$H_2O_2 + h\nu \rightarrow 2OH$$

$$OH + H_2O_2 \rightarrow H_2O + HO_2$$

$$HO_2 + HO_2 \rightarrow H_2O_2 + O_2$$

Since the OH radical reacts very rapidly with hydrogen peroxide, the first two steps may be combined to give:

$$3H_2O_2 + h\nu \rightarrow 2H_2O + 2HO_2$$

The general process we wish to examine is therefore:

$$3A + h\nu \rightarrow 2Z + B$$

$$Z + Z \rightarrow A + C$$

Z is a second-order radical whose kinetic behavior has already been examined. The rate of formation of the radical Z is given by

$$P = 2\sigma I_o[A]$$

and has units of molecules/cm^3·sec.

The differential rate equation for the reactant A can be written

$$\frac{d\,A}{dt} = -\frac{3P}{2} + \frac{Q}{2}[Z]^2 \qquad \text{when the lamp is on}$$

and

$$\frac{d\,A}{dt} = \frac{Q}{2}[Z]^2 \qquad \text{when the lamp is off.}$$

A term for the flow of reactant A into the cell must be included to make the concentration of A vary periodically. The flow term is equal to the average rate of reactant destruction which is P/2. The complete differential equations including flow are

$$\frac{d[A]}{dt} = \frac{P}{2} - \frac{3P}{2} + \frac{Q}{2}[Z]^2 \qquad \text{when the lamp is on}$$

and

$$\frac{d[A]}{dt} = \frac{P}{2} + \frac{Q}{2}[Z]^2 \qquad \text{when the lamp is off.}$$

The concentration profile of the reactant A is calculated over a flashing cycle from the rate of radical formation P, the rate constant for radical-radical reaction Q, and the concentration profile of the radical Z. Then a Fourier analysis of the concentration modulation of the reactant is performed and the amplitude and phase shift of the fundamental are extracted. The Fortran program which performs this calculation follows.

```
      TANH[Z,C]#Ø.5*ALOG[1&Z/C]-Ø.5*ALOG[1-Z/C]
      TANH[D]#[EXP[D]-EXP[-D]]/[EXP[D]&EXP[-D]]
      DIMENSION XTHETA[4ØØ],Y[1],YTHETA[4ØØ],COSSUM[3],SINSUM[3],
     1SINV[4ØØ,3],COSV[4ØØ,3]
      PI#3.1416
      A#1.ØE 13
      B#1.ØE-11
      G#SQRT[A*B]
      H#SQRT[A/B]
      ANGLEINCREMENT#2*PI/4ØØ
      THETA#-PI
      DO 17 I#1,4ØØ
      DO 18 J#1,3
      SINV[I,J]#SIN[[2*J-1]*THETA]
18    COSV[I,J]#COS[[2*J-1]*THETA]
17    THETA#THETA&ANGLEINCREMENT
16    ACCEPT 1,XPI1,XPI2,XO,F
1     FORMAT[3E15.5,F1Ø.3]
      DELTAT#1/F/4ØØ.
      HOPE#TANH[XPI1,H]
      THETA#-PI
      R#2*PI*F
      DO 5 I#1,2ØØ
      WTHETA#[THETA&PI]*G/R&HOPE
      XTHETA[I]#H*TANH[WTHETA]
5     THETA#THETA&ANGLEINCREMENT
      THETA#Ø.
      DO 6 I#2Ø1,4ØØ
      XTHETA[I]#R*XO/[R&B*XO*THETA]
6     THETA#THETA&ANGLEINCREMENT
      YTHETA[Ø]#1.ØE 15
      DO 7 I#1,2ØØ
7     YTHETA[I]#YTHETA[I-1]&[-1.ØØE 13&Ø.5*B*XTHETA[I]**2]*DELTAT
      DO 8 I#2Ø1,4ØØ
8     YTHETA[I]#YTHETA[I-1]&[5.ØE 12&Ø.5*B*XTHETA[I]**2]*DELTAT
      PRINT 9, F
```

```
9       FORMAT[1H1,4X,$THE REACTANT CONCENTRATION PROFILE AT $,F7.3,
       1$   CPS IS $,//]
        PRINT 1Ø,YTHETA
1Ø      FORMAT[4X,8E15.5]
        PRINT 11, YTHETA[1],YTHETA[2ØØ],YTHETA[4ØØ]
11      FORMAT [//4X,3E15.5]
        THETA#-PI
        DO 2 L#1,3
        SINSUM[L]#Ø
2       COSSUM[L]#Ø
        DO 4 I#1,4ØØ
        DO 12 L#1,3
        SINSUM[L]#SINSUM[L]&YTHETA[I]*SINV[I,L]
12      COSSUM[L]#COSSUM[L]&YTHETA[I]*COSV[I,L]
4       CONTINUE
        PRINT 13,[I,SINSUM[I],I,COSSUM[I],I#1,3]
13      FORMAT [/4X,$SIN COEFFICIENT[$,I1,$] # $,E15.5,
       14ØX,$COS COEFFICIENT [$,I1,$] #$, E15.5]
        AMPLITUDE#SQRT[SINSUM[1]**2&COSSUM[1]**2]*2/4ØØ
        PHASE#57.296*ATAN[-COSSUM[1],-SINSUM[1]]
        T#1/F
        TN#1Ø/F
        PRINT 14,AMPLITUDE,PHASE
14      FORMAT [4X,$AMPLITUDE # $,E15.5/4X,$PHASE # $,F7.3]
        PRINT 15,T,TN,F
15      FORMAT [4X,$PERIOD # $,F1Ø.4/4X,$PERIOD NORMALIZED # $,F1Ø.4
       1/4X,$FREQUENCY # $,F1Ø.4]
        GO TO 16
        END
```

APPENDIX D

The Effect of a Moving Average Curve Smooth on the Spectral Resolution

Consider the ideal triangular slit function Y whose width at half-height is N data points and whose peak is Y_o. The slope of the sides of the slit function is $0.5Y_o/(N-1)/2 = Y_o/(N-1)$.

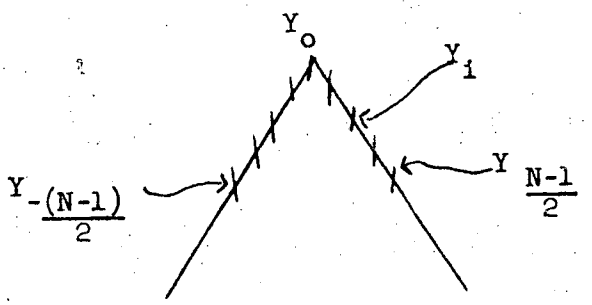

The slit function at any point Y_i can be found from the slope but it is unnecessary.

Applying a moving average curve of M data points, where $M \leq N$, to the slit function generates a new slit function Y' where the peak is given by:

$$Y'_o = \frac{Y_o}{M}\left(1 + 2\left(1 - \frac{1}{N-1}\right) + 2\left(1 - \frac{2}{N-1}\right) + \ldots 2\left(1 - \frac{(M-1)/2}{N-1}\right)\right)$$

As long as $M \leq N$, $Y'_i = Y_i$ for $i = (N-1)/2$ so the number of points N' per slit width of the new slit function is given by the equation

$$\frac{Y'_o}{2} = Y_o\left(1 - \left(\frac{N-1}{2}\right)\left(\frac{1}{N-1}\right)\right).$$

The last two equations have been used to calculate slit width for

3, 5, 7, and 9 point curve smooths. Values of N' are presented in Table XII as functions of N and M.

Table XII

Number of points N' per slit width of a slit function originally N points wide modified by a curve smooth of M points

M \ N	3	5	7	9
3	3.67	5.67	7.67	9.67
5	----	6.20	8.20	10.20
7	----	----	8.71	10.71
9	----	----	----	11.22

APPENDIX E

After the ultraviolet spectrum of HO_2 had been observed in the photolysis of hydrogen peroxide, Earl Morris conducted experiments to observe HO_2 in another chemical system. The reaction he chose was the photolysis of chlorine in the presence of hydrogen peroxide. The expected elementary reactions are:

$$Cl_2 + h\nu \rightarrow 2Cl$$
$$Cl + H_2O_2 \rightarrow HCl + HO_2$$
$$HO_2 + HO_2 \rightarrow H_2O_2 + O_2$$

Two G.E. F64T6-BL black lamps provide the photolysis light over the region 3200 to 3800A°. The photon flux was 4.2×10^{16} photons/cm^2·sec.; the effective cross-section for absorption of the photolysis light by chlorine is 9.2×10^{-20} cm^2/molecule. The absorption cross-section of hydrogen peroxide at these wave lengths is very low ($<2\times10^{-21}cm^2$/molecule)

Reactant concentrations during the photolysis were: $[Cl_2] = 1.7\times10^{16}$molecules/$cm^3$ and $[H_2O_2] = 1.5\times10^{16}$molecules/$cm^3$. The observed modulation spectrum at 2 Hz is presented in the following table.

Table XIII

λA°	Amplitude*	Phase Shift
2500	1593	-52.4°
2400	5494	-21.0°
2300	11629	-18.3°
2250	13947	-17.8°
2200	17258	-17.6°
2150	19279	-17.6°
2100	20496	-16.9°
2050	20650	-16.9°
2000	20205	-15.6°
1950	17644	-14.6°

*The amplitudes are not frequency normalized.

ACKNOWLEDGEMENTS

I am grateful to Dr. Harold P. Johnston for his gentle and patient guidance of this research. His practice of granting each student a large degree of autonomy encourages the student to develop his own scientific potential and inclinations, while his example of a creative scientist provides the student with an invaluable model of scientific thought and approach to physical problems.

My experience at this university has been enrichened by the graduate students and post-doctoral fellows with whom I have worked and shared ideas. Dr. L. W. Richards deserves special mention for the valuable assistance he probided in the early phases of this work.

I am indebted to the National Science Foundation for a Graduate Fellowship which supported my studies during the first two years. This work has been funded by the United States Public Health Service and the Atomic Energy Commission.

REFERENCES

1. H. S. Johnston and F. Cramarossa, Advances in Photochemistry 4, 1. Interscience Publishers, New York (1966).

2. R. G. W. Norrish and B. A. Thrush, Quart. Rev. (London) 10, 149 (1956).

3. R. G. W. Norrish, Proc. Chem. Soc. 1958, 247.

4. R. G. W. Norrish, Am. Sci. 50, 131 (1962).

5. R. G. W. Norrish, Science 149, 1470 (1965).

6. R. G. W. Norrish, Chem. Brit. 1, 289 (1965).

7. A. M. Bass and H. P. Broida (edotors), Formation and Trapping of Free Radicals, Academic Press, New York (1960).

8. C. V. Crews, Unpublished review of radicals studied by ultraviolet, visible, and infrared spectroscopy in matrix isolation from 1959 to 1967.

9. H. S. Johnston, G. E. McGraw, T. T. Paukert, L. W. Richards, and J. van den Bogaerde, Proc. Natl. Acad. Sci. 57, 1146 (1967).

10. J. van den Bogaerde, Ph.D. Thesis, University of California, Berkeley (1969).

11. E. D. Morris, Ph. D. Thesis, University of California, Berkeley (1969).

12. A. L. Marshall, J. Phys. Chem. 30, 34, 1078 (1926).

13. H. S. Taylor, Trans. Faraday Soc. 21, 560 (1926).

14. B. Lewis and G. von Elbe, Third Symposium on Combustion and Flames and Explosion Phenomena, Williams and Wilkins Co., Baltimore (1949) p. 484.

15. B. Lewis and G. von Elbe, Combustion, Flames, and Explosions of Gases, Academic Press, New York (1961).

16. R. R. Baldwin, L. Mayor, and P. Doran, Trans. Faraday Soc. 56, 93 (1960).

17. R. R. Baldwin and L. Mayor, Trans. Faraday Soc. 56, 80, 103 (1960).

18. R. H. Burgess and J. C. Robb, Chem. Soc. Spec. Pub. No. 9, 167 (1957).

19. G. J. Minkoff and C. F. H. Tipper, Chemistry of Combustion Reactions, Butterworths, London (1962).

20. L. J. Heidt and G. S. Forbes, J. Am. Soc. 56, 1671, 2365 (1934).

21. D. H. Volman, J. Am. Chem. Soc. 73, 1018 (1951).

22. R. G. W. Norrish and R. P. Wayne, Proc. Roy. Soc. A288, 200 (1965).

23. D. H. Volman, Advances in Photochemistry 1, 43, Interscience Publ., New York (1963).

24. W. D. McGrath and R. G. W. Norrish, Proc. Roy. Soc. A254, 317 (1960).

25. D. H. Volman, J. Chem. Phys. 17, 947 (1949).

26. W. Forst and P. A. G. Giguere, J. Phys. Chem. 62, 340 (1958).

27. R. R. Baldwin, P. Doran, and L. Mayor, Eighth Combustion Symposium Williams and Wilkins Co., Balitmore (1962) p. 103.

28. R. R. Baldwin, D. Jackson, R. W. Walker, and S. J. Webster, Trans. Faraday Soc. 63, 1676 (1967).

29. R. R. Baldwin and D. Brattan, Eighth Combustion Symposium, Williams and Wilkins Co., Baltimore (1962) p. 110.

30. R. R. Baldwin, D. Jackson, R. W. Walder, and S. J. Webster, Tenth Combustion Symposium, Combustion Institute, Pittsburg (1965) p. 423.

31. D. E. Hoare, Proc. Roy. Soc. A291, 73 (1966).

32. N. R. Greiner, J. Chem. Phys. 45, 99 (1966); J. Phys. Chem. 72, 406 (1968).

33. S. N. Foner and R. L. Hudson, J. Chem. Phys. 36, 2681 (1962).

34. S. N. Foner and R. L. Hudson, J. Chem. Phys. 21, 1608 (1953).

35. A. J. B. Robertson, Applied Mass Spectrometry, Institute of Petroleum, London (1954).

36. K. U. Ingold and W. A. Bryce, J. Chem. Phys. 24, 360 (1956).

37. D. J. Fabian and W. A. Bryce, Seventh International Symposium on Combustion, Butterworths Scientific Publications, London (1959) p. 150.

38. D. E. Milligan and M. E. Jacox, J. Chem. Phys. 38, 2627 (1963), 40, 605 (1964).

39. J. F. Ogilvie, Spectrochimica Acta 23A, 737 (1967).

40. G. Czapski and L. M. Dorfman, J. Phys. Chem. 68, 1169 (1964).

41. S. N. Foner and R. L. Hudson, Mass Spectrometry of Inorganic Free Radicals, Advances in Chemistry Series No. 36 (1962) p. 42.

42. M. Green and J. W. Linnett, J. Chem. Soc. 1960, 4959.

43. M. E. Boyd, J. Chem. Phys. 37, 1317 (1962).

44. A. D. Walsh, J. Chem. Soc. 1953, 2288.

45. F. W. Dalby, Can. J. Phys. 36, 1336 (1958).

46. H. Margeneau and G. S. Murphy, The Mathematics of Physics and Chemistry, D. Van Nostrand Co., Inc., Princeton, N. J. (1956) p. 41.

47. A. Savitzky and M. J. E. Golay, Anal. Chem. 36, 1627 (1964).

48. T. A. Brubaker and D. R. Stevens, J. Comput. Phys. 2, 465 (1968).

49. G. A. Cook, A. D. Kiffer, C. V. Klumpp, A. H. Malik, and L. A. Spence, "Separation of Ozone from Oxygen by a Sorption Press Process" in Ozone Chemistry and Technology Advances in Chemistry Advances in Chemistry Series No. 21 (1959) p. 44.

50. P. A. Giguere, J. Chem. Phys. 18, 88 (1950).

51. R. B. Holt, C. K. McLane, and O. Oldenberg, J. Chem. Phys. 16, 225, 638 (1948).

52. G. Herzberg, Molecular Structure and Molecular Spectra I. Spectra of Diatomic Molecules, D. Van Nostrand Co., Princeton, N. J. (1950) p. 560.

53. H. C. Urey, L. H. Dawsey, and F. O. Rice, J. Am. Chem. Soc. 51, 1371 (1929).

54. R. L. Redington, W. B. Olson, and P. C. Cross, J. Chem. Phys. 36, 1311 (1962).

55. G. Herzberg, Molecular Structure and Molecular Spectra II. Infrared and Raman Spectra of Polyatomic Molecules, D. Van Nostrand Co., Princeton, N. J. (1945) p. 400.

56. G. Herzberg, Molecular Structure and Molecular Spectra II. Infrared and Raman Spectra of Polyatomic Molecules, D. Van Nostrand Co., Princeton, N. J. (1945) p. 489.

57. S. L. Gerhard and D. M. Dennison, Phys. Rev. 43, 197 (1933).

58. M. K. Wilson and R. M. Badger, J. Chem. Phys. 16, 741 (1948).

59. W. C. Schumb, C. N. Satterfield, and R. L. Wentworth, Hydrogen Peroxide, Reinhold Publishing Corp., New York (1955) p. 287.

60. N. S. Bayliss and E. G. McRae, J. Phys. Chem. 58, 1002 (1954), 61, 562 (1957).

61. I. A. Zhmyrev, V. V. Zelinski, V. P. Kolobkov, A. S. Kochemirovskii, and I. I. Reznikova, Opt. and Spect. 8, 214 (1960).

62. I. A. Zhmyreva and I. I. Reznikova, Opt. and Spect. 10, 142 (1961).

63. N. G. Bakhshiev, Bull. Acad. Sci. USSR, Phys. 26, 1252 (1963).

64. E. M. Arnett and D. Hufford, J. Am. Chem. Soc. 88, 3140 (1966).

65. M. B. Ledger and P. Suppan, Spectrochimica Acta 23A, 641 (1967).

66. G. C. Pimentel and A. L. McClellan, The Hydrogen Bond , W. H. Freeman and Co., San Francisco (1960) p. 157.

67. N. G. Bakshiev, Optics and Spectroscopy, 7, 29 (1959).

68. D. L. Baulch, D. D. Drysdale, and A. C. Lloyd, Critical Evaluation of Rate Data for Homogeneous Gas-Phase Reactions of Interest in High-Temperature Systems, School of Chemistry, The University, Leeds (1969) p. 39.

LEGAL NOTICE

This report was prepared as an account of Government sponsored work. Neither the United States, nor the Commission, nor any person acting on behalf of the Commission:

A. Makes any warranty or representation, expressed or implied, with respect to the accuracy, completeness, or usefulness of the information contained in this report, or that the use of any information, apparatus, method, or process disclosed in this report may not infringe privately owned rights; or

B. Assumes any liabilities with respect to the use of, or for damages resulting from the use of any information, apparatus, method, or process disclosed in this report.

As used in the above, "person acting on behalf of the Commission" includes any employee or contractor of the Commission, or employee of such contractor, to the extent that such employee or contractor of the Commission, or employee of such contractor prepares, disseminates, or provides access to, any information pursuant to his employment or contract with the Commission, or his employment with such contractor.

TECHNICAL INFORMATION DIVISION
LAWRENCE RADIATION LABORATORY
UNIVERSITY OF CALIFORNIA
BERKELEY, CALIFORNIA 94720